



PRELIMINARY STUDY OF L'AQUILA EARTHQUAKE GROUND MOTION RECORDS V5.20



Eugenio Chioccarelli, Flavia De Luca and Iunio Iervolino

eugenio.chioccarelli@unina.it; flavia.deluca@unina.it; iunio.iervolino@unina.it

Dipartimento di Ingegneria Strutturale, Università di Napoli Federico II.

Index

1. What's New	1
2. Introduction	1
3. Geographic Information.....	3
4. Horizontal Component - Plots for Spectral Periods	6
5. Horizontal Component - Plots for Distance Bins	8
6. Vertical Component - Plots for Spectral Periods.....	12
7. Vertical Component - Plots for Distance Bins	15
8. Peak Values Tables.....	19
9. Horizontal Component – Plots of Integral parameters (Durations).....	23
10. Integral Values Tables	24
11. Horizontal Component – Inelastic Spectra	28
12. Vertical Component – Inelastic Spectra	31
13. Horizontal Component –Specific Hysteretic Energy Inelastic Spectra.....	35
14. Vertical Component –Specific Hysteretic Energy Inelastic Spectra	39
15. Horizontal Component –Number of Equivalent Cycles Spectra.....	43
16. Vertical Component –Number of Equivalent Cycles Spectra	47
References.....	51

1. What's New

This report may be subjected to editing and revisions, check www.reluis.it for updates

New elements of this version are:

- Maps of geographic positions of fault surface, accelerometric stations, soil type, PGV and PGA recorded;
- **As a function of epicentral distance and for fixed spectral ordinate, the Sabetta and Pugliese attenuation law has been compared with the values recorded at the various stations; Attenuation law has been plotted for $M=5.8$ (M_L) and $M=6.2$ (M_W);**
- **As a function of fault distance, the Sabetta and Pugliese attenuation law has been compared with the values of PGA recorded at the various stations; Attenuation law has been plotted for $M=5.8$ (M_L) and $M=6.2$ (M_W);**
- Inelastic pseudo-acceleration spectra with a constant strength reduction factor have been replaced by inelastic acceleration spectra with constant ductility;
- Specific hysteretic energy inelastic spectra for horizontal and vertical component;
- Number of equivalent cycles spectra for horizontal and vertical component;

2. Introduction

Accelerometric National Network (RAN) has made available the records of the recent earthquake with epicenter in the Abruzzo (date 6/04/09 1.32AM – UTC; Magnitude 5.8).

Signals, corrected with a linear baseline correction and with a Butterworth bandpass filter (Freq1=0.1, Freq2=25, Order 4), have been processed to get preliminary information about characteristic parameters of the records. Peak values, integral parameters and two different measures of duration have been computed for each component registered by the 57 accelerometric stations. **Corrected records and details of correction are available on the Reluis website (<http://www.reluis.it>).**

First, in Chapter 3, it shows maps with the following elements:

- Rupture surface projection (D. Cheloni, personal communication), accelerometric station codes, most damaged towns and soil classification for each accelerometric station. This classification, in accordance with Eurocode8, is provided by National Institute of Geophysics and Volcanology (INGV) and is basically obtained from national geological classification in scale 1:100000;
- Recorded values of PGV and PGA at each stations.

In order to analyze peak values, data have been processed and compared to the Attenuation law of Sabetta and Pugliese (1996) in term of peak ground acceleration (PGA), peak ground velocity (PGV) and spectral acceleration (Sa) for stiff soil. Comparisons have been made adopting magnitude equal to 5.8 and 6.2; these are M_L and M_w of studied earthquake, respectively. Because each accelerometric station has produced two records of the same signal in two horizontal directions perpendicular to each other, the horizontal record chosen is that characterized by the higher PGA. This solution will be used for also for the other results unless explicitly indicated. As a function of epicentral distance and for fixed spectral ordinate, the average attenuation law (and its standard deviation) have been compared with the points corresponding to the values recorded at the various stations.

PGA values of horizontal and vertical component has been compared also with Sabetta and Pugliese attenuation law as function of fault distance.

Signals recorded were also grouped in bins of 10 km of epicentral distance and the average spectrum of each bin was compared with the average spectrum obtained from the attenuation law for a distance equal to the average distance of the records of each bin and magnitude equal to 5.8.

Moreover *Peak Ground Acceleration* (PGA), *Peak Ground Velocity* (PGV) and *Peak Ground Displacement* (PGD) are calculated for the two horizontal direction and for the vertical one. They are reported in Tables 1, 2 3.

Arias Intensity (I_A) and *Cosenza and Manfredi Index* (I_D) are the integral parameters computed for each record. Iervolino et al. attenuation law in term of I_D have been compared with I_D values computed for horizontal component of each record.

Durations computed for each record are: *Significant Duration* (S_d) and *Bracketed Duration* (B_d), the former estimated between 5% and 95% of the I_A , the latter assuming as reference value 0.05 PGA.

The same maximum PGA based criteria previously considered for peak parameters have been assumed to choose the values of I_A , I_D , S_d and B_d to be plotted.

In Tables 4, 5 and 6 are reported integral parameters for the three directions of each record.

In sections 11 and 12 signals were grouped in bins of 10 km of epicentral distance and average constant ductility acceleration spectra of each bin are plotted for different values of the ductility factor q ($S_{d,in}/S_{d,el}$). In particular q is equal to 2, 4 and 6. Hardening ratio of inelastic system is 0.03. Plots show also mean elastic spectrum of the bin

For the same bins of records and considering a non-linear system with a constant strength reduction factor R_s ($F_{el,max}/F_y$), in sections 13 to 16, specific hysteretic energy (E_H) spectra have been computed in addition to the number of equivalent cycles (N_e) spectra for inelastic

N_e has been computed according to (1).

$$N_e = \frac{E_h}{F_y (\delta_{max} - \delta_y)} + 1 \quad (1)$$

R_s factors used are 2, 4, 6, 8 and 10.

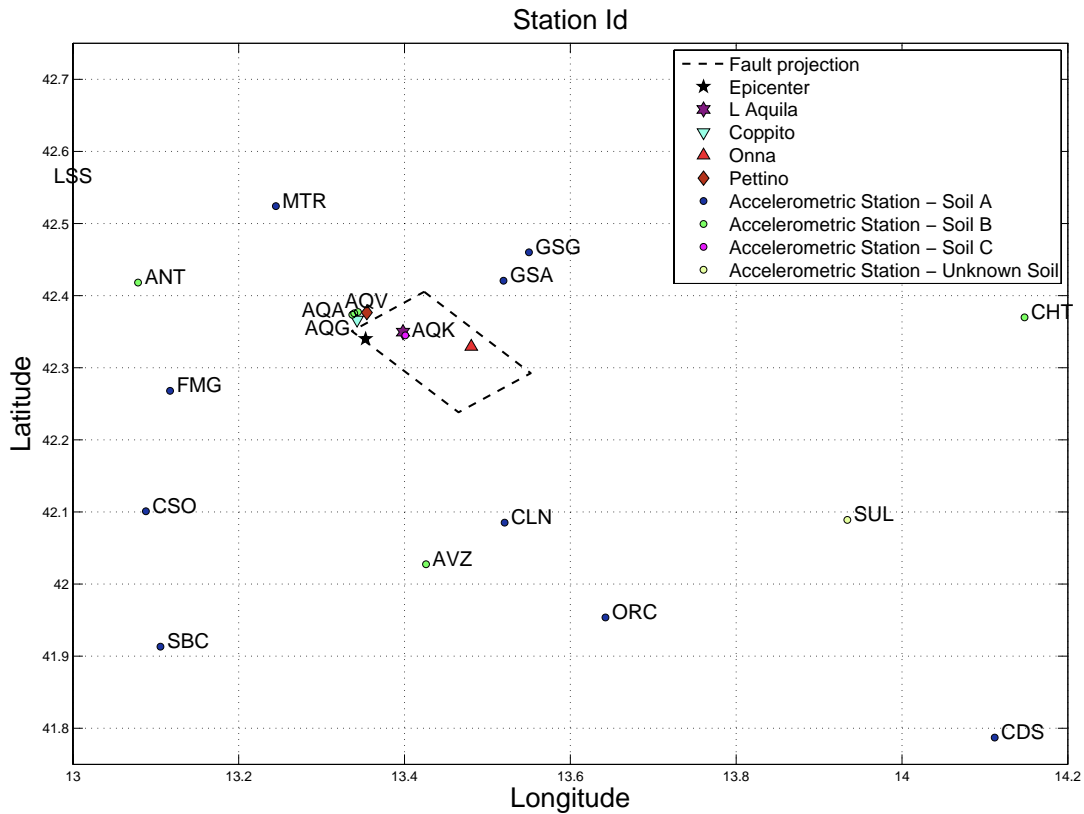
In the following are reported the results described above.

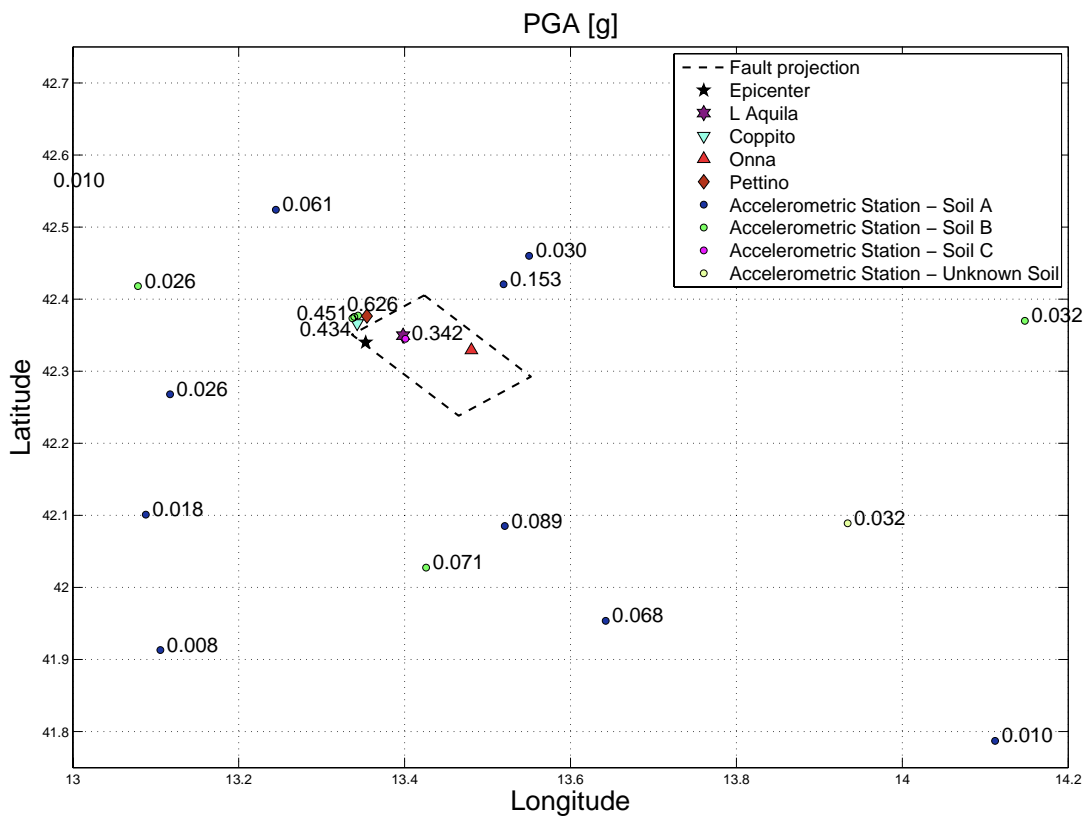
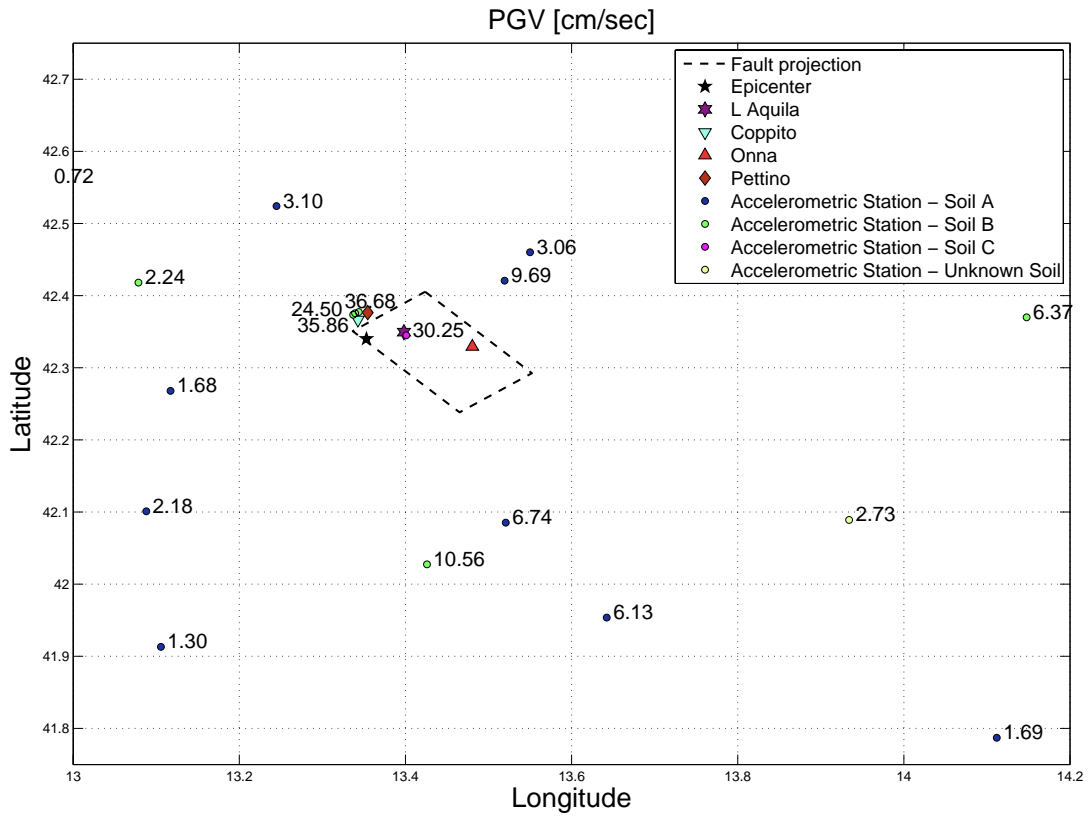
3. Geographic Information

In Table 1 is possible to relate record id to the station id, geographic coordinates of the station in addition to information of the soil type in some cases. These data are a gentle concession of DPC-S4 project (<http://esse4.mi.ingv.it/>). Soil type marked with a star (*) means that the identification has been carried out from Italian geological maps (1:100.000 scale).

Record Identifier	Station Id	Latitude	Longitude	Station Na	Altitude (m)	Soil Type
GX066	AQV	42.38	13.34	L'AQUILA - V. ATERNO - CENTRO VALLE	692	C
FA030	AQG	42.37	13.34	L'AQUILA - V. ATERNO - COLLE GRILLI	721	B*
CU104	AQA	42.38	13.34	L'AQUILA - V. ATERNO - F. ATERNO	693	C*
AM043	AQK	42.34	13.40	L'AQUILA - V. ATERNO - AQUIL PARK IN	726	B*
EF021	GSA	42.42	13.52	GRAN SASSO (LAB. INFN ASSERGI)	1,062	A*
TK003	CLN	42.09	13.52	CELANO	803	A*
BI016	AVZ	42.03	13.43	AVEZZANO	746	B*
CR008	ORC	41.95	13.64	ORTUCCHIO (NUOVA)	732	A*
BY048	MTR	42.52	13.24	MONTEREALE	975	A*
CR003	SUL	42.089	13.934	SULMONA		
EK007	CHT	42.37	14.15	CHIETI	109	B
GE1463	GSG	42.46	13.55	GRAN SASSO (LAB. INFN GALLERIA)	1,200	A*
BX007	FMG	42.27	13.12	FIAMIGNANO	1,071	A*
DF006	ANT	42.42	13.08	ANTRODOCO	568	B*
BY003	CSO	42.10	13.08	CARSOLI	653	A*
EI160	BOJ	41.48	14.47	BOJANO (NUOVA)	537	B*
BH003	CDS	41.79	14.11	CASTEL DI SANGRO	932	A*
BN048	TMO	41.989	14.975	TERMOLI		
ZC002	LSS	42.56	12.97	LEONESSA (NUOVA)	1,065	A*
HB060	SPO	42.73	12.74	SPOLETO	476	A*
BS029	CSS	41.486	13.823	CASSINO		
CU008	MMP1	42.25	12.75	MOMPEO1	474	A*
BW024	SPC	42.743	12.74	SPOLETO (CANTINA)		
BC018	ISR	41.611	14.236	ISERNIA		
AL104	PTF	41.696	14.702	PETRELLA TIFERNINA		
CQ001	SBC	41.91	13.11	SUBIACO	680	A*
CB004	ASS	43.07	12.60	ASSISI	390	A*
AY026	SPC	41.807	15.165	SERRACAPRIOLA		
IY045	SSR	41.691	15.374	S.SEVERO		
AU056	CMR	41.883	14.712	CASTELMAURO		
AY081	CTL	43.955	12.736	CATTOLICA		
BD004	SCM	41.71	14.98	S. CROCE DI MAGLIANO	676	B*

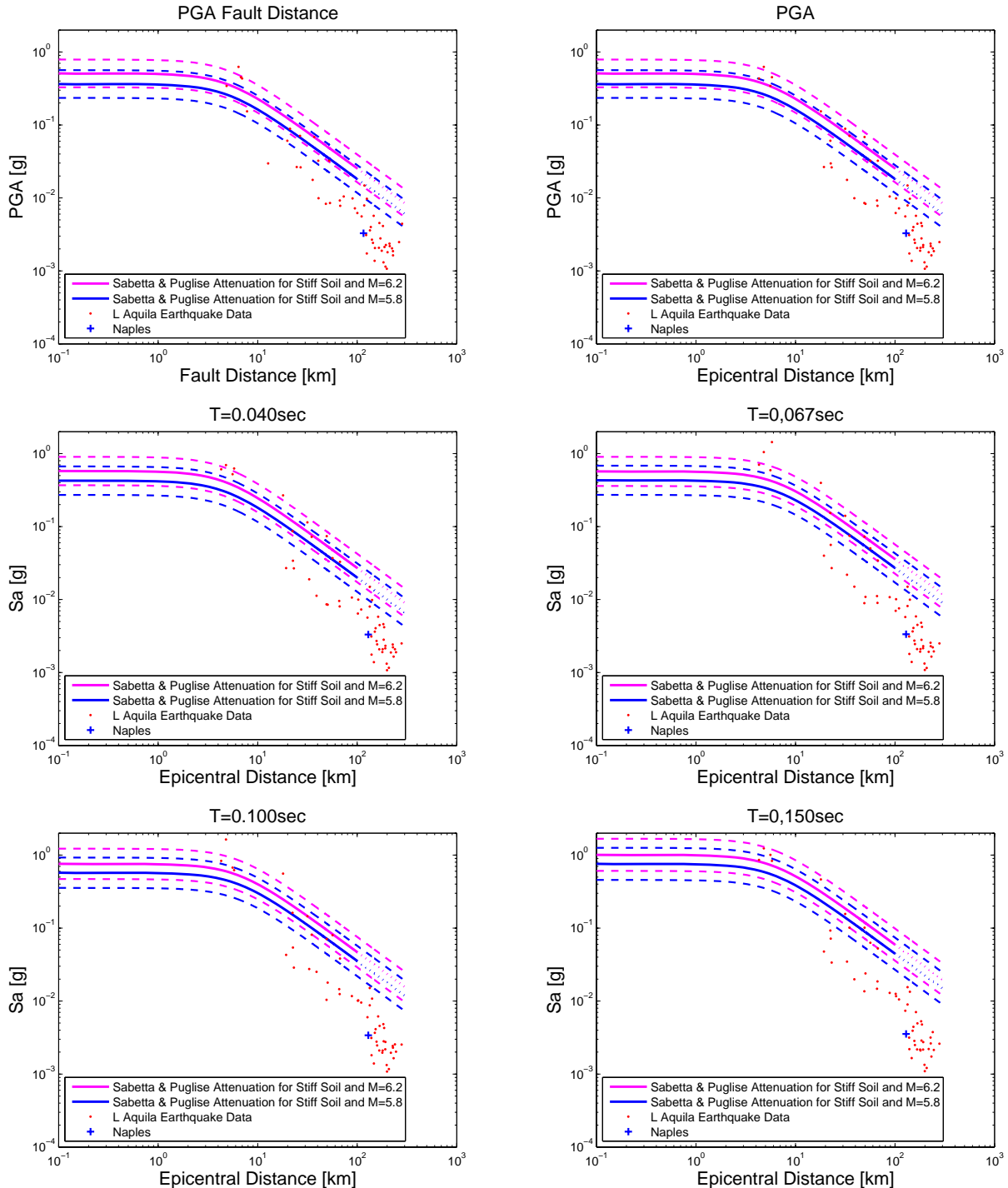
CA056	SNS	43.57	12.14	SANSEPOLCRO	371	C*
QX001	VRP	41.33	14.13	VAIRANO PATENORA	209	A*
BB007	SEP	41.63	14.88	S. ELIA A PIANISI	649	A*
GK004	CMB	41.563	14.652	CAMPOBASSO		
BM444	NAP	40.80	14.18	NAPOLI OVEST	205	C*
FO003	TLS	41.22	14.53	TELESE TERME	124	A*
AY017	RIC	41.483	14.838	RICCIA		
QI081	MNN	41.634	15.911	MANFREDONIA		
DF032	SNM	43.93	12.45	SAN MARINO	743	A*
BU012	MNG	41.704	15.958	MONTE S.ANGELO		
AR042	GNL	40.84	16.03	GENZANO DI LUCANIA		A*
DM033	VIE	41.877	16.165	VIESTE		
BX001	BNE	41.13	14.78	BENEVENTO (NUOVA)	221	B*
EC009	CAN	41.203	15.475	CANDELA		
AV122	BDT	43.71	12.19	BADIA TEDALDA	795	A*
BS035	SDG	41.709	15.733	S.GIOVANNI ROTONDO		
BQ056	CNM	41.62	15.10	CASALNUOVO MONTEROTARO (NUOVA)	462	
EB150	CER	41.26	15.91	CERIGNOLA		
AT182	FOR	44.20	12.04	FORLI' (NUOVA)	77	C
AR006	PDM	41.36	14.39	PIEDIMONTE MATESE	340	C*
BG067	STN	41.02	15.11	STURNO	684	A*
BA125	AVL	40.92	14.79	AVELLINO	423	B*
BM130	PIC	42.85	11.68	PIANCASTAGNAIO	832	B*
AO008	BBN	43.75	11.82	BIBBIENA (NUOVA)	471	A*
EH008	STL	40.54	15.64	SATRIANO DI LUCANIA	748	A*

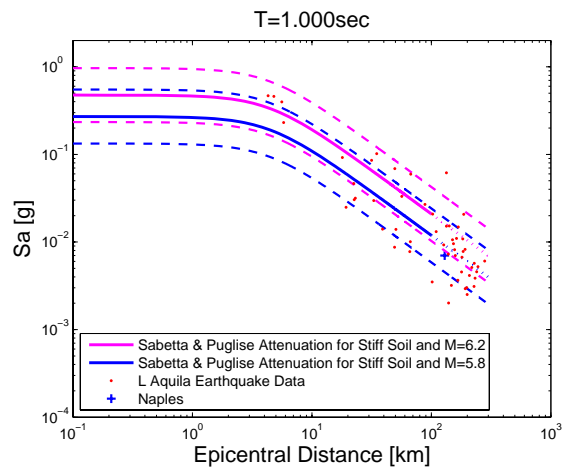
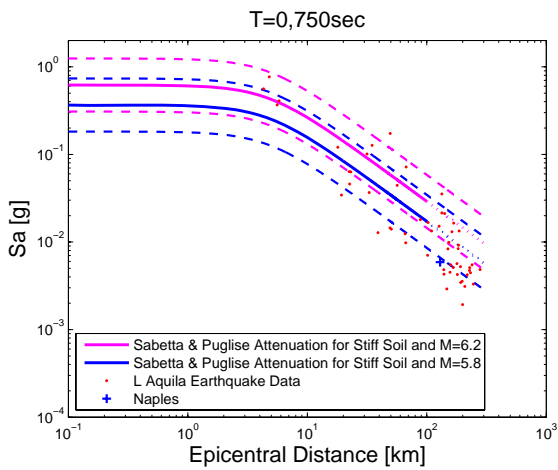
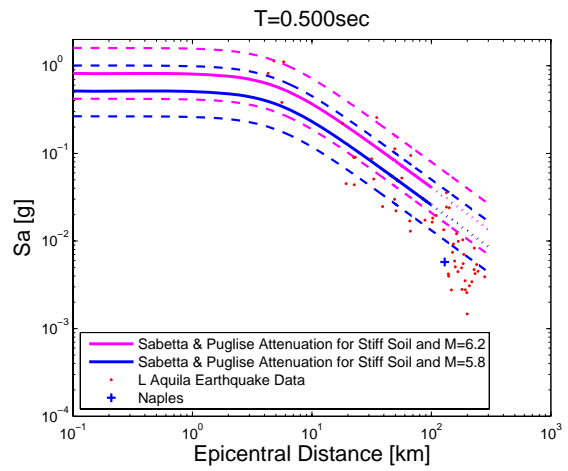
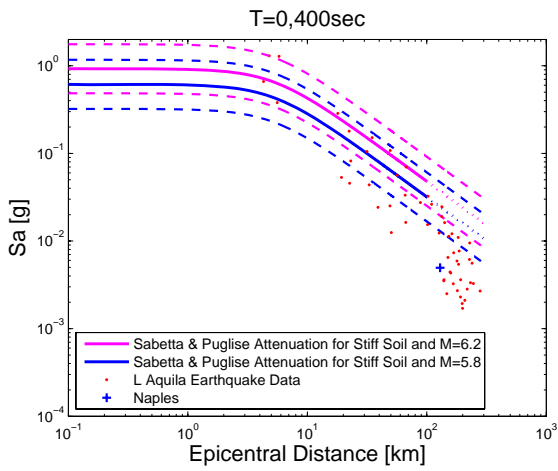
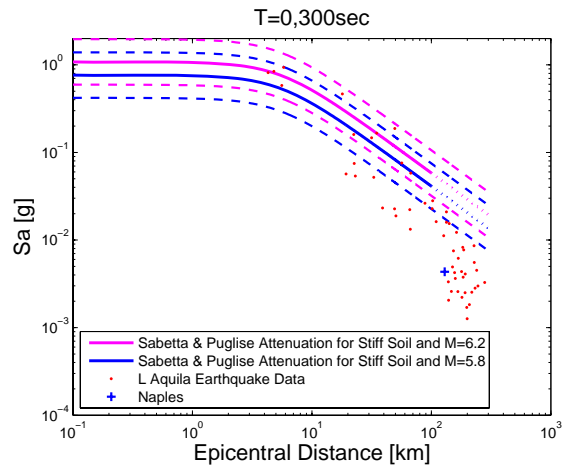
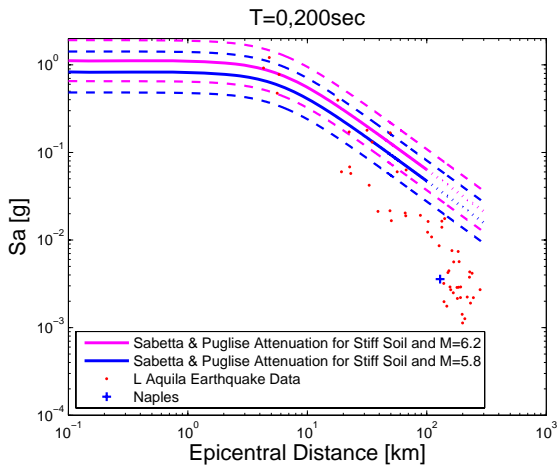


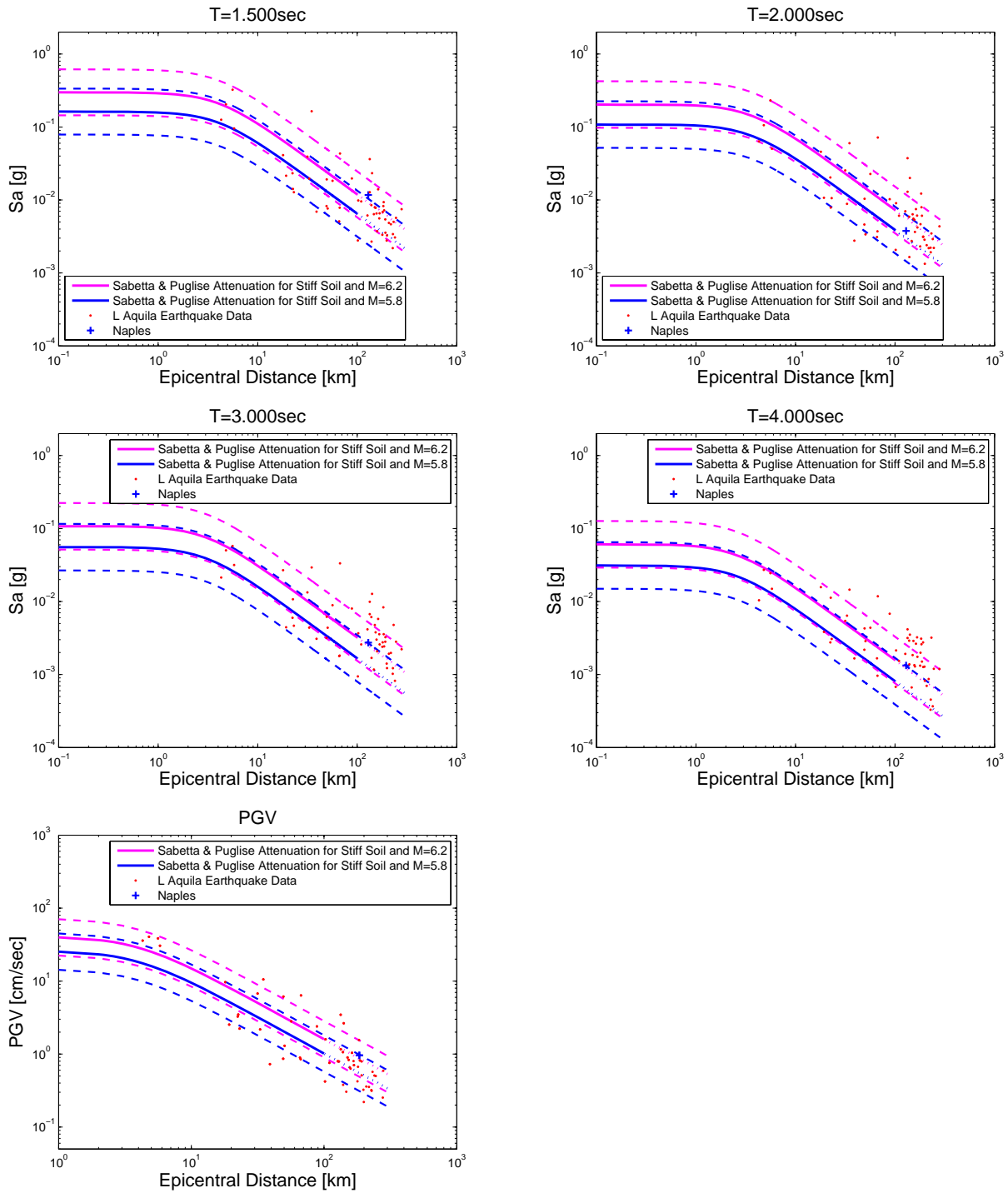


4. Horizontal Component - Plots for Spectral Periods

In this section are reported plots comparing the Attenuation law of Sabetta and Pugliese (1996) to spectral acceleration values recorded at different epicentral distance or fault distance (only for PGA).

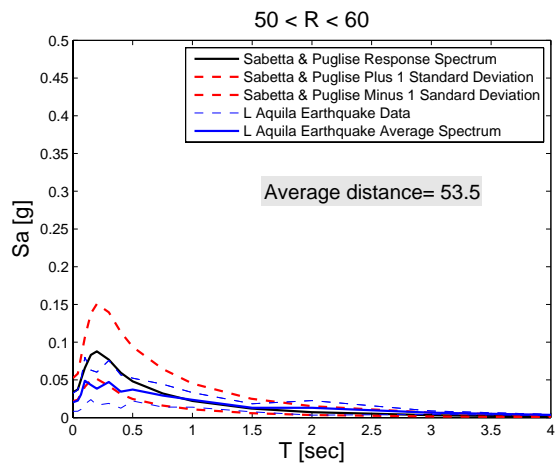
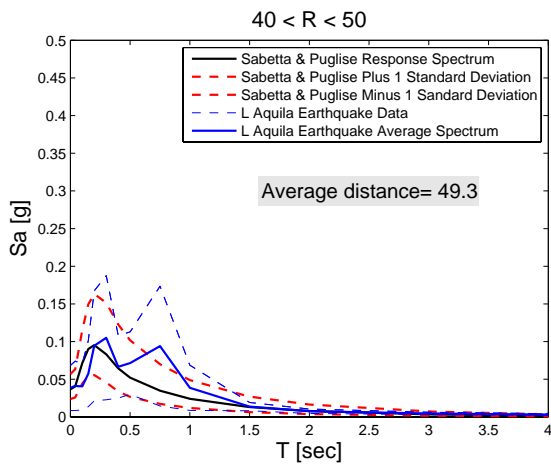
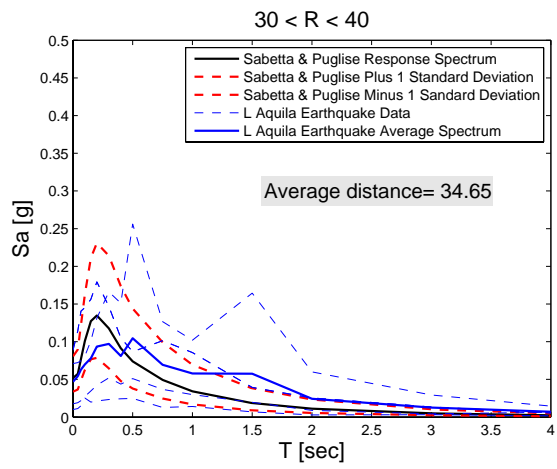
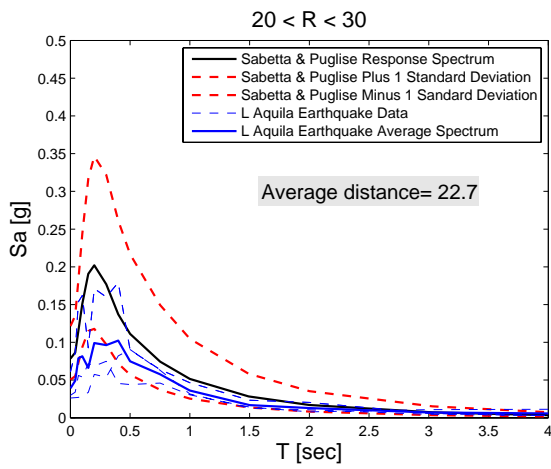
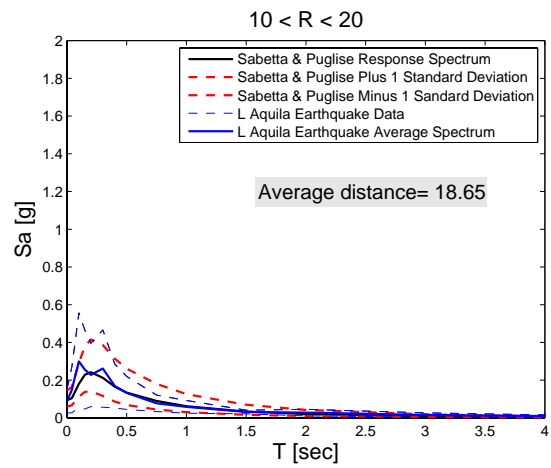
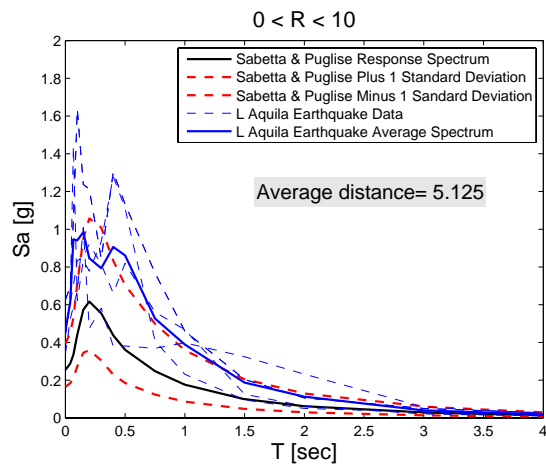


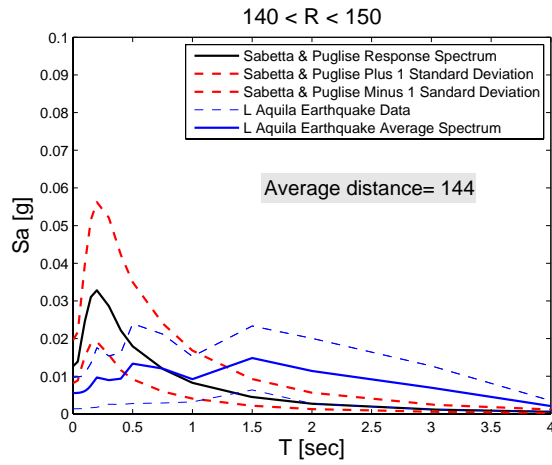
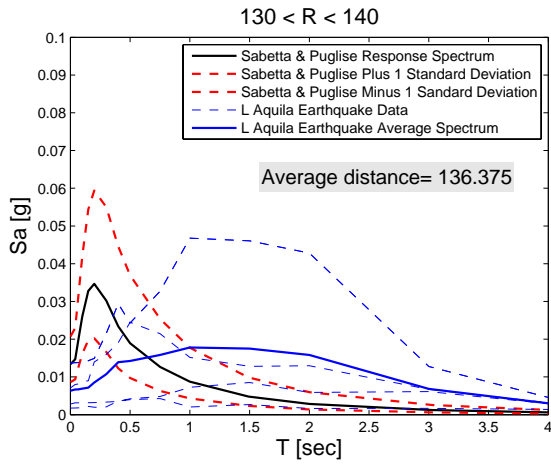
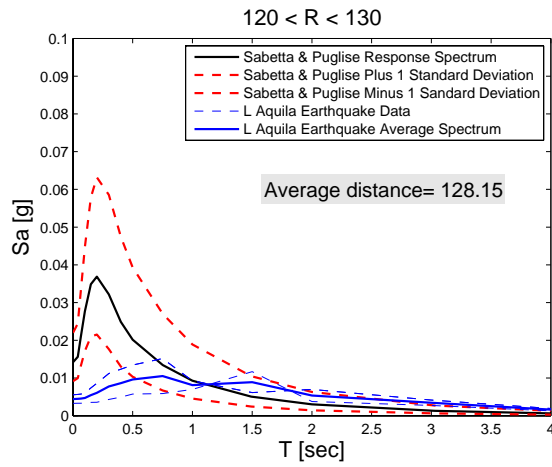
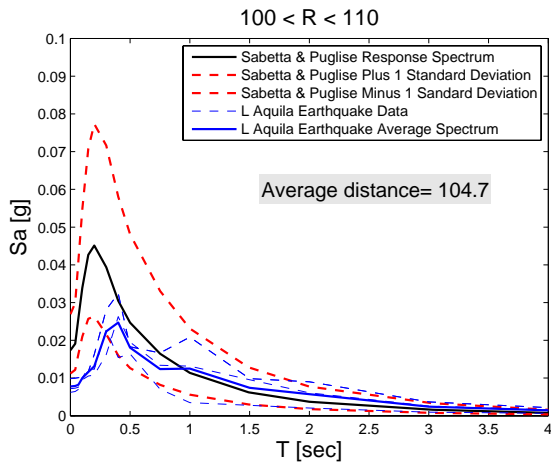
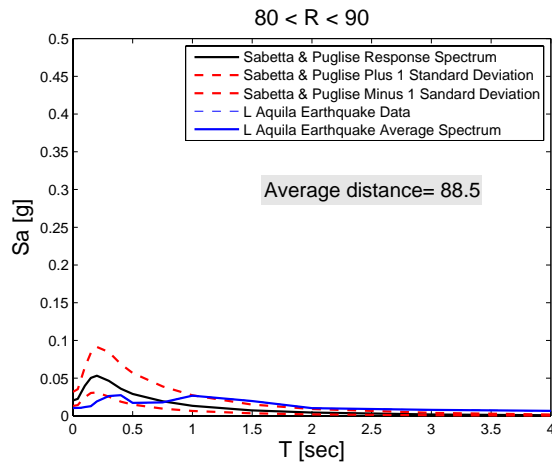
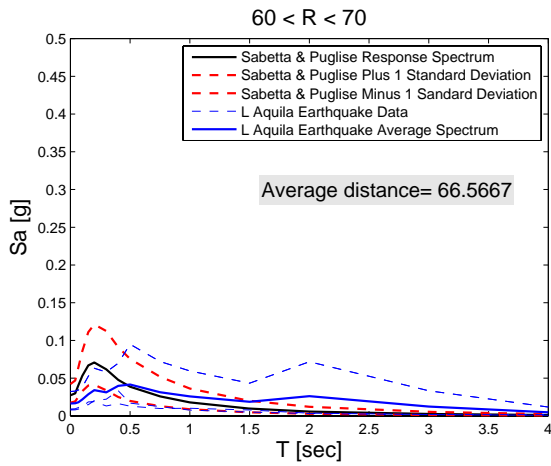


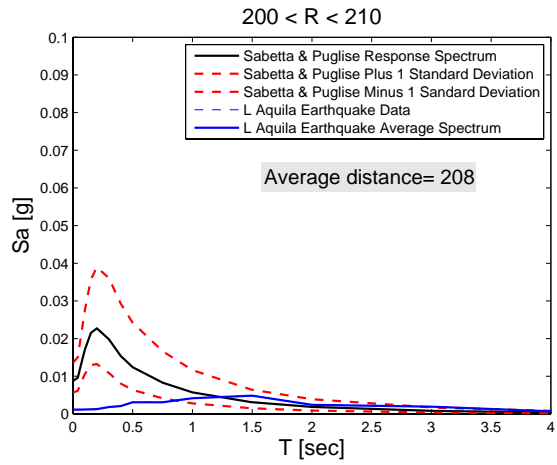
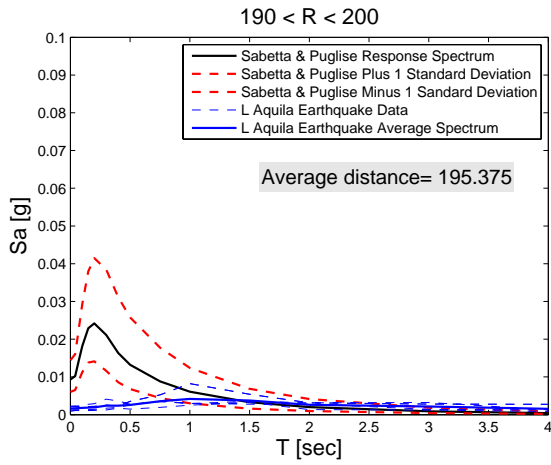
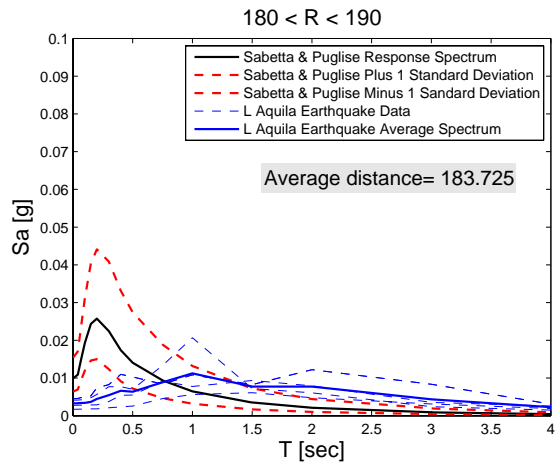
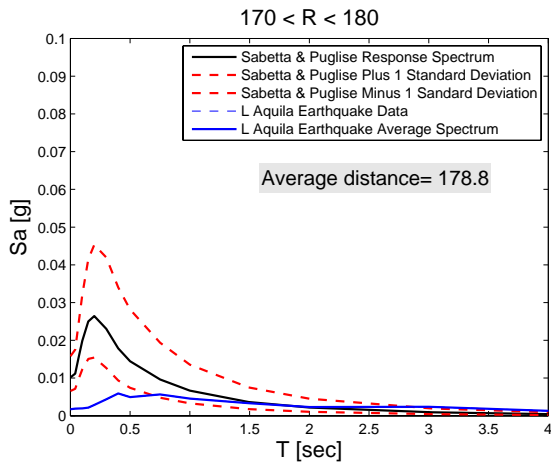
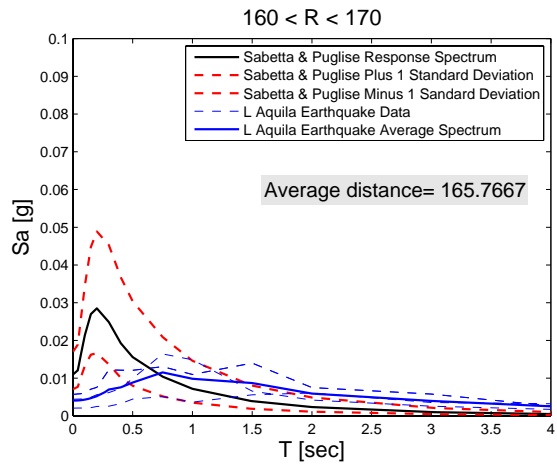
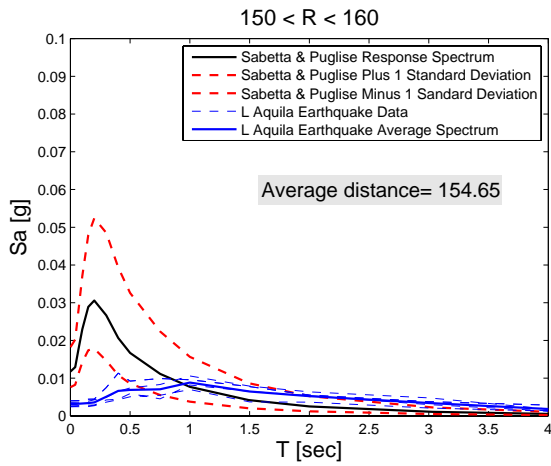


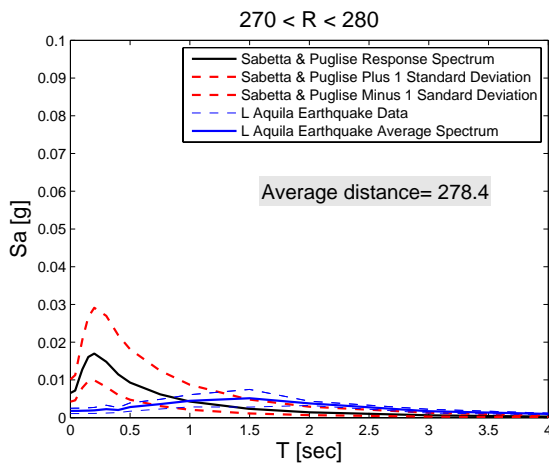
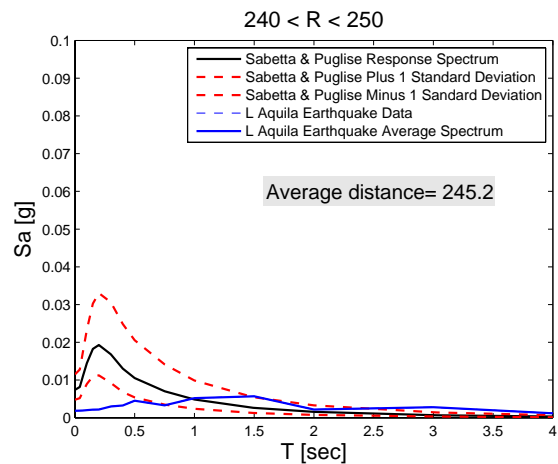
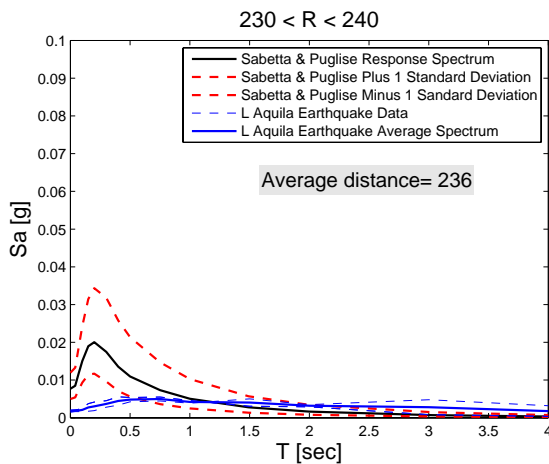
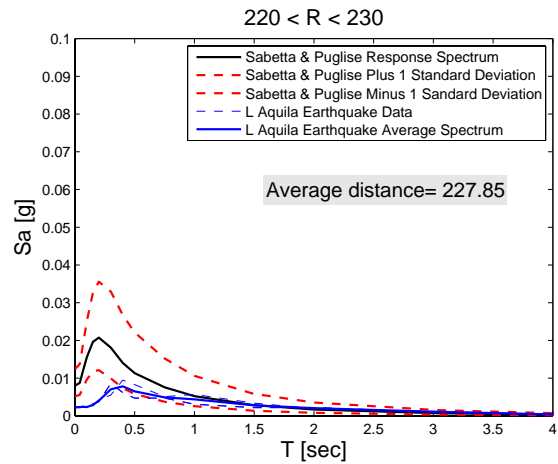
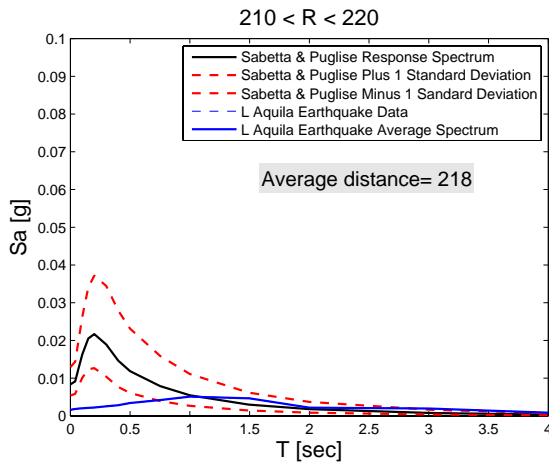
5. Horizontal Component - Plots for Distance Bins

Signals recorded were grouped in bins of 10 km of epicentral distance (R) and the average pseudo-acceleration spectrum of each bin was compared with the average spectrum obtained from the attenuation law for a distance equal to the average distance of the records of each bin and magnitude equal to 5.8. Plots are reported below.



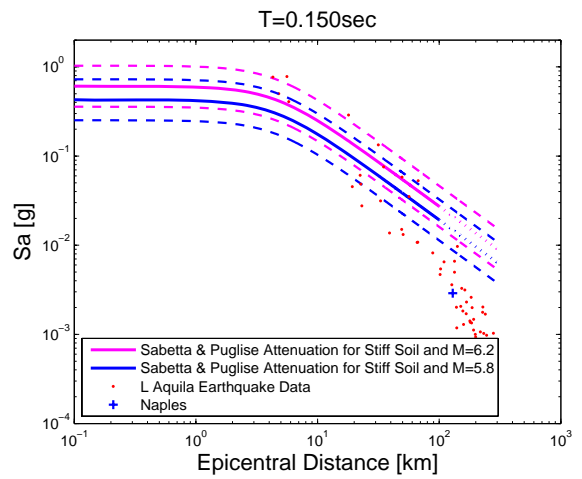
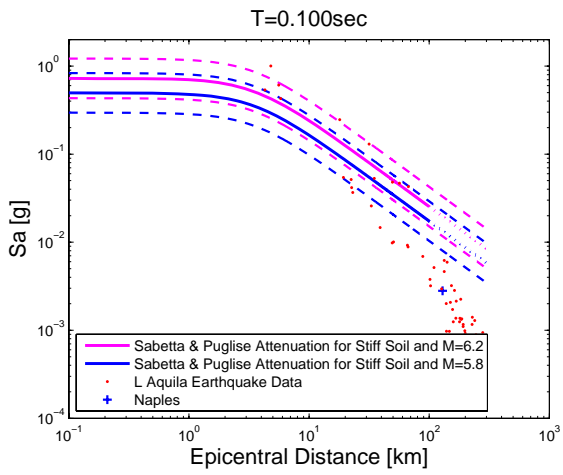
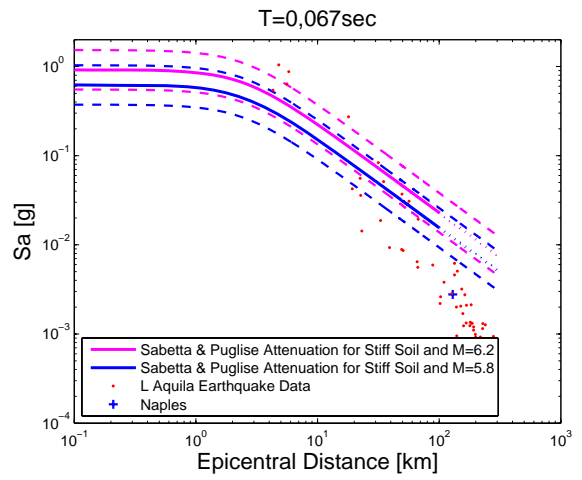
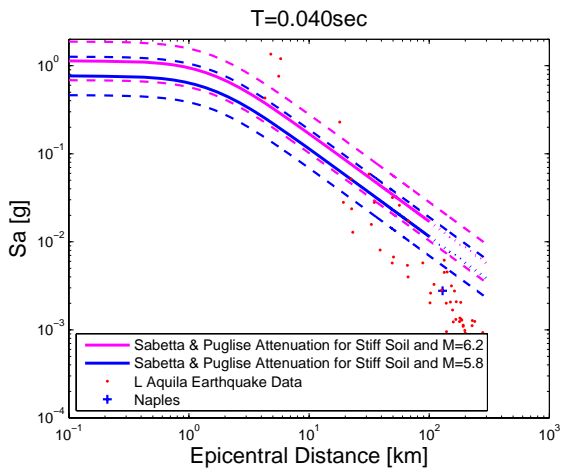
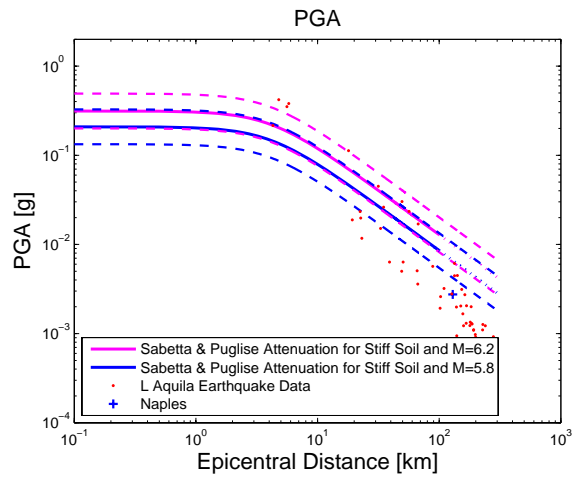
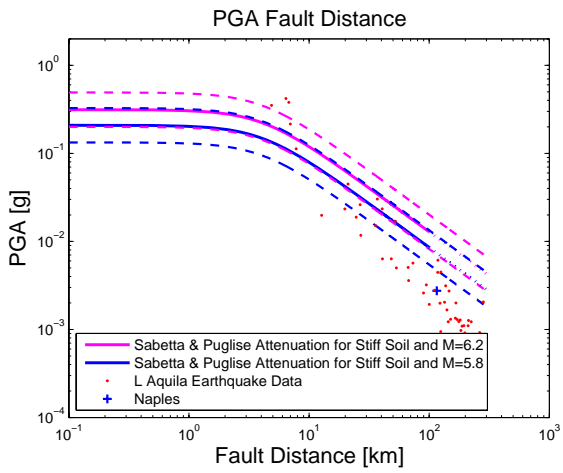


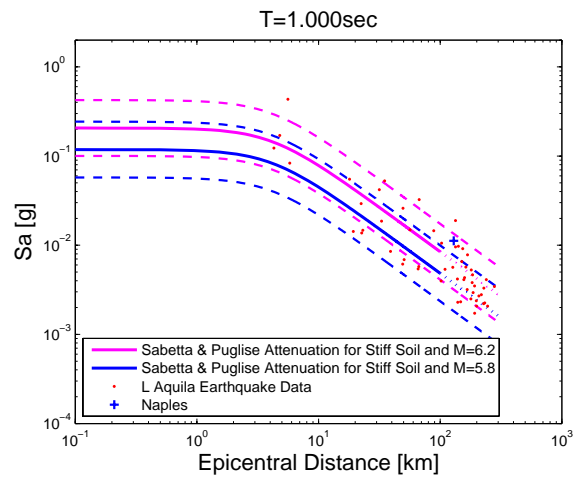
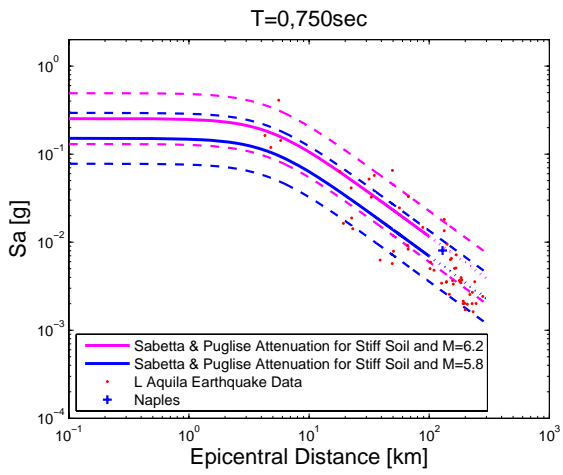
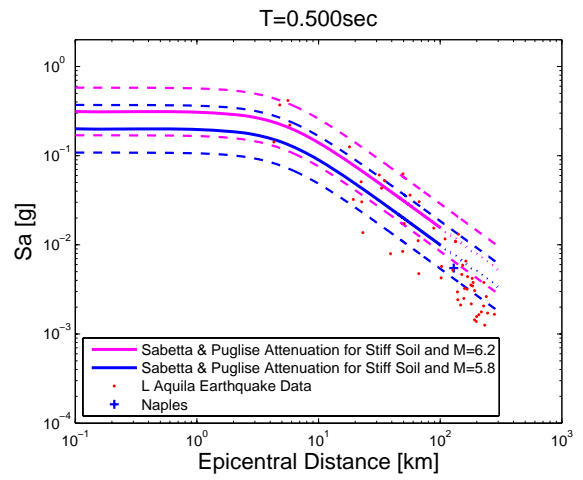
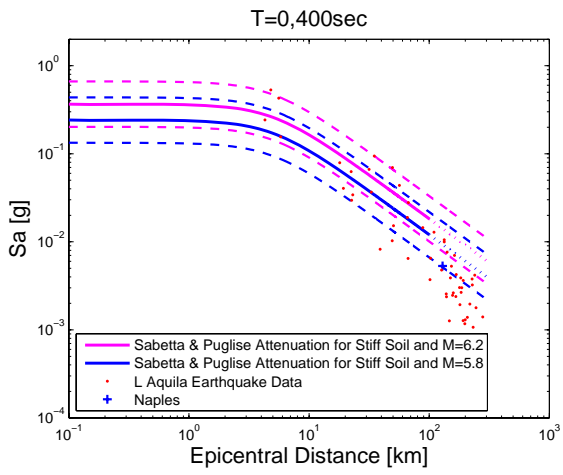
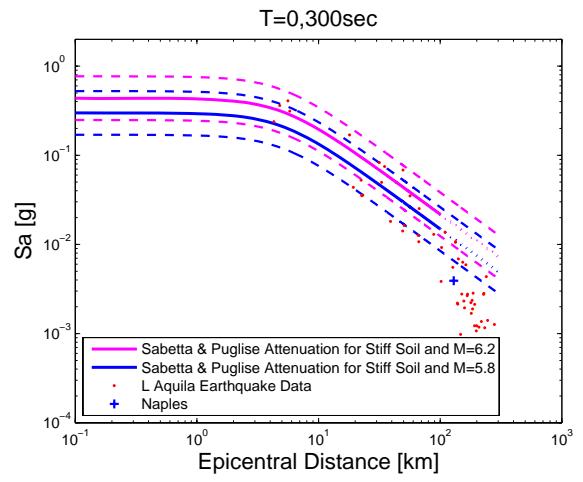
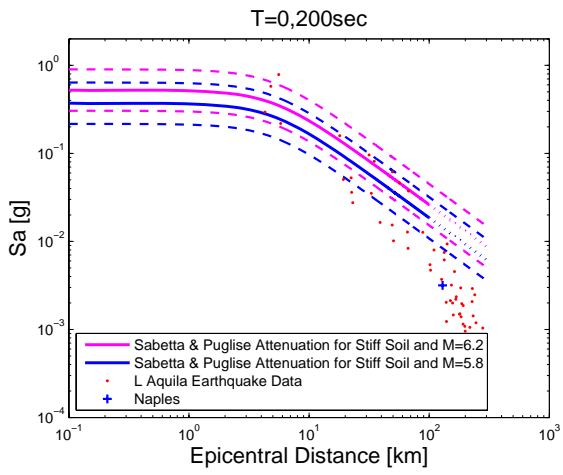


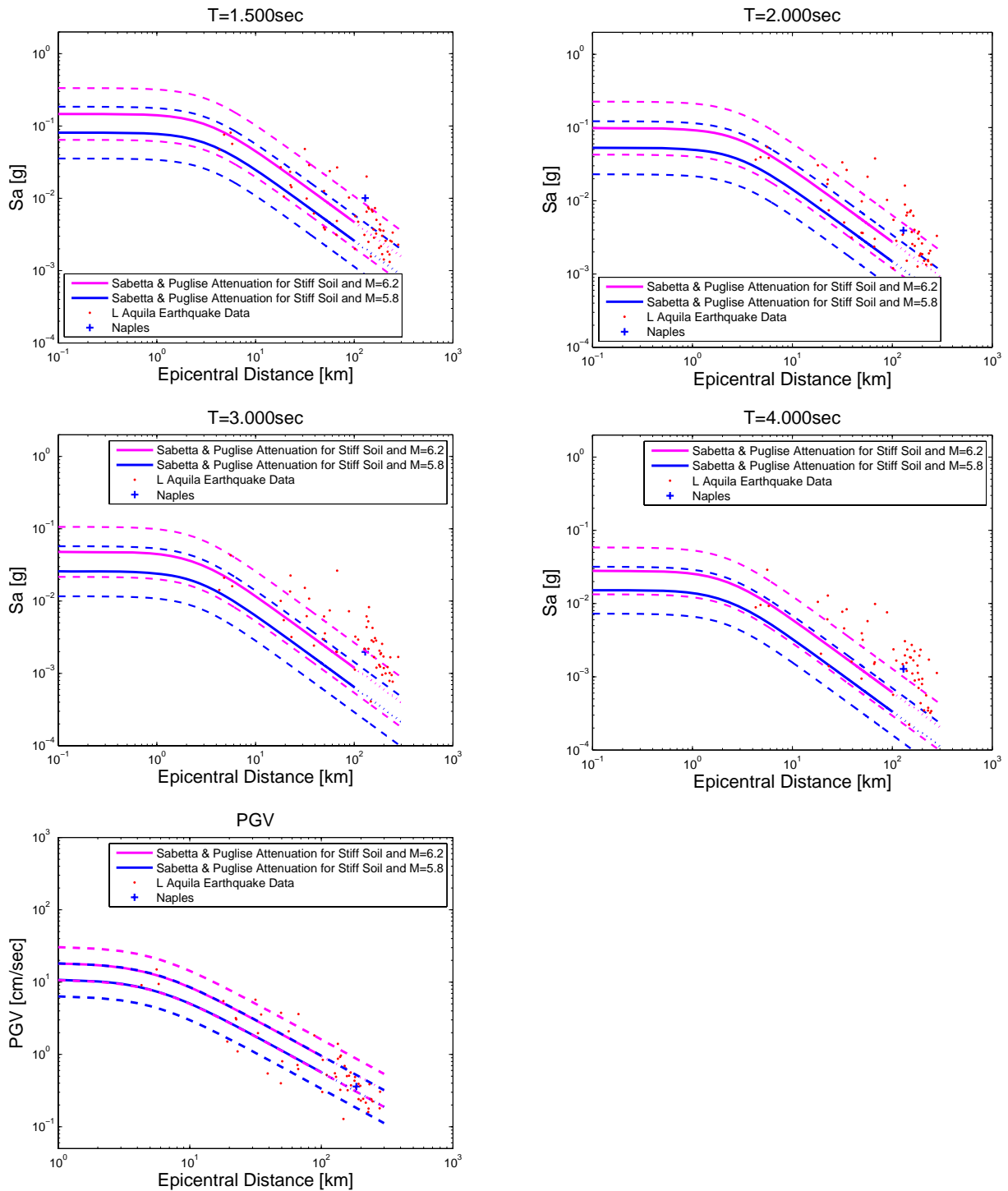


6. Vertical Component - Plots for Spectral Periods

In this section are reported plots comparing the Attenuation law of Sabetta and Pugliese (1996) to spectral acceleration values recorded at different epicentral distance or fault distance (only for PGA).

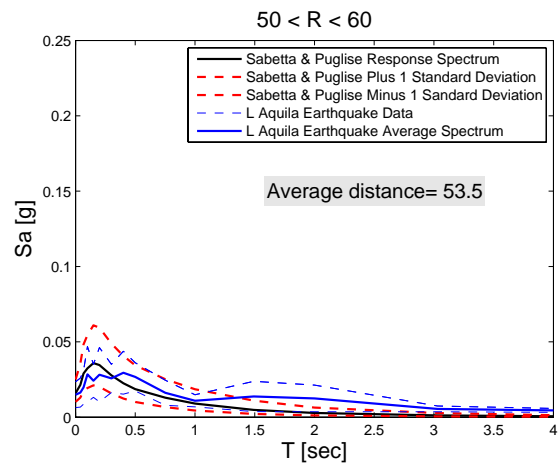
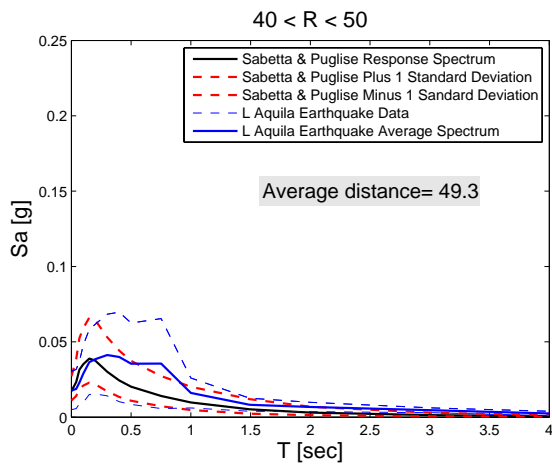
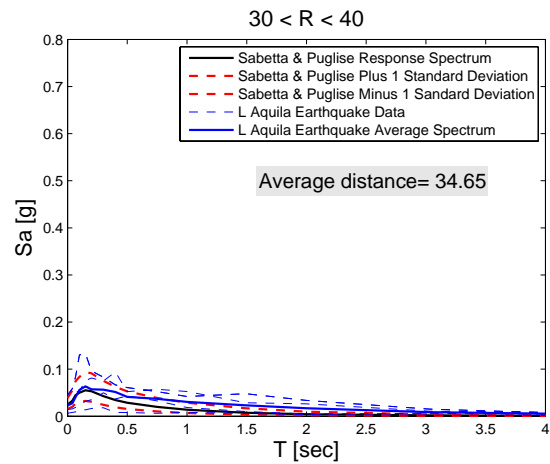
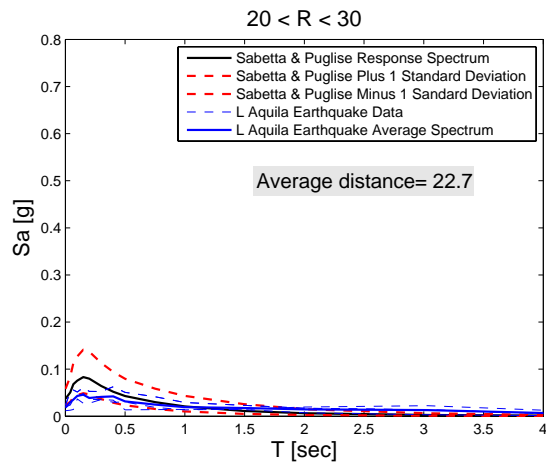
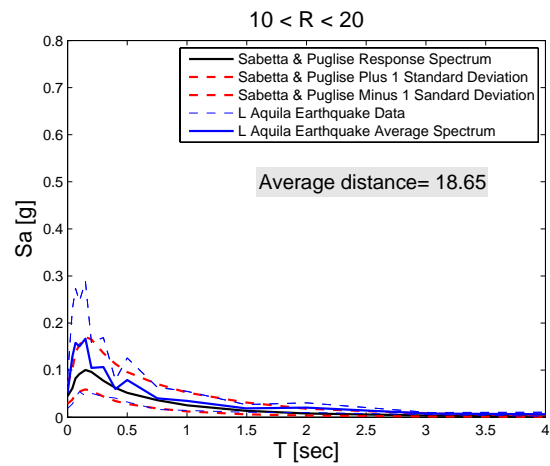
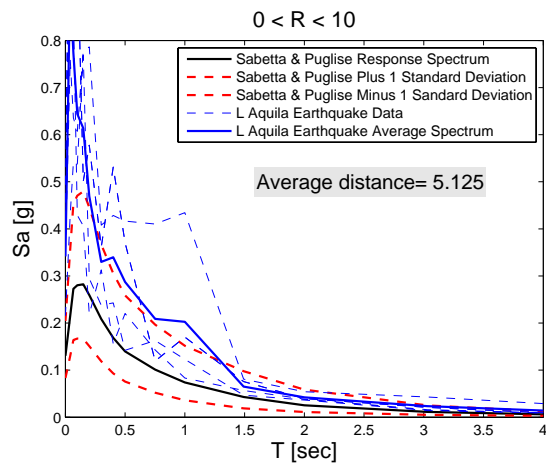


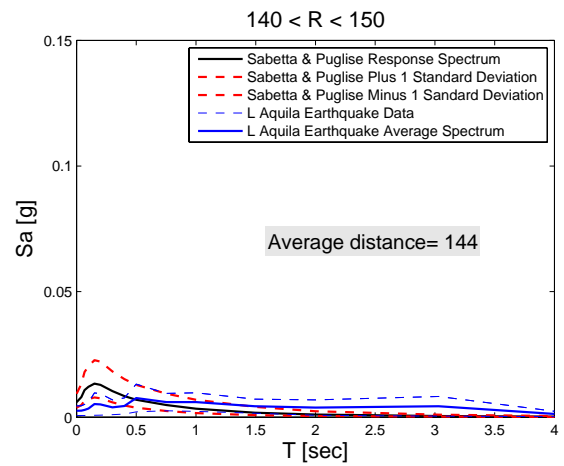
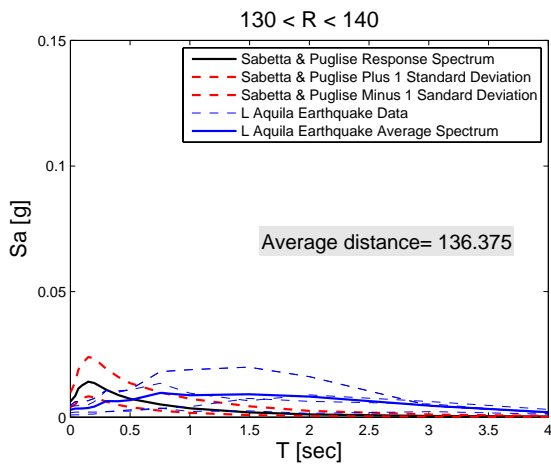
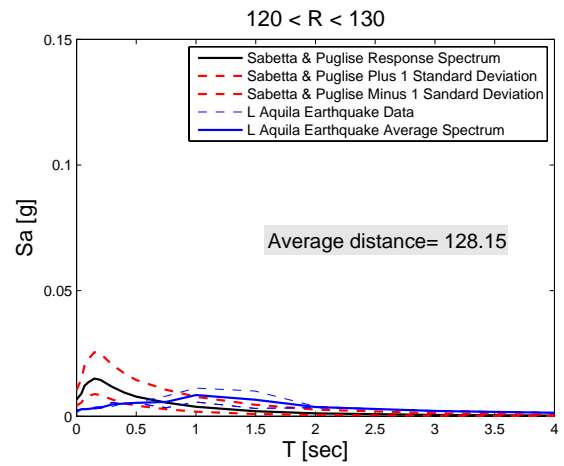
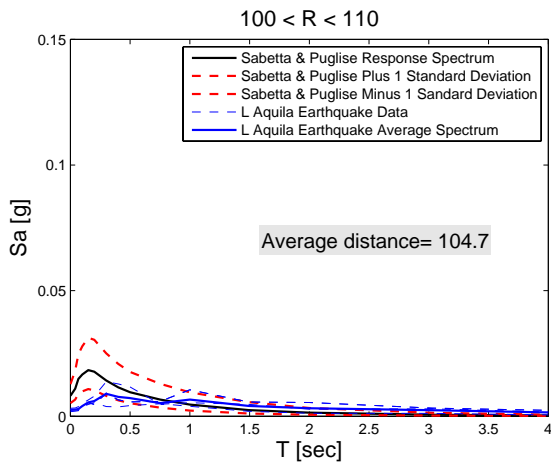
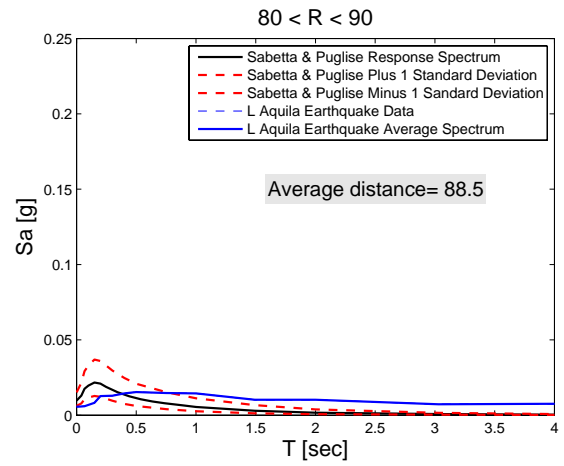
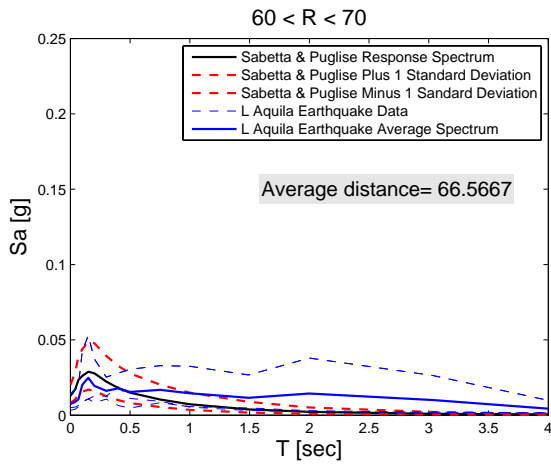


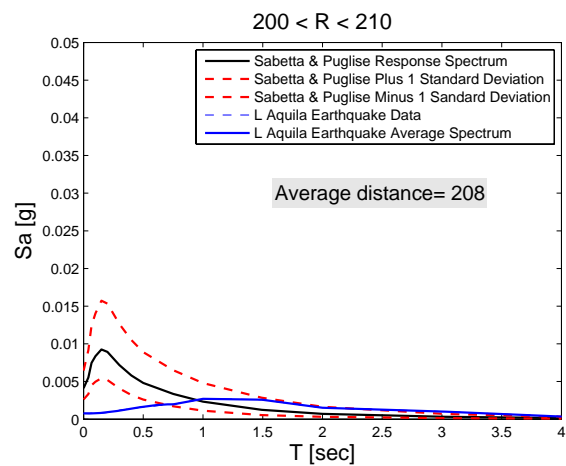
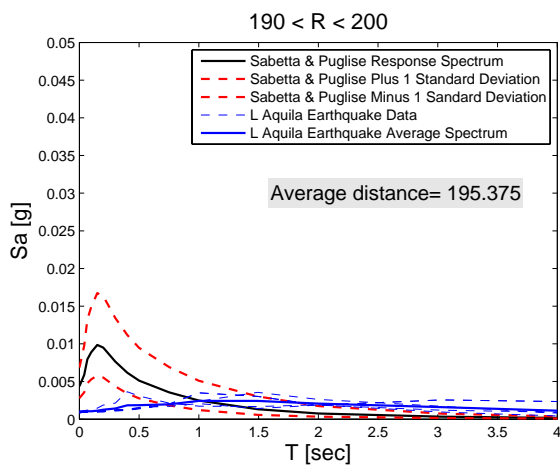
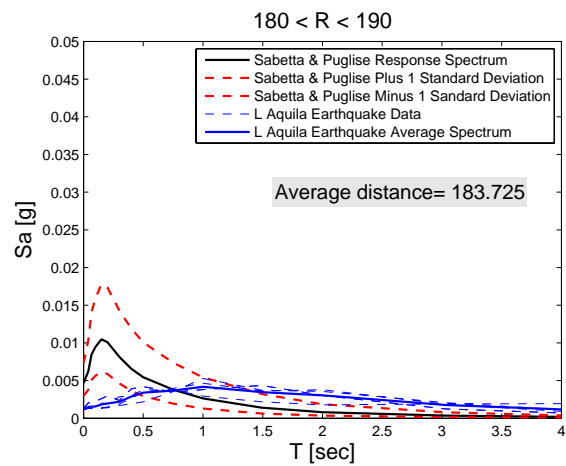
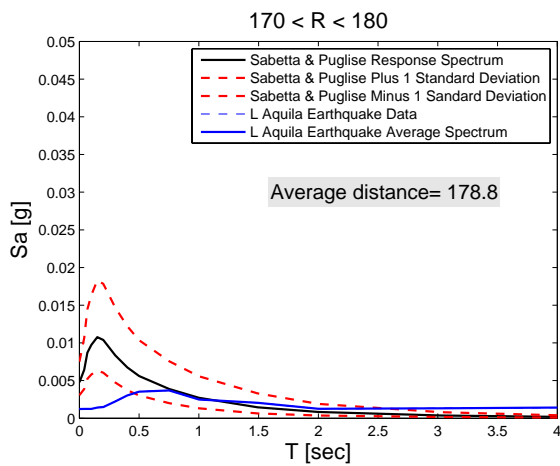
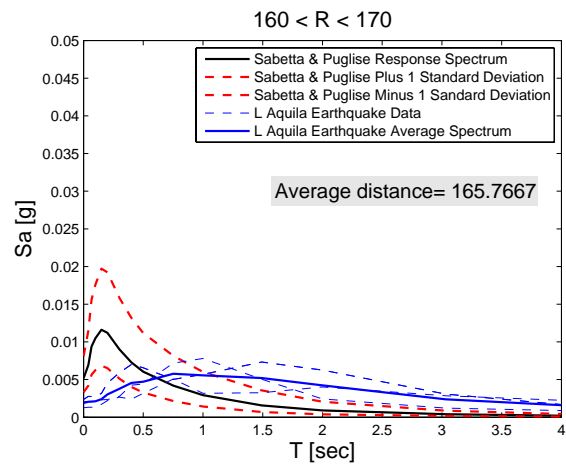
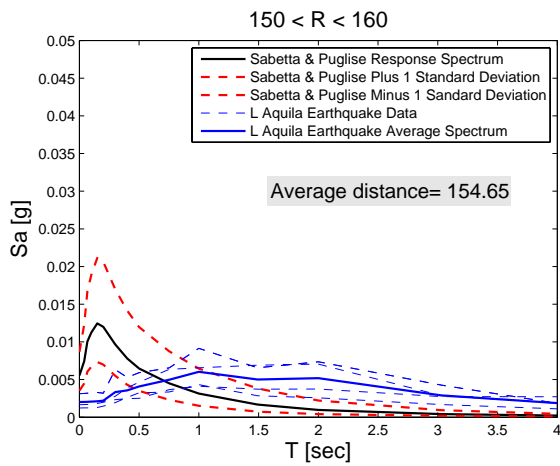


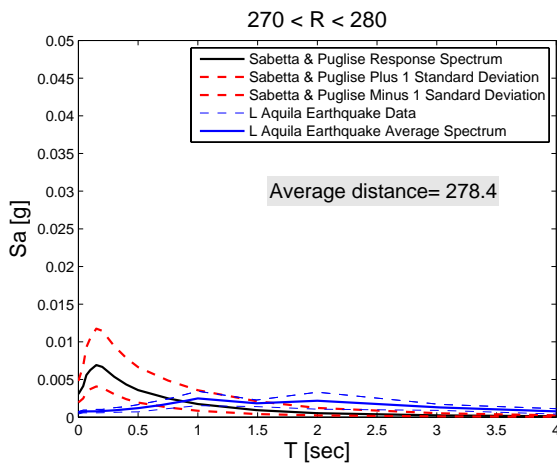
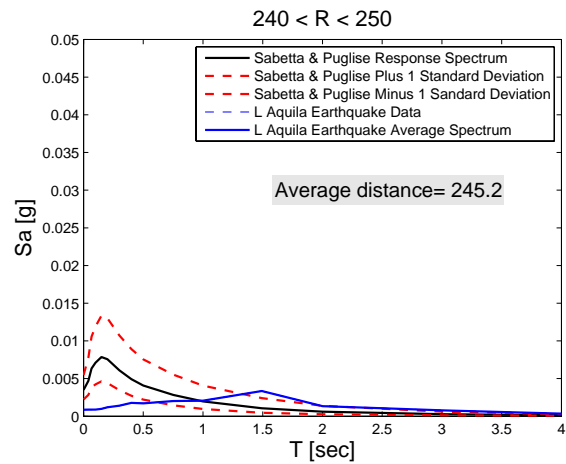
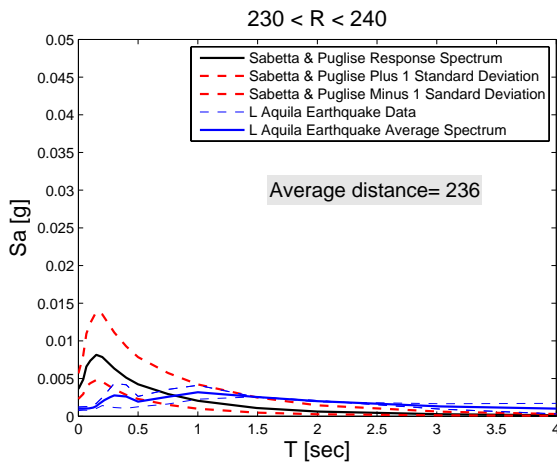
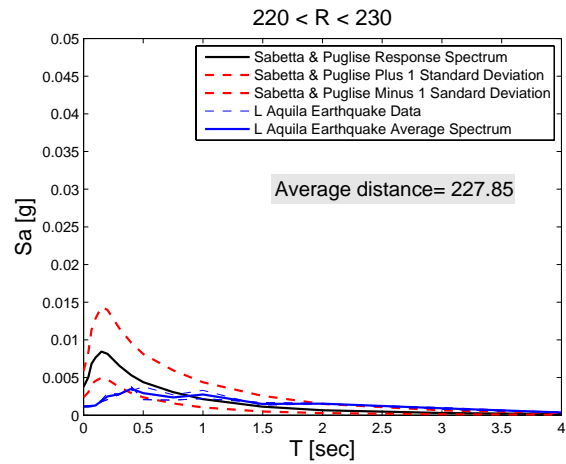
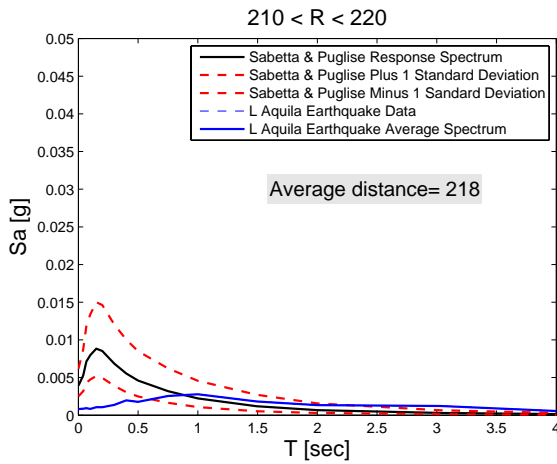
7. Vertical Component - Plots for Distance Bins

Signals recorded were grouped in bins of 10 km of epicentral distance (R) and the average pseudo-acceleration spectrum of each bin was compared with the average spectrum obtained from the attenuation law for a distance equal to the average distance of the records of each bin and magnitude equal to 5.8. Plots are reported below.









8. Peak Values Tables

Tables show peak values for all record in X direction (Table 1), Y direction (Table 2) and Z direction (Table 3).

Table 1 – Peak Values for Direction X

Record Identifier	PGA	PGV	PGD	Epicentral Distance
	[cm/s ²]	[cm/s]	[cm]	[km]
GX066	613.8	36.7	8.4	4.8

FA030	408.2	33.6	7.9	4.3
CU104	386.8	30.5	6.4	5.8
AM043	335.5	30.3	7.8	5.6
EF021	150.6	9.7	3.0	18
TK003	79.2	4.6	2.6	31.6
BI016	60.6	10.5	4.6	34.9
CR008	67.1	6.1	1.3	49.4
BY048	42.4	3.3	1.0	22.4
CR003	31.7	2.7	0.8	56.5
EK007	31.8	6.4	2.9	67.1
GE1463	20.1	3.5	1.6	22.6
BX007	23.7	2.5	1.2	19.3
DF006	19.6	1.9	0.4	23.1
BY003	17.3	2.2	1.0	33
EI160	13.4	3.5	1.0	133.5
BH003	9.1	2.4	0.8	88.5
BN048	9.6	2.5	0.8	140.9
ZC002	9.7	0.7	0.3	39.1
HB060	6.1	0.7	0.2	65.9
BS029	8.7	1.6	0.9	102.7
CU008	8.4	0.9	0.3	49.2
BW024	7.7	0.8	0.2	66.7
BC018	7.1	0.8	0.3	109.7
AL104	7.7	1.2	0.5	133.7
CQ001	5.4	0.9	0.6	50.5
CB004	6.1	0.4	0.1	101.7
AY026	2.9	0.7	0.3	162.4
IY045	3.9	1.1	0.4	183.4
AU056	5.5	0.8	0.3	126.9
AY081	4.0	0.7	0.3	186.6
BD004	3.2	0.8	0.5	153.2
CA056	4.3	0.7	0.2	168
QX001	3.1	0.8	0.4	129.4
BB007	3.5	0.8	0.7	150.4
GK004	2.9	1.1	0.7	138.9
BM444	2.4	0.9	0.5	184.5
FO003	2.4	0.6	0.3	158.5
AY017	2.2	0.7	0.4	156.5
QI081	2.3	0.2	0.1	227.3
DF032	2.1	0.8	0.5	191.8
BU012	2.1	0.3	0.1	228.4
AR042	2.0	0.5	0.3	279.4
DM033	2.0	0.3	0.1	239.7
BX001	1.7	0.5	0.3	180.4
EC009	1.8	0.4	0.2	218
AV122	1.8	0.3	0.1	178.8
BS035	1.3	0.2	0.1	192
BQ056	2.0	0.8	0.6	166.9
EB150	1.8	0.5	0.2	245.2
AT182	1.6	0.6	0.4	232.3
AR006	1.7	0.3	0.2	139.4
BG067	1.1	0.4	0.2	208
BA125	1.0	0.3	0.2	198.1

BM130	0.9	0.2	0.1	147.1
AO008	0.7	0.2	0.2	199.6
EH008	1.1	0.3	0.1	277.4

Table 2 – Peak Values for Direction Y

Record Identifier	PGA	PGV	PGD	Epicentral Distance
	[cm/s ²]	[cm/s]	[cm]	[km]
GX066	586.2	40.5	4.1	4.8
FA030	426.1	35.9	3.9	4.3
CU104	442.0	24.5	3.9	5.8
AM043	333.6	38.5	11.8	5.6
EF021	146.6	7.4	2.2	18
TK003	87.1	6.7	1.9	31.6
BI016	69.6	10.6	4.4	34.9
CR008	39.9	3.7	0.9	49.4
BY048	59.6	3.1	0.7	22.4
CR003	25.9	2.8	1.1	56.5
EK007	29.9	5.4	2.6	67.1
GE1463	29.2	3.1	1.8	22.6
BX007	26.0	1.7	0.6	19.3
DF006	25.8	2.2	0.5	23.1
BY003	17.1	1.4	0.6	33
EI160	14.5	3.0	0.8	133.5
BH003	10.3	1.7	1.0	88.5
BN048	8.7	2.6	1.2	140.9
ZC002	7.6	0.7	0.2	39.1
HB060	9.1	0.9	0.3	65.9
BS029	9.7	1.4	0.6	102.7
CU008	6.3	0.6	0.4	49.2
BW024	5.7	0.8	0.2	66.7
BC018	5.9	0.7	0.3	109.7
AL104	6.7	1.0	0.6	133.7
CQ001	8.1	1.3	0.7	50.5
CB004	3.3	0.4	0.2	101.7
AY026	5.6	1.0	0.4	162.4
IY045	4.4	1.6	0.7	183.4
AU056	4.0	0.7	0.5	126.9
AY081	3.3	0.8	0.3	186.6
BD004	3.9	0.8	0.5	153.2
CA056	3.4	0.5	0.2	168
QX001	3.2	0.8	0.3	129.4
BB007	3.3	0.9	0.7	150.4
GK004	3.0	0.9	0.6	138.9
BM444	2.7	1.0	0.6	184.5
FO003	2.0	0.6	0.3	158.5
AY017	2.6	0.6	0.4	156.5
QI081	1.3	0.3	0.2	227.3
DF032	1.8	0.7	0.6	191.8
BU012	2.1	0.3	0.2	228.4
AR042	2.4	0.6	0.2	279.4
DM033	1.9	0.5	0.2	239.7
BX001	2.0	0.7	0.4	180.4

EC009	1.4	0.3	0.2	218
AV122	1.9	0.4	0.2	178.8
BS035	2.2	0.5	0.3	192
BQ056	2.0	0.8	0.5	166.9
EB150	1.2	0.3	0.2	245.2
AT182	1.4	0.5	0.4	232.3
AR006	1.3	0.4	0.2	139.4
BG067	1.0	0.3	0.2	208
BA125	1.3	0.3	0.4	198.1
BM130	1.3	0.3	0.1	147.1
AO008	1.0	0.2	0.1	199.6
EH008	0.8	0.2	0.1	277.4

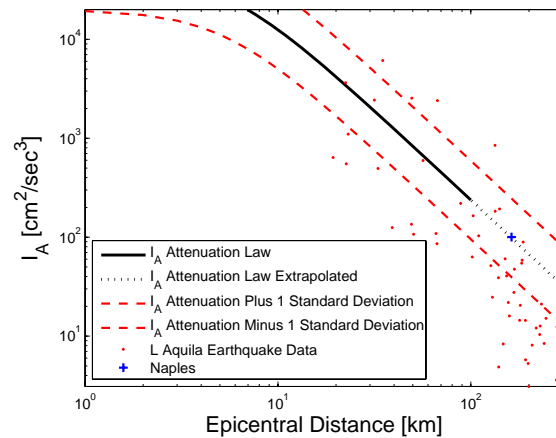
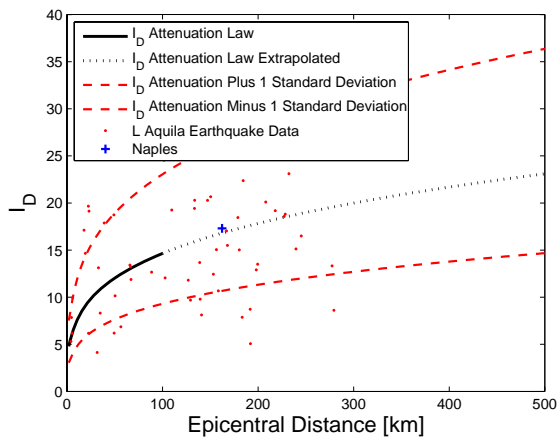
Table 3 – Peak Values for Direction Z

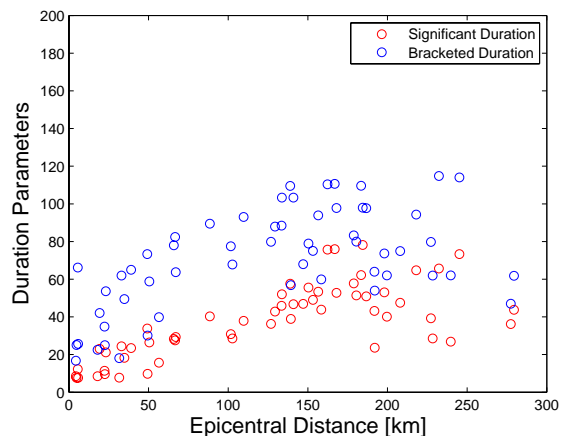
Record Identifier	PGA	PGV	PGD	Epicentral Distance
	[cm/s ²]	[cm/s]	[cm]	[km]
GX066	411.7	13.4	2.5	4.8
FA030	211.4	9.1	1.9	4.3
CU104	373.2	9.4	1.9	5.8
AM043	343.8	15.0	4.9	5.6
EF021	110.3	5.5	1.5	18
TK003	44.1	5.7	1.9	31.6
BI016	25.7	3.6	1.3	34.9
CR008	29.7	3.8	0.6	49.4
BY048	22.9	3.2	0.8	22.4
CR003	23.0	2.1	1.0	56.5
EK007	16.7	3.6	1.7	67.1
GE1463	19.4	3.0	1.8	22.6
BX007	18.5	1.5	0.4	19.3
DF006	11.5	1.1	0.2	23.1
BY003	14.8	2.0	0.7	33
EI160	6.0	1.4	0.5	133.5
BH003	5.6	1.8	0.9	88.5
BN048	4.4	1.0	0.4	140.9
ZC002	6.2	0.5	0.3	39.1
HB060	5.0	0.7	0.3	65.9
BS029	2.5	0.8	0.6	102.7
CU008	4.9	0.4	0.2	49.2
BW024	3.5	0.6	0.2	66.7
BC018	3.1	0.5	0.3	109.7
AL104	4.4	0.9	0.4	133.7
CQ001	6.2	0.8	0.6	50.5
CB004	1.9	0.3	0.1	101.7
AY026	2.7	0.5	0.2	162.4
IY045	2.0	0.3	0.1	183.4
AU056	2.7	0.5	0.3	126.9
AY081	1.3	0.4	0.2	186.6
BD004	3.1	0.6	0.2	153.2
CA056	2.0	0.4	0.2	168
QX001	2.7	0.5	0.3	129.4
BB007	2.0	0.7	0.6	150.4
GK004	2.0	0.9	0.5	138.9

BM444	1.3	0.4	0.3	184.5
FO003	1.2	0.3	0.3	158.5
AY017	1.6	0.5	0.4	156.5
QI081	1.1	0.2	0.1	227.3
DF032	1.1	0.4	0.2	191.8
BU012	1.2	0.2	0.1	228.4
AR042	0.9	0.3	0.1	279.4
DM033	1.2	0.2	0.1	239.7
BX001	1.3	0.5	0.3	180.4
EC009	0.8	0.2	0.1	218
AV122	1.2	0.4	0.2	178.8
BS035	1.1	0.2	0.1	192
BQ056	1.3	0.6	0.4	166.9
EB150	0.9	0.2	0.1	245.2
AT182	0.8	0.4	0.2	232.3
AR006	0.9	0.3	0.2	139.4
BG067	0.8	0.2	0.1	208
BA125	1.0	0.4	0.3	198.1
BM130	0.7	0.1	0.0	147.1
AO008	0.9	0.2	0.2	199.6
EH008	0.6	0.2	0.1	277.4

9. Horizontal Component – Plots of Integral parameters (Durations)

Plots show integral parameters for the horizontal direction of higher PGA of each accelerometric station. Arias intensity attenuation is plotted for M=5.8.





10. Integral Values Tables

Tables show integral values for all record in X direction (Table 4), Y direction (Table 5) and Z direction (Table 6).

Table 4 – Integral parameters for Direction X

Record Identifier	I_A	I_D	S_d	B_d	$I_A/(\pi/2g)$	Epicentral Distance
	[cm/s]	[/]	[s]	[s]	[cm ² /s ³]	
GX066	283.0	7.8	7.6	25.1	176732.8	4.8
FA030	129.6	5.9	8.0	15.4	80950.8	4.3
CU104	158.9	8.4	7.4	67.0	99228.7	5.8
AM043	100.3	6.2	12.2	66.2	62620.4	5.6
EF021	40.0	17.1	8.4	22.5	24962.4	18
TK003	3.7	6.3	6.6	20.3	2334.5	31.6
BI016	7.8	7.7	20.9	50.5	4866.3	34.9
CR008	4.1	6.2	9.8	30.1	2546.7	49.4
BY048	3.4	15.1	15.1	40.7	2098.5	22.4
CR003	1.0	6.9	15.7	39.9	595.0	56.5
EK007	3.9	11.9	29.3	63.8	2404.8	67.1
GE1463	0.6	5.5	11.6	31.9	387.2	22.6
BX007	1.2	12.5	18.6	51.0	746.9	19.3
DF006	0.9	14.2	24.6	58.6	538.4	23.1
BY003	0.8	13.1	24.4	61.9	495.4	33
EI160	1.3	17.7	55.1	88.6	822.2	133.5
BH003	0.4	11.6	31.3	91.4	252.8	88.5
BN048	0.3	8.1	46.7	103.3	193.0	140.9
ZC002	0.2	17.9	23.5	65.0	125.0	39.1
HB060	0.1	16.3	29.2	83.9	65.3	65.9
BS029	0.2	8.4	25.9	63.4	116.2	102.7
CU008	0.2	18.7	33.7	73.3	135.2	49.2
BW024	0.1	13.2	27.5	82.5	86.0	66.7
BC018	0.2	19.3	37.9	93.0	103.1	109.7
AL104	0.3	20.3	52.0	103.3	182.9	133.7

CQ001	0.1	13.7	24.9	61.9	65.3	50.5
CB004	0.1	24.5	30.9	77.5	63.1	101.7
AY026	0.1	29.1	82.1	111.5	60.2	162.4
IY045	0.1	10.2	54.9	109.6	44.2	183.4
AU056	0.1	11.8	36.3	79.8	51.5	126.9
AY081	0.1	30.1	50.9	97.7	89.3	186.6
BD004	0.1	18.6	42.6	74.9	49.3	153.2
CA056	0.1	15.5	52.7	97.9	47.5	168
QX001	0.0	12.0	47.8	88.0	29.8	129.4
BB007	0.1	20.7	55.6	78.9	60.4	150.4
GK004	0.1	13.0	54.1	107.8	40.1	138.9
BM444	0.1	22.9	74.7	98.0	49.7	184.5
FO003	0.0	10.7	43.8	59.9	16.0	158.5
AY017	0.0	16.6	57.0	93.7	23.5	156.5
QI081	0.0	18.6	39.3	79.8	10.4	227.3
DF032	0.0	8.7	43.1	63.9	14.4	191.8
BU012	0.0	18.8	28.6	62.0	12.6	228.4
AR042	0.0	12.0	43.5	61.9	12.8	279.4
DM033	0.0	15.1	26.8	62.0	8.4	239.7
BX001	0.0	23.1	49.4	79.7	18.2	180.4
EC009	0.0	19.2	64.7	94.3	12.1	218
AV122	0.0	22.5	55.5	81.0	11.5	178.8
BS035	0.0	10.3	36.8	53.8	2.5	192
BQ056	0.0	17.0	75.9	110.6	27.6	166.9
EB150	0.0	16.5	73.4	114.0	15.1	245.2
AT182	0.0	23.1	65.7	114.8	21.1	232.3
AR006	0.0	9.8	38.9	56.9	4.9	139.4
BG067	0.0	20.1	47.5	74.9	8.1	208
BA125	0.0	18.5	55.9	73.9	6.0	198.1
BM130	0.0	29.0	54.3	68.0	4.5	147.1
AO008	0.0	15.4	43.7	61.9	2.4	199.6
EH008	0.0	13.3	36.2	46.9	3.6	277.4

Table 5 – Integral parameters for Direction Y

Record Identifier	IA	ID	Sd	Bd	IA/($\pi/2g$)	Epicentral Distance
	[cm/s]	[/]	[s]	[s]	[cm2/s3]	[km]
GX066	199.7	5.3	7.7	25.0	124699.3	4.8
FA030	129.8	5.3	8.5	16.8	81038.2	4.3
CU104	172.6	10.0	7.6	25.6	107794.1	5.8
AM043	119.8	5.8	11.3	66.3	74811.7	5.6
EF021	43.7	25.1	8.8	25.4	27268.2	18
TK003	3.9	4.1	7.7	18.1	2428.2	31.6
BI016	9.8	8.3	18.3	49.5	6105.5	34.9
CR008	2.5	10.8	13.7	42.3	1578.6	49.4
BY048	5.8	19.7	11.4	34.8	3636.1	22.4
CR003	1.0	8.6	14.7	46.1	628.0	56.5
EK007	3.2	12.6	30.4	63.5	2012.5	67.1
GE1463	0.9	6.2	9.5	25.0	551.9	22.6
BX007	1.0	14.7	23.0	42.0	640.4	19.3
DF006	1.8	19.1	21.2	53.6	1102.5	23.1
BY003	0.6	14.5	24.6	56.2	358.1	33
EI160	1.4	19.4	45.9	88.5	848.6	133.5

BH003	0.4	12.7	40.3	89.5	219.2	88.5
BN048	0.3	8.0	44.1	100.9	183.9	140.9
ZC002	0.2	17.8	29.6	74.3	99.0	39.1
HB060	0.2	13.4	28.3	78.0	109.0	65.9
BS029	0.3	12.1	28.5	67.8	164.4	102.7
CU008	0.1	22.2	35.2	82.1	85.6	49.2
BW024	0.1	16.7	31.1	80.0	73.9	66.7
BC018	0.2	24.3	37.3	87.0	102.1	109.7
AL104	0.3	24.0	63.5	107.2	167.7	133.7
CQ001	0.2	10.1	26.4	58.8	107.0	50.5
CB004	0.0	24.2	39.3	90.6	29.8	101.7
AY026	0.2	17.3	75.7	110.3	100.2	162.4
IY045	0.1	7.9	62.2	109.6	54.6	183.4
AU056	0.1	14.9	40.8	81.7	40.2	126.9
AY081	0.1	26.2	56.3	99.7	71.4	186.6
BD004	0.1	12.4	49.0	75.0	40.6	153.2
CA056	0.1	23.0	55.3	97.1	40.9	168
QX001	0.0	9.7	42.8	88.0	24.8	129.4
BB007	0.1	19.2	52.0	79.0	57.7	150.4
GK004	0.1	13.7	57.6	109.5	38.9	138.9
BM444	0.1	22.4	78.2	98.0	58.6	184.5
FO003	0.0	15.8	41.0	60.0	17.7	158.5
AY017	0.0	15.0	53.4	93.9	21.9	156.5
QI081	0.0	15.3	38.5	79.8	6.4	227.3
DF032	0.0	8.4	44.5	63.8	10.5	191.8
BU012	0.0	17.3	28.5	60.7	10.2	228.4
AR042	0.0	8.6	43.8	61.8	12.4	279.4
DM033	0.0	10.1	27.3	62.0	9.5	239.7
BX001	0.0	15.0	51.4	79.9	20.5	180.4
EC009	0.0	26.3	60.0	95.1	12.8	218
AV122	0.0	18.4	57.8	83.2	14.5	178.8
BS035	0.0	5.1	23.6	54.0	5.8	192
BQ056	0.0	15.4	71.7	109.7	23.4	166.9
EB150	0.0	33.3	72.6	115.0	11.7	245.2
AT182	0.0	17.5	68.5	115.0	13.2	232.3
AR006	0.0	11.8	43.9	56.9	6.0	139.4
BG067	0.0	21.0	54.0	75.0	6.6	208
BA125	0.0	12.9	53.0	73.7	5.3	198.1
BM130	0.0	20.3	46.9	68.0	8.3	147.1
AO008	0.0	13.5	40.1	62.0	3.1	199.6
EH008	0.0	16.0	39.2	47.0	2.7	277.4

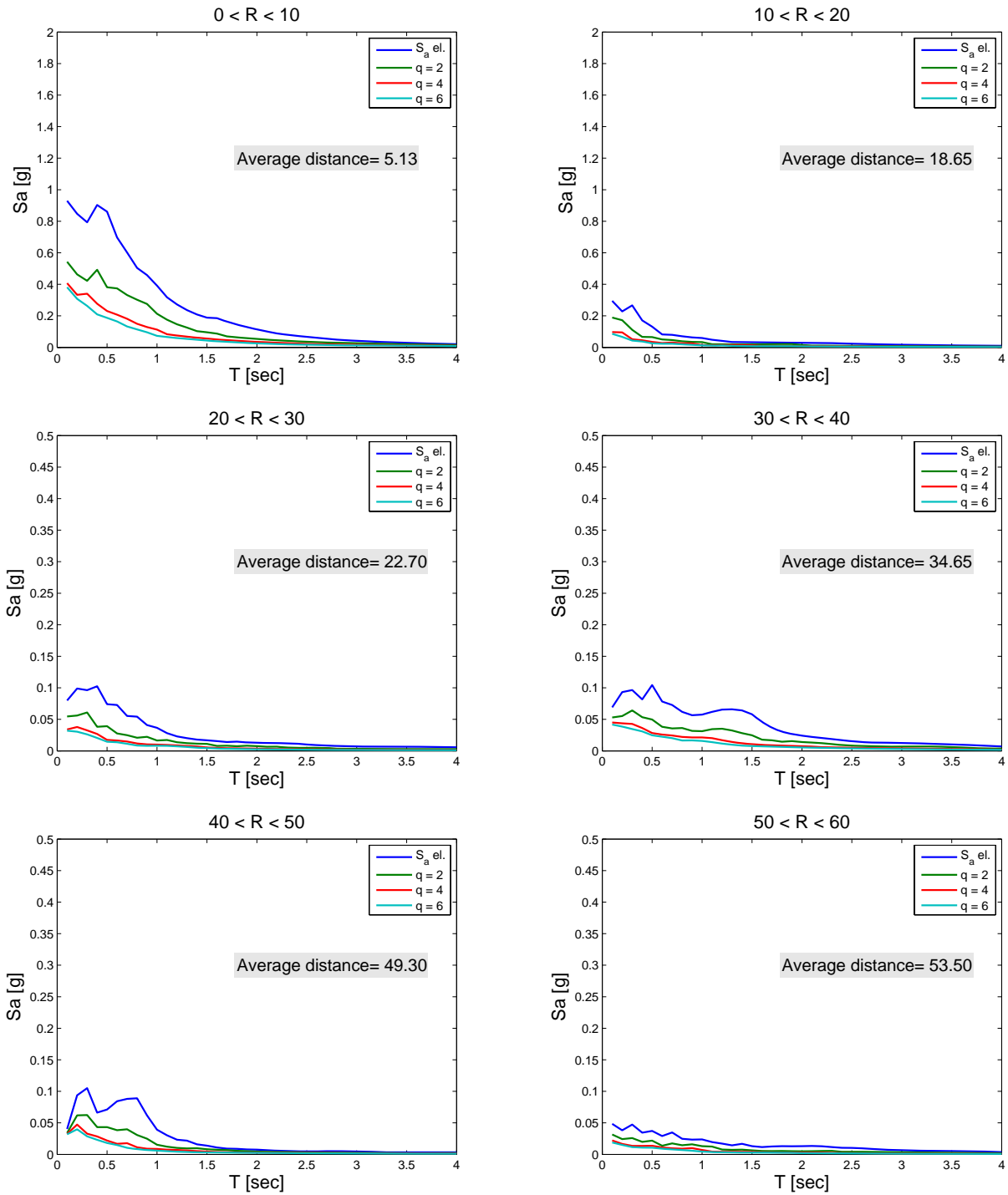
Table 6 – Integral parameters for Direction Z

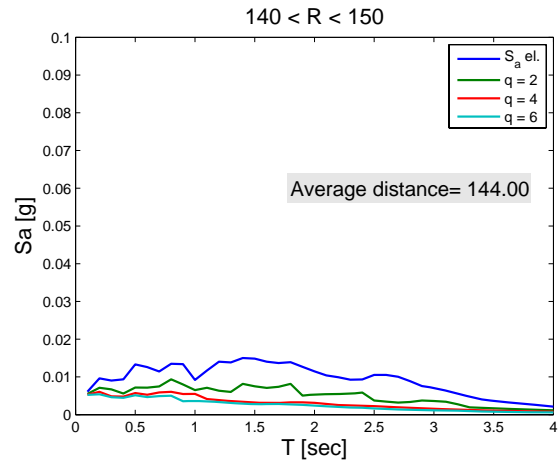
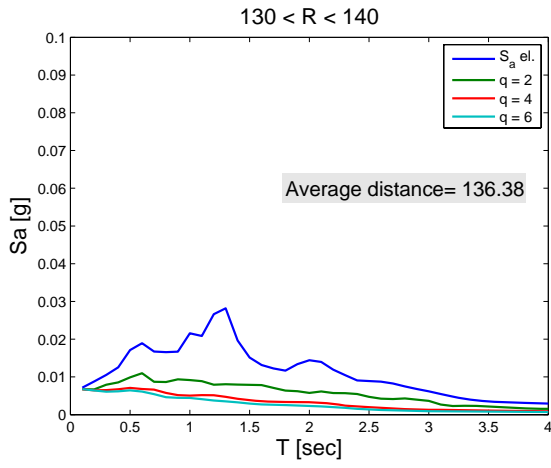
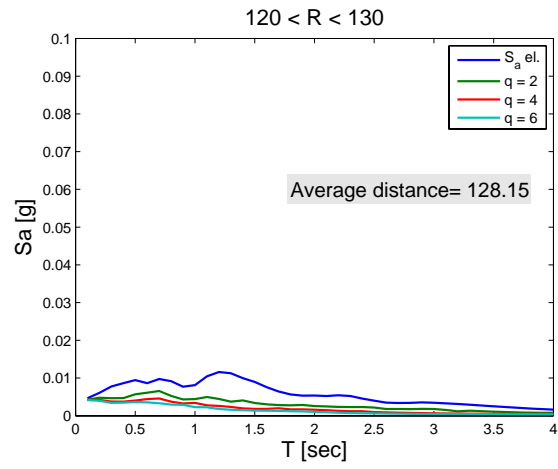
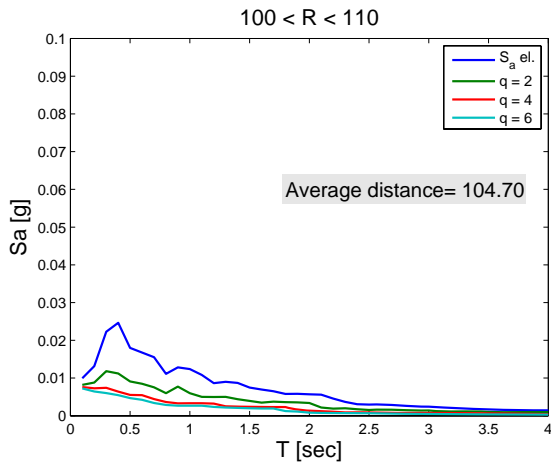
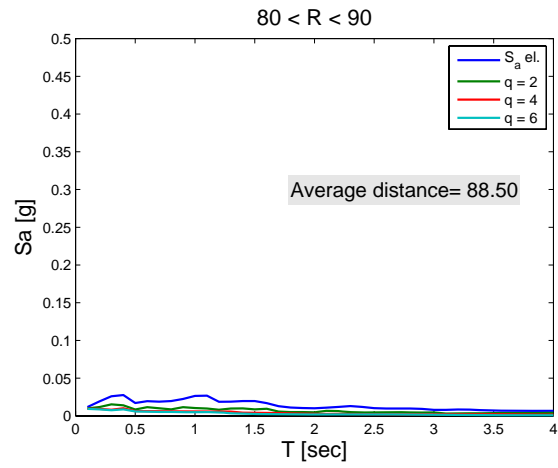
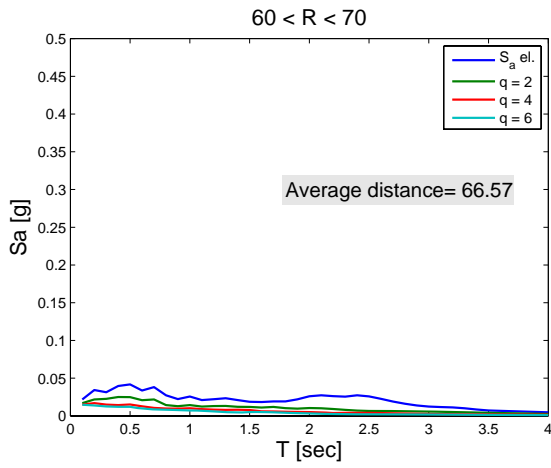
Record Identifier	IA	ID	Sd	Bd	IA/($\pi/2g$)	Epicentral Distance
	[cm/s]	[/]	[s]	[s]	[cm ² /s ³]	[km]
GX066	89.6	10.1	6.1	14.1	55933.9	4.8
FA030	31.4	10.2	8.3	16.7	19598.1	4.3
CU104	52.9	9.4	6.7	12.0	33034.1	5.8
AM043	111.4	13.5	10.5	23.0	69557.0	5.6
EF021	13.5	14.0	9.5	21.3	8445.4	18
TK003	1.7	4.2	8.3	25.4	1059.4	31.6
BI016	2.4	16.3	17.9	55.3	1491.6	34.9

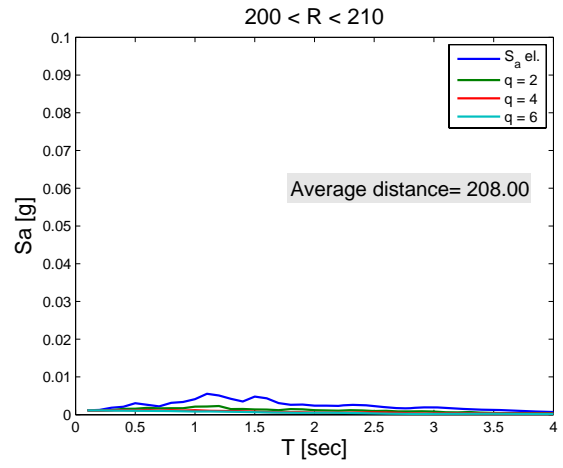
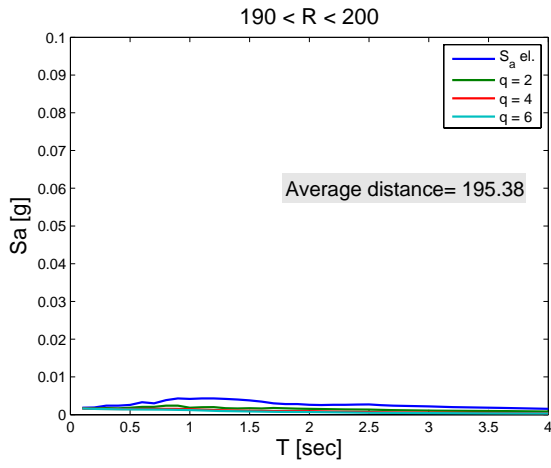
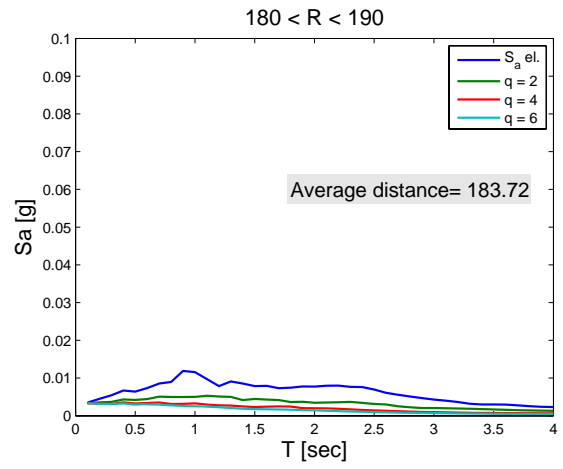
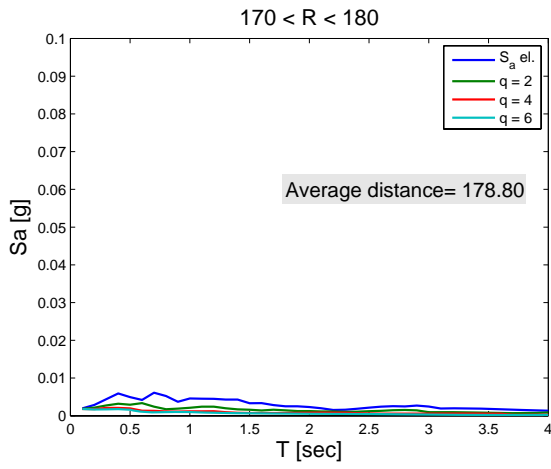
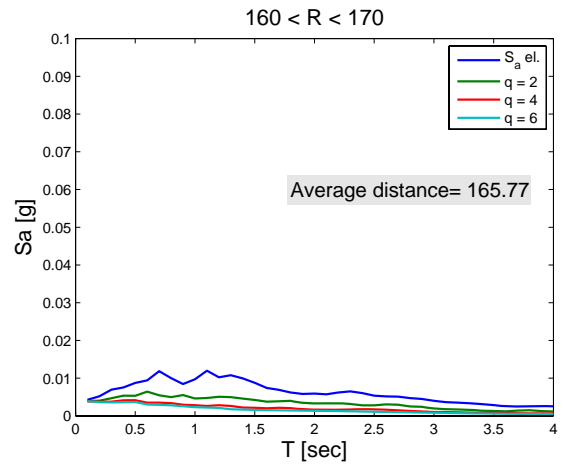
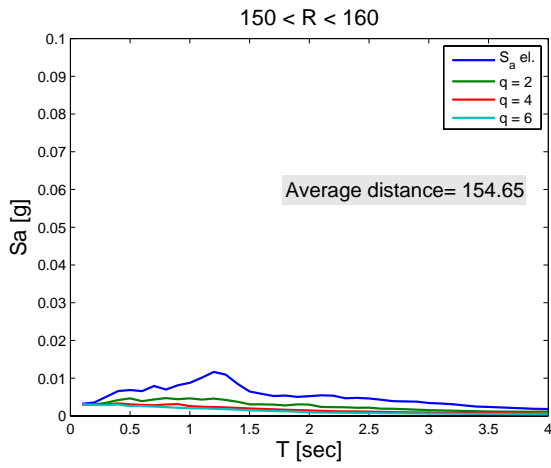
CR008	0.9	4.8	13.3	28.3	531.0	49.4
BY048	1.3	11.3	19.4	45.1	824.1	22.4
CR003	0.5	6.3	22.8	46.1	304.3	56.5
EK007	1.3	13.7	35.3	66.2	824.6	67.1
GE1463	0.6	6.5	14.4	33.0	386.6	22.6
BX007	0.8	18.3	21.6	45.1	509.3	19.3
DF006	0.3	15.3	22.4	56.1	193.1	23.1
BY003	0.5	10.3	20.6	50.1	299.8	33
EI160	0.3	19.3	59.1	93.0	162.8	133.5
BH003	0.2	11.6	33.6	92.1	118.5	88.5
BN048	0.1	16.1	78.4	105.6	68.1	140.9
ZC002	0.1	14.2	32.1	73.0	48.1	39.1
HB060	0.1	11.1	33.3	81.2	39.5	65.9
BS029	0.0	12.8	40.4	89.2	27.5	102.7
CU008	0.1	23.2	37.0	81.7	45.4	49.2
BW024	0.1	14.7	41.6	84.0	32.5	66.7
BC018	0.1	19.1	38.8	92.0	31.3	109.7
AL104	0.1	17.5	58.0	106.2	66.9	133.7
CQ001	0.1	11.9	25.0	60.8	59.6	50.5
CB004	0.0	17.9	42.9	90.0	10.2	101.7
AY026	0.0	22.6	72.2	113.4	30.7	162.4
IY045	0.0	15.3	69.7	111.9	10.4	183.4
AU056	0.0	10.7	55.5	81.8	16.0	126.9
AY081	0.0	17.6	65.2	102.4	8.1	186.6
BD004	0.1	17.2	52.3	75.0	33.9	153.2
CA056	0.0	21.5	62.6	101.1	16.2	168
QX001	0.0	19.2	37.6	85.7	25.3	129.4
BB007	0.0	20.2	56.9	79.0	28.1	150.4
GK004	0.0	15.4	69.2	111.7	27.7	138.9
BM444	0.0	27.0	76.2	98.0	12.4	184.5
FO003	0.0	15.5	43.6	60.0	6.0	158.5
AY017	0.0	18.1	54.3	93.8	14.8	156.5
QI081	0.0	18.2	55.4	81.0	3.1	227.3
DF032	0.0	13.1	48.3	64.0	5.5	191.8
BU012	0.0	13.7	34.8	62.0	3.0	228.4
AR042	0.0	18.2	45.0	62.0	5.0	279.4
DM033	0.0	15.0	31.5	62.0	4.4	239.7
BX001	0.0	19.8	51.9	80.0	12.7	180.4
EC009	0.0	22.9	81.9	96.0	3.9	218
AV122	0.0	12.0	63.3	83.7	6.3	178.8
BS035	0.0	9.0	27.8	54.0	2.4	192
BQ056	0.0	21.6	73.6	111.7	15.6	166.9
EB150	0.0	28.0	83.5	116.0	5.4	245.2
AT182	0.0	17.2	82.9	115.0	5.2	232.3
AR006	0.0	12.9	46.3	57.0	3.9	139.4
BG067	0.0	15.7	53.0	75.0	2.9	208
BA125	0.0	12.6	42.9	74.0	4.4	198.1
BM130	0.0	24.2	51.3	68.0	2.0	147.1
AO008	0.0	10.5	44.7	61.9	2.2	199.6
EH008	0.0	8.1	35.3	47.0	0.8	277.4

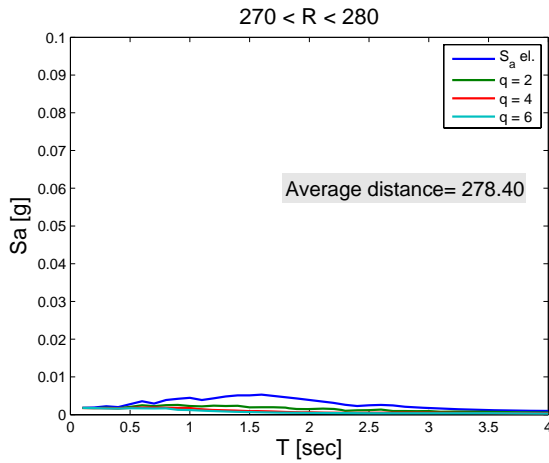
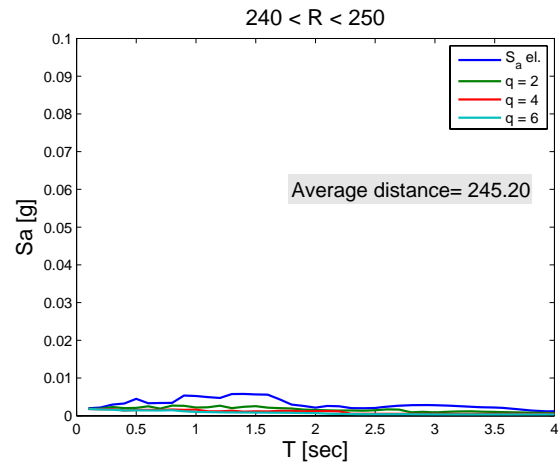
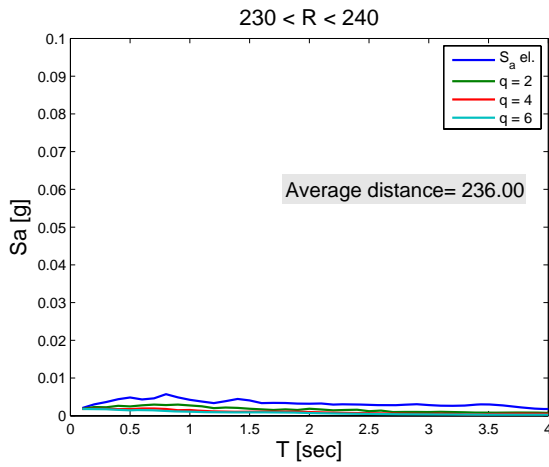
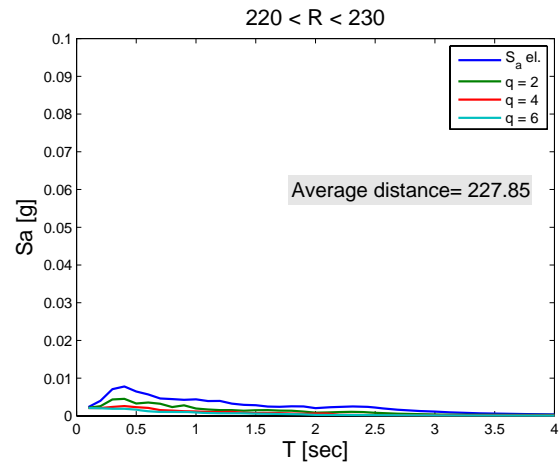
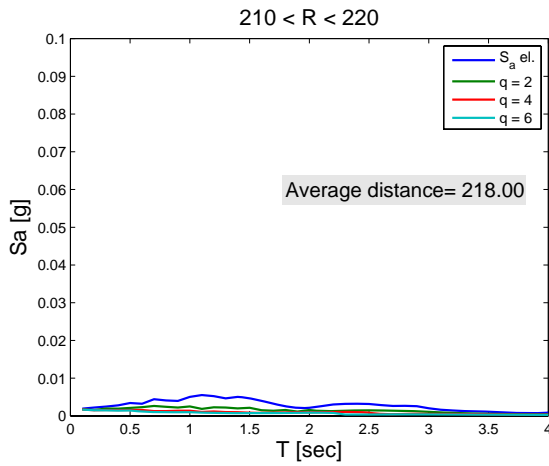
11. Horizontal Component – Inelastic Spectra

Horizontal records are grouped in bins of 10 km of epicentral distance (R) and average inelastic acceleration spectra of each bin are plotted for different values of ductility factor q. Hardening ratio of inelastic system is equal to 0.03. Plots show also mean elastic pseudo-acceleration spectrum of bins.



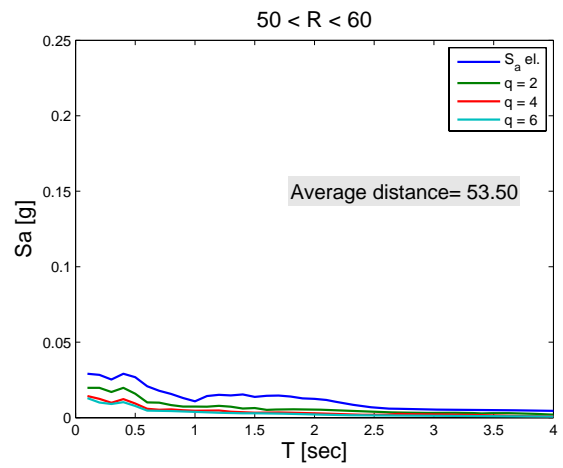
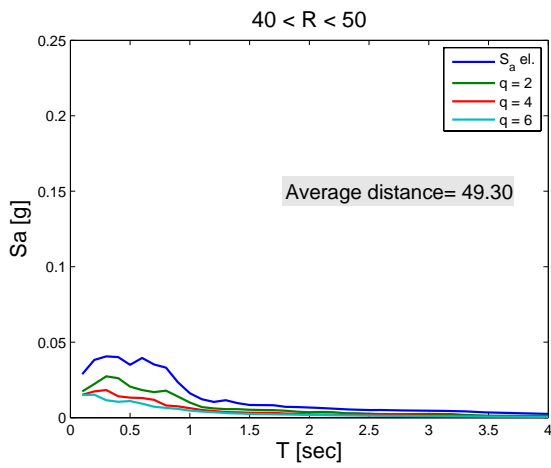
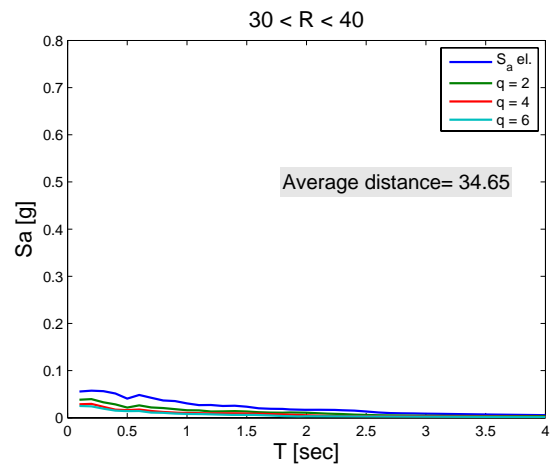
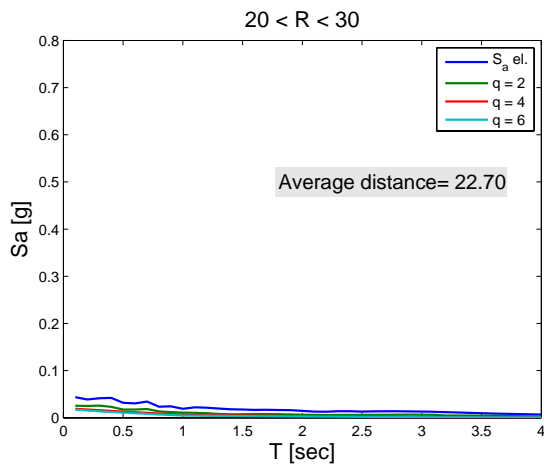
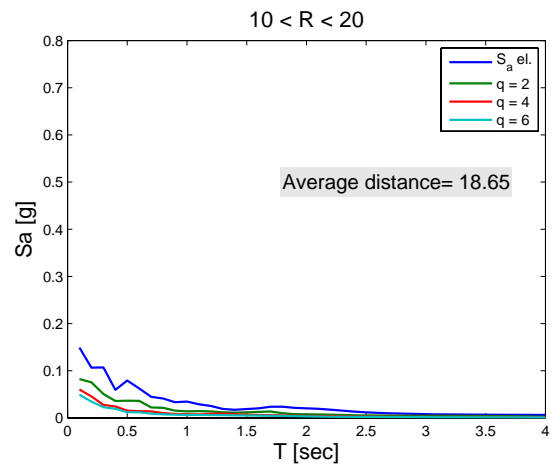
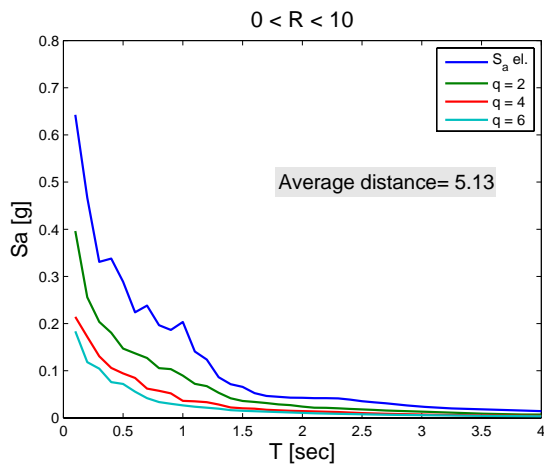


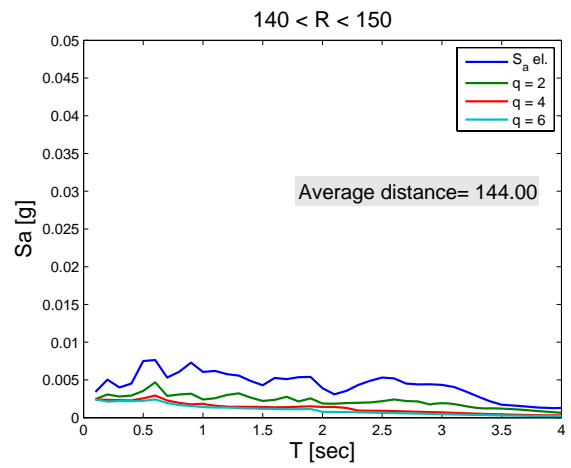
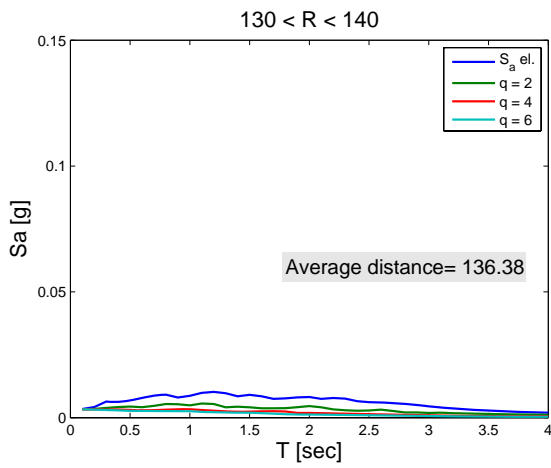
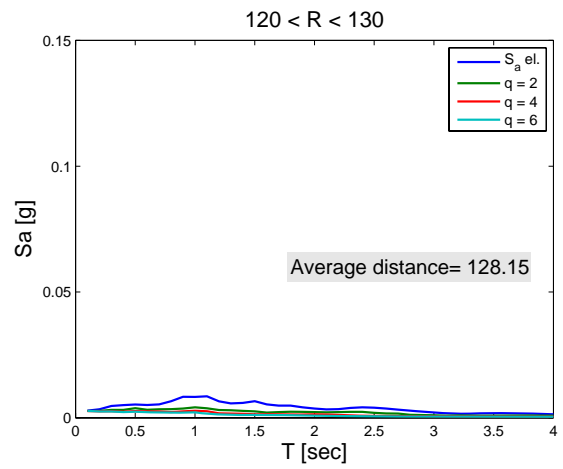
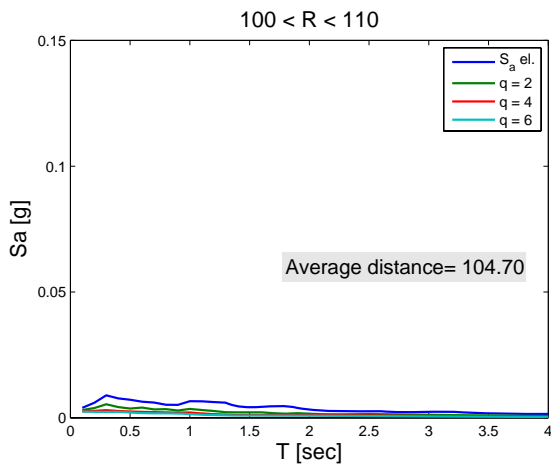
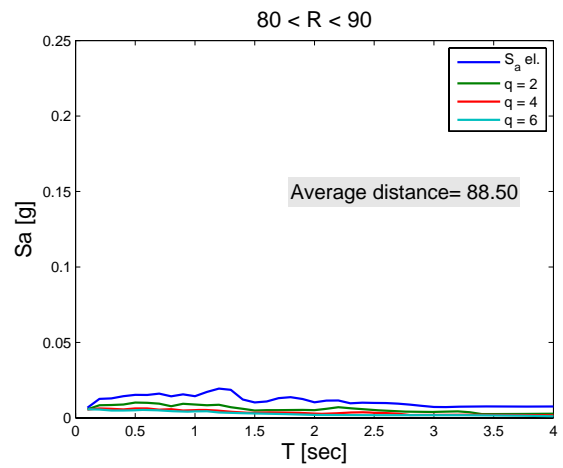
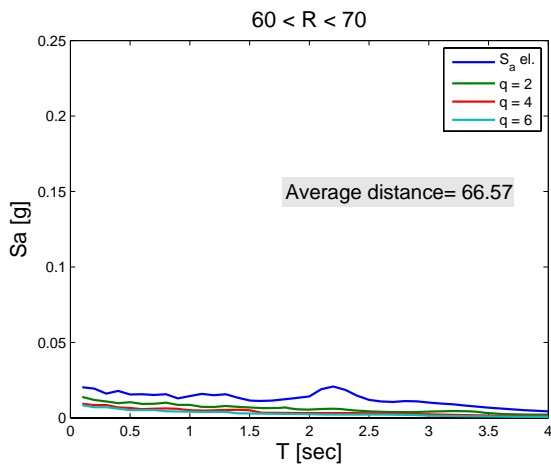


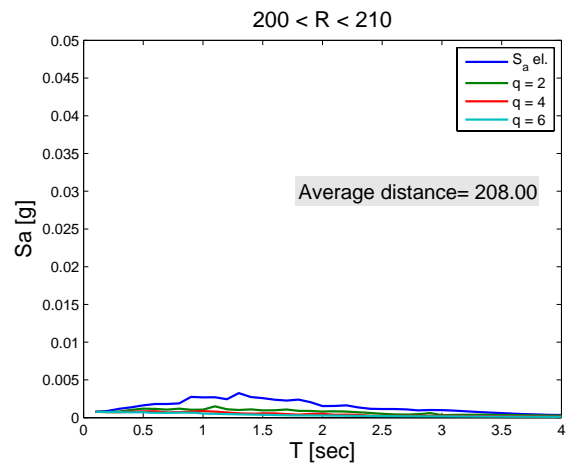
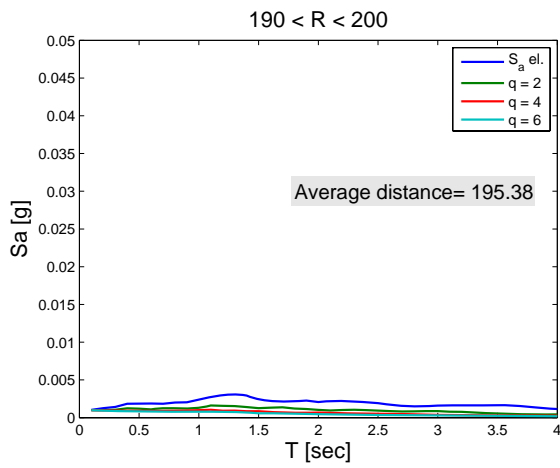
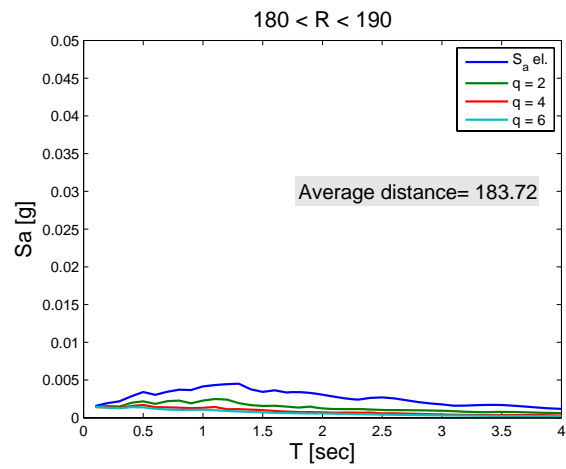
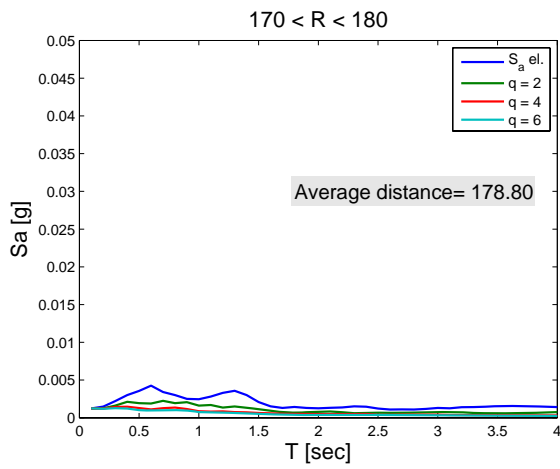
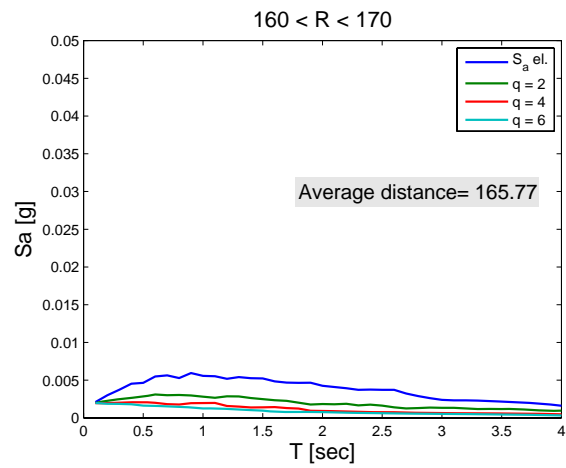
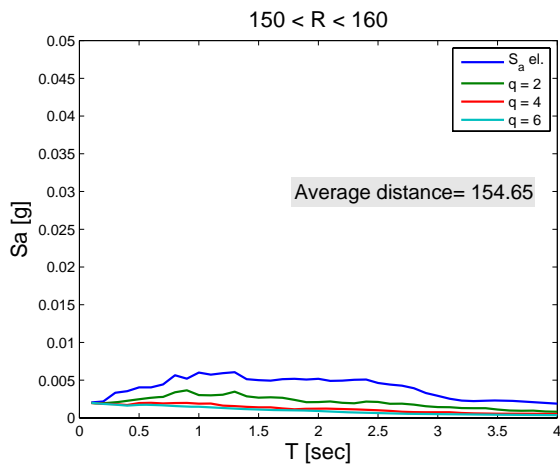


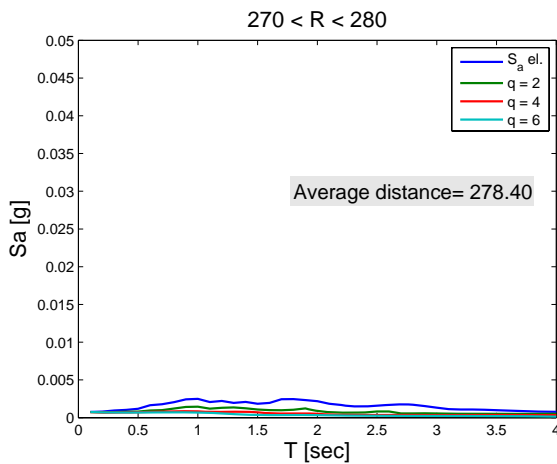
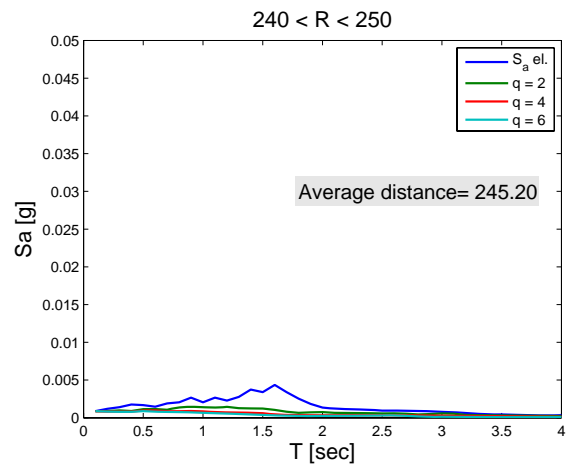
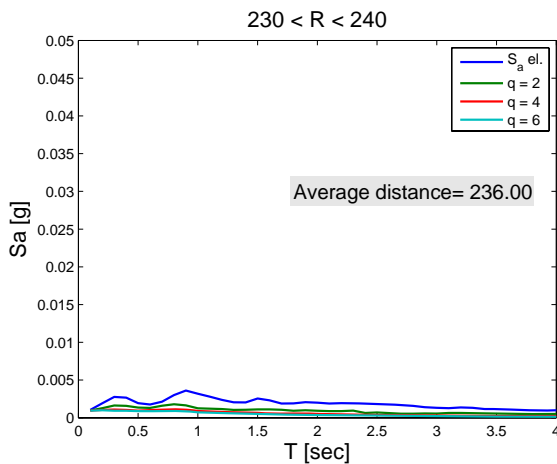
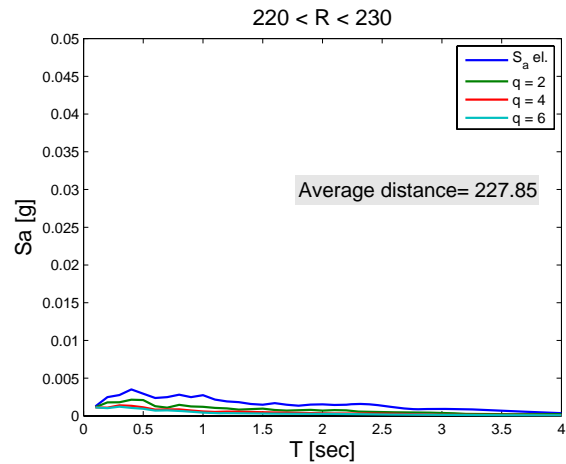
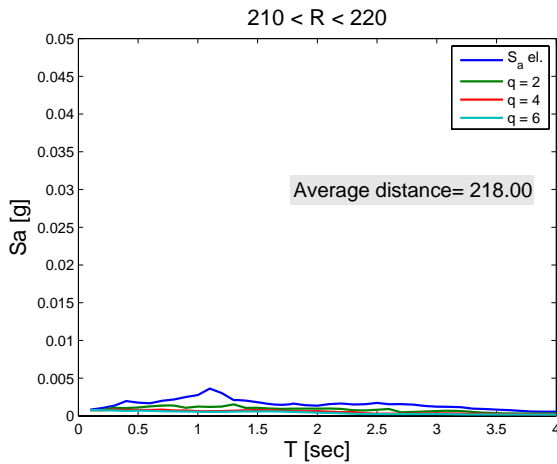
12. Vertical Component – Inelastic Spectra

Vertical records are grouped in bins of 10 km of epicentral distance (R) and average inelastic acceleration spectra of each bin are plotted for different values of ductility factor q. Hardening ratio of inelastic system is equal to 0.03. Plots show also mean elastic pseudo-acceleration spectrum of bins.



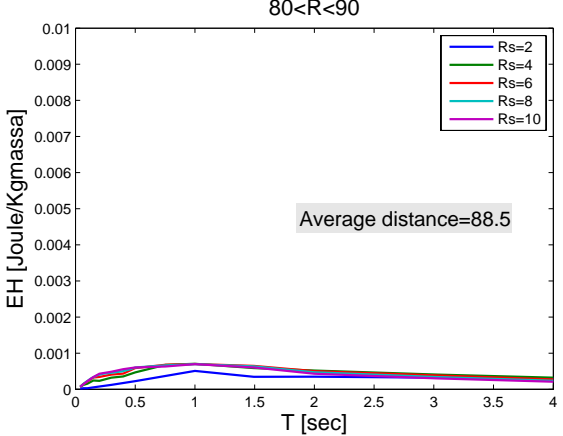
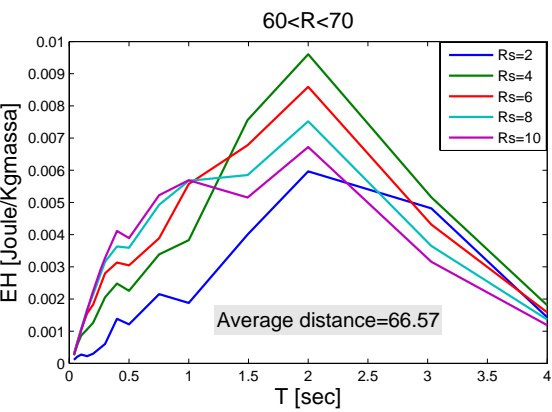
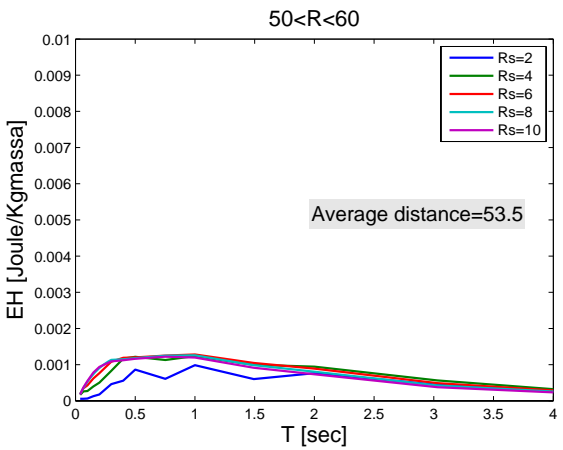
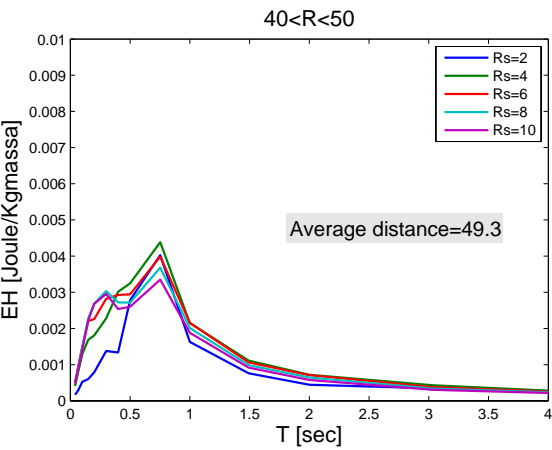
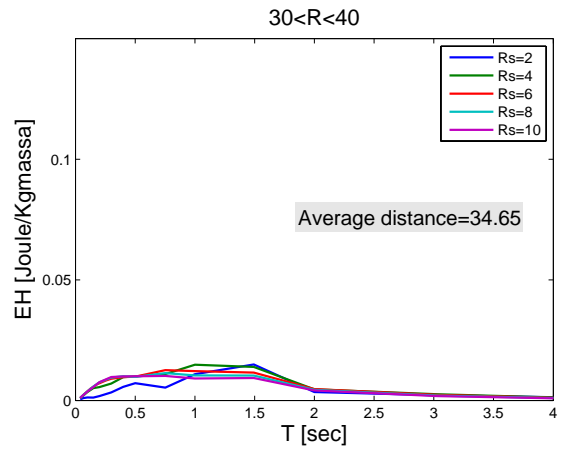
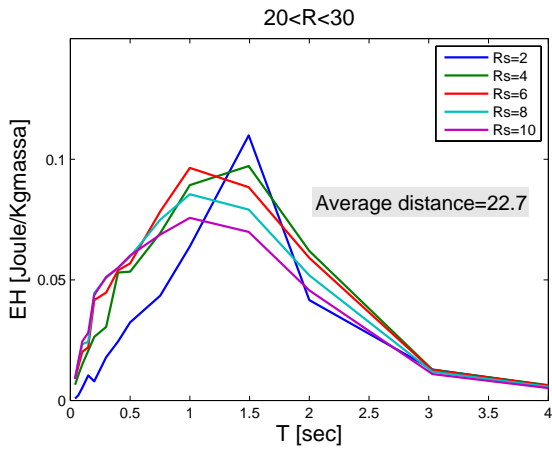
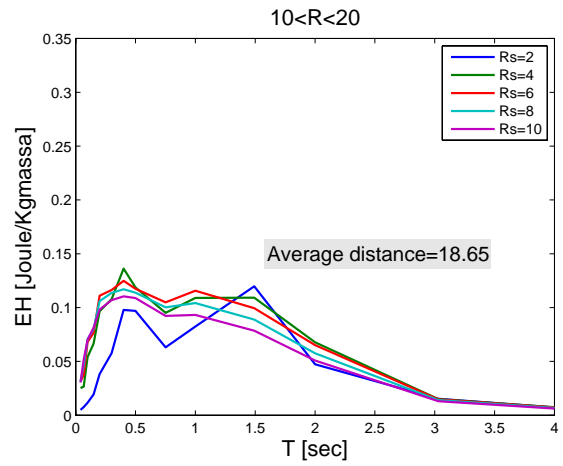
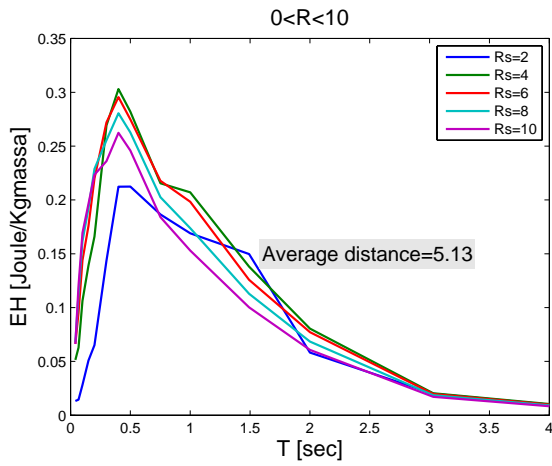


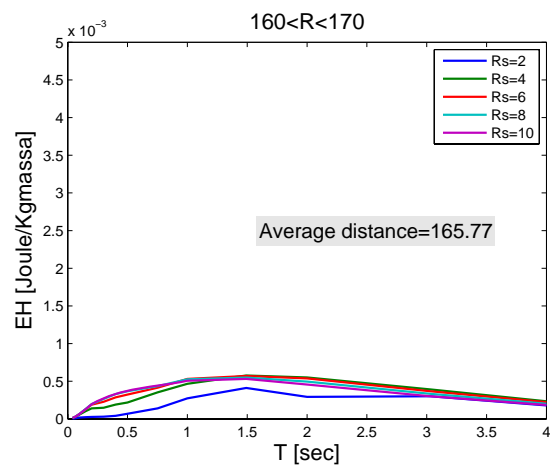
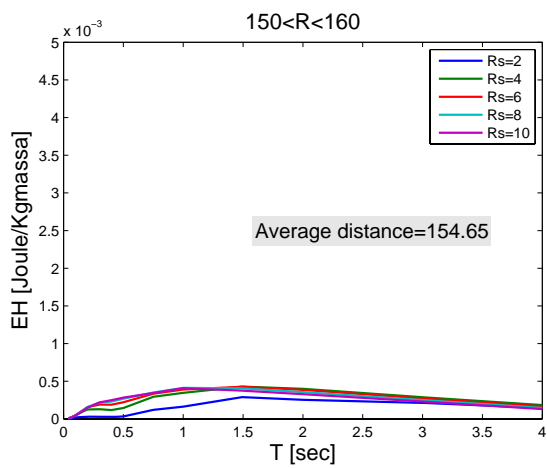
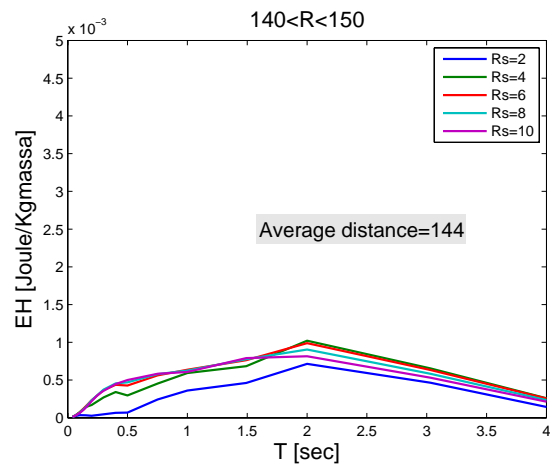
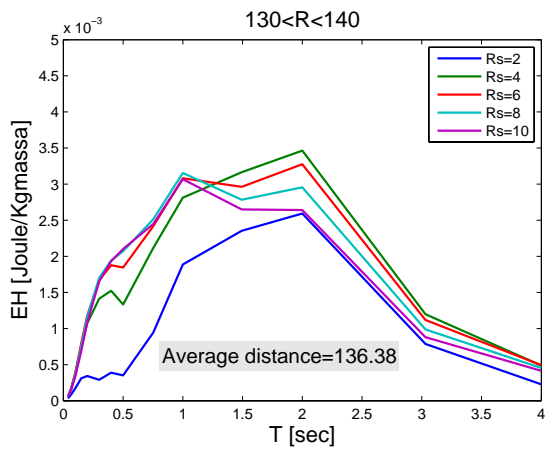
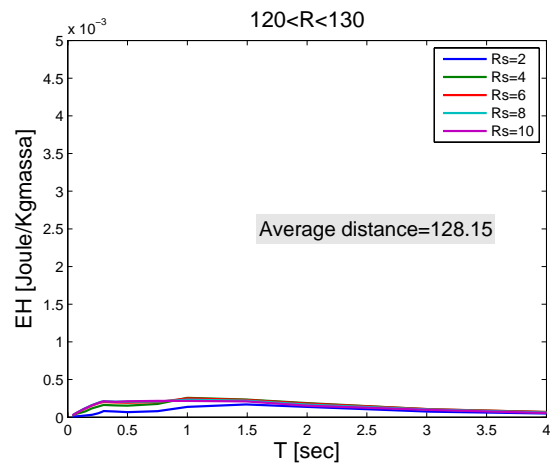
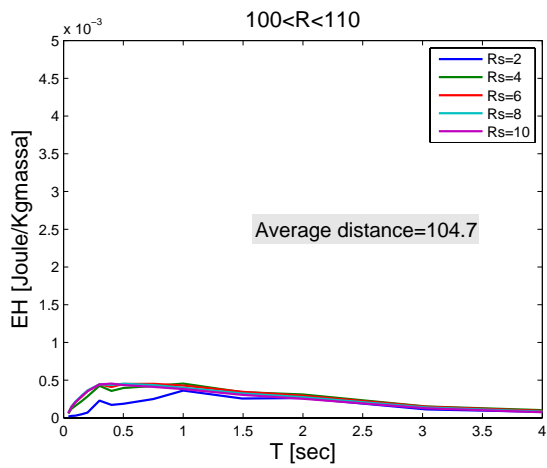


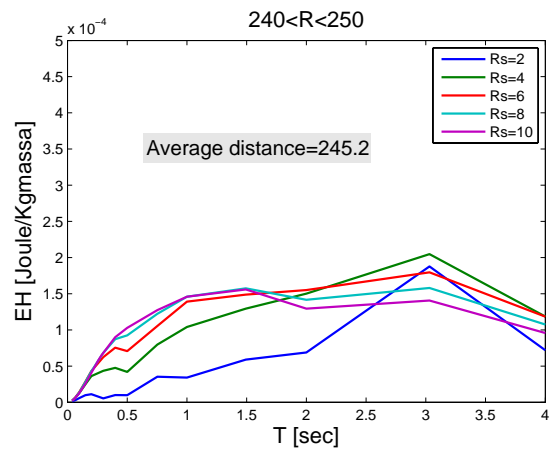
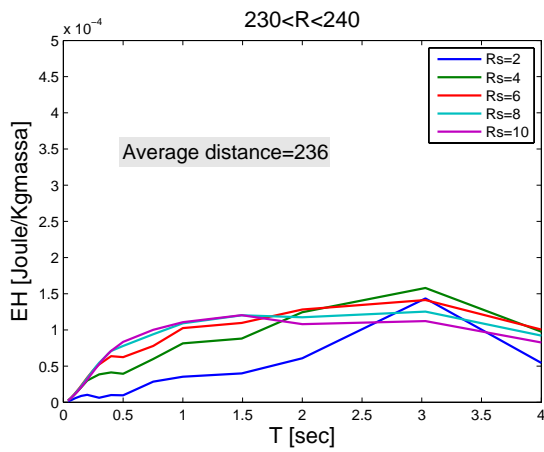
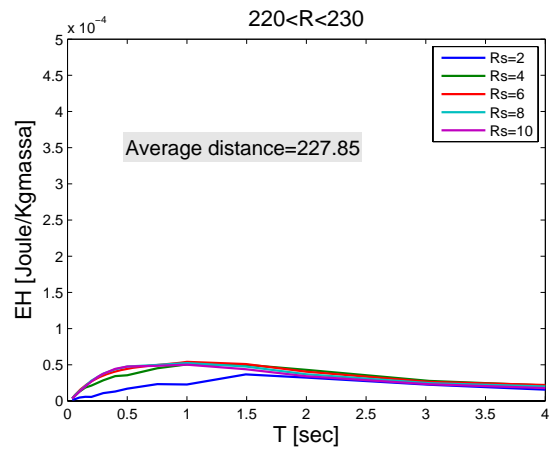
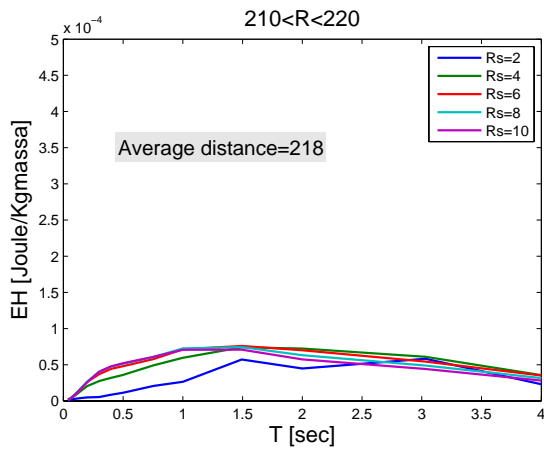
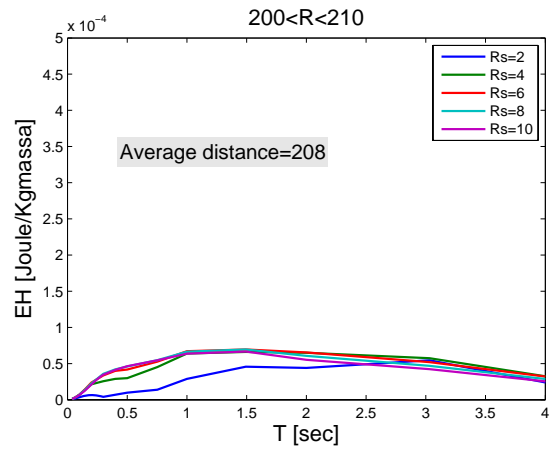
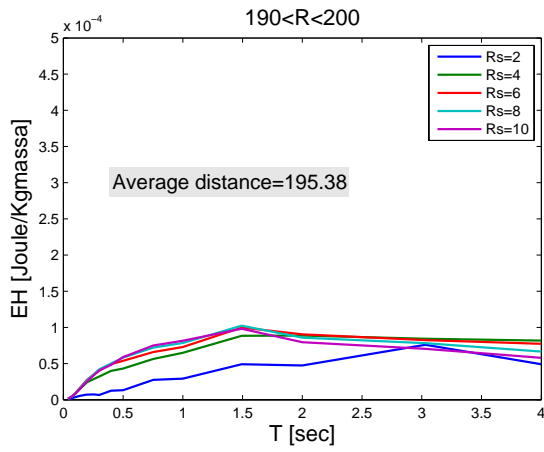
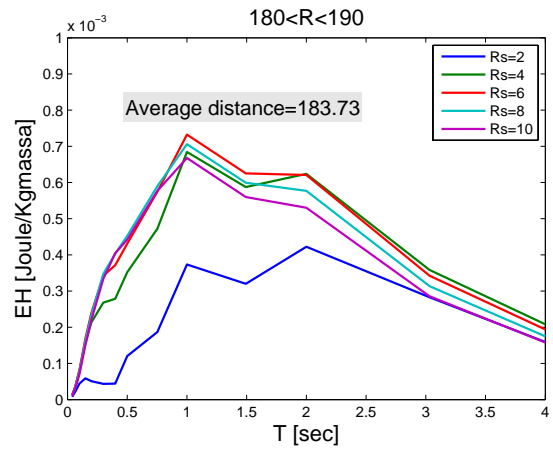
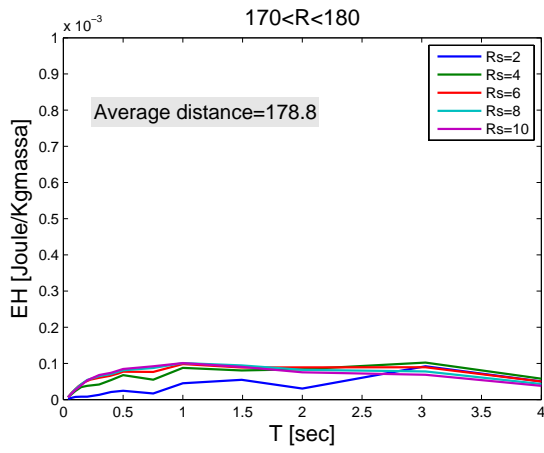


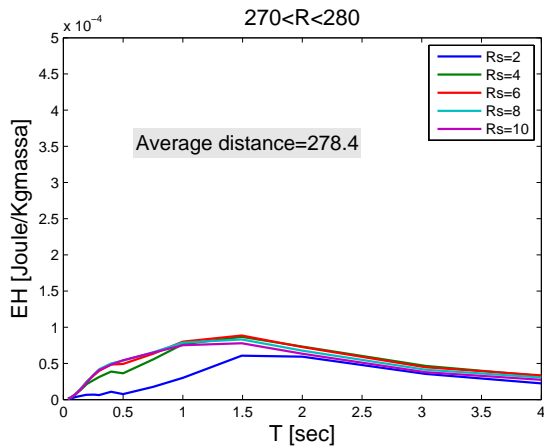
13. Horizontal Component – Specific Hysteretic Energy Inelastic Spectra

Horizontal records are grouped in bins of 10 km of epicentral distance (R) and average specific hysteretic energy inelastic spectra of each bin are plotted for different values of the strength reduction factor R_s ($F_{el,max}/F_y$). Hardening ratio of inelastic system is equal to 0.03. Plots have been put in different scale (plot on the same line have the same scale) because of the slide change in energy passing through a bin to another.



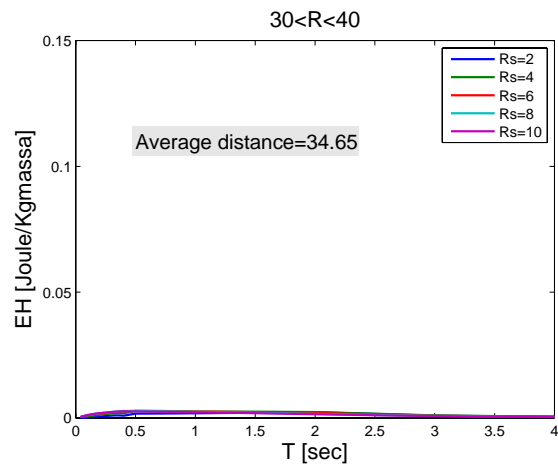
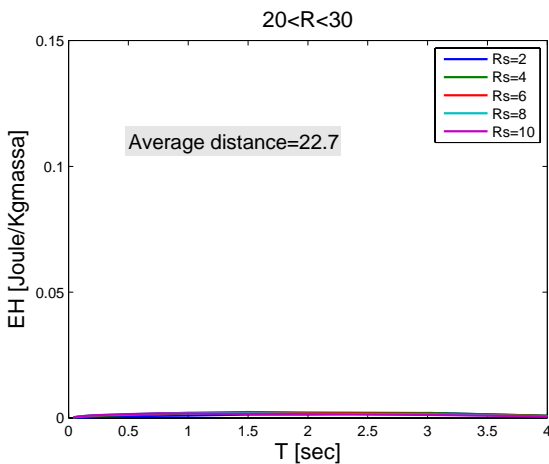
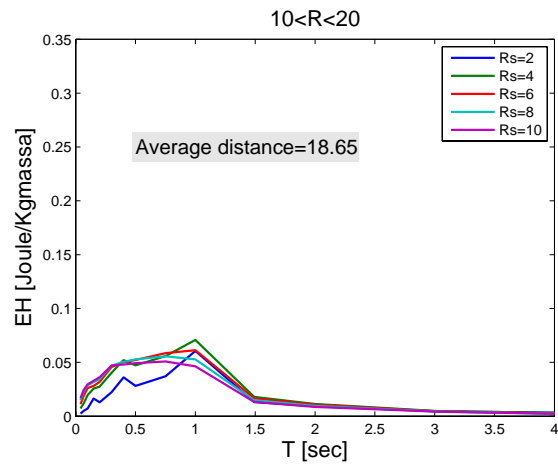
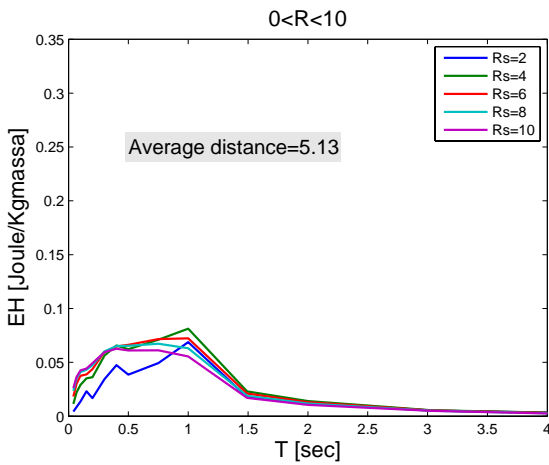


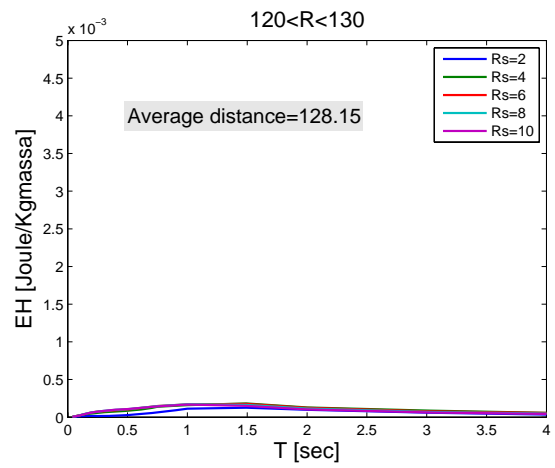
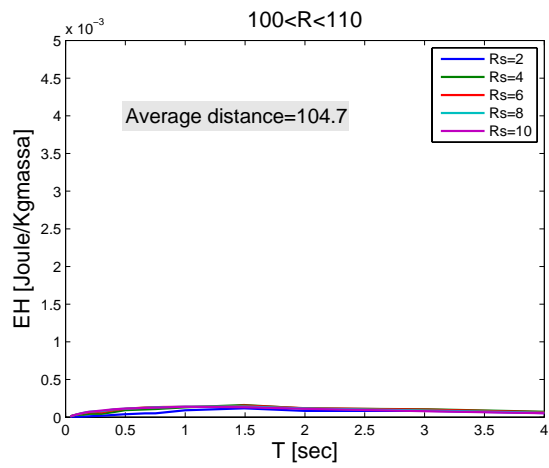
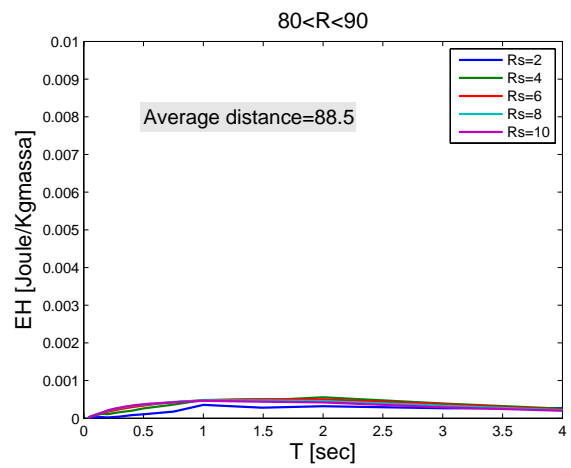
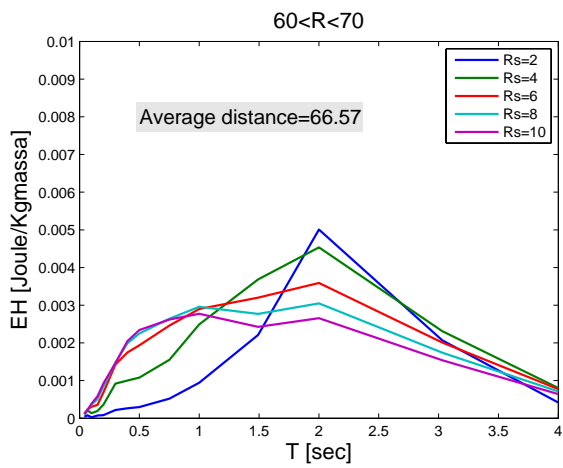
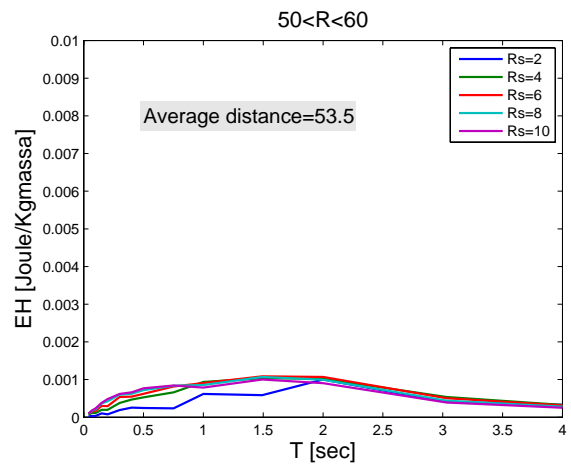
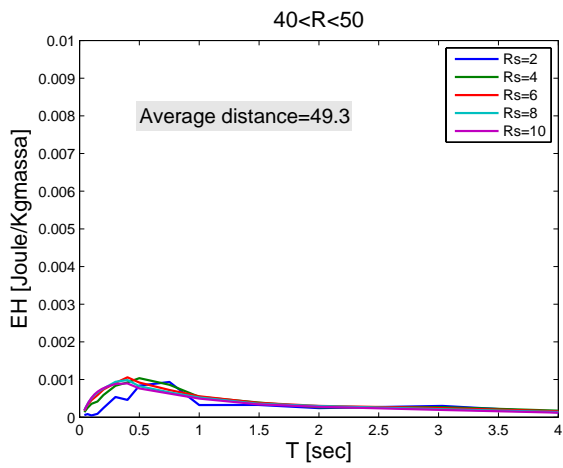


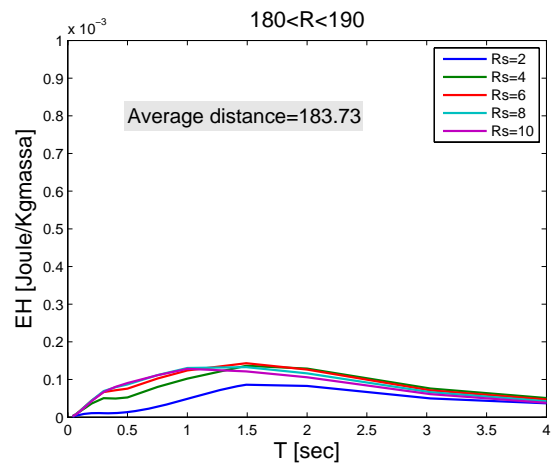
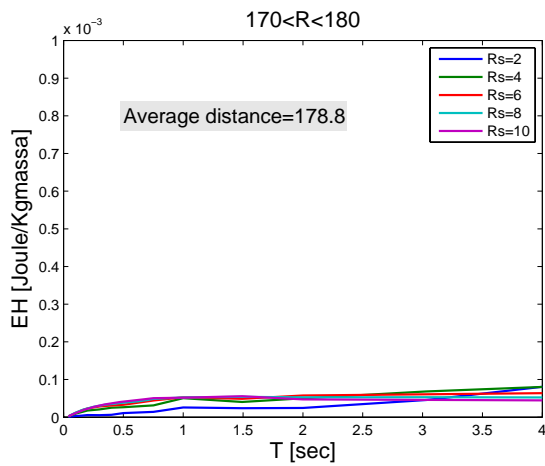
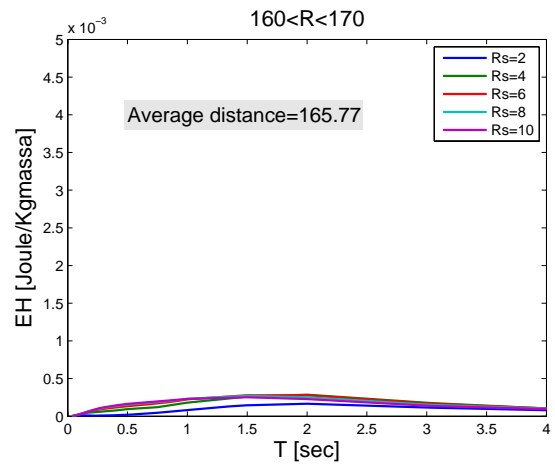
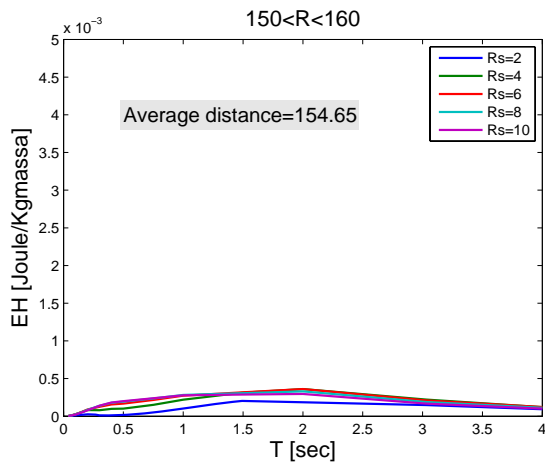
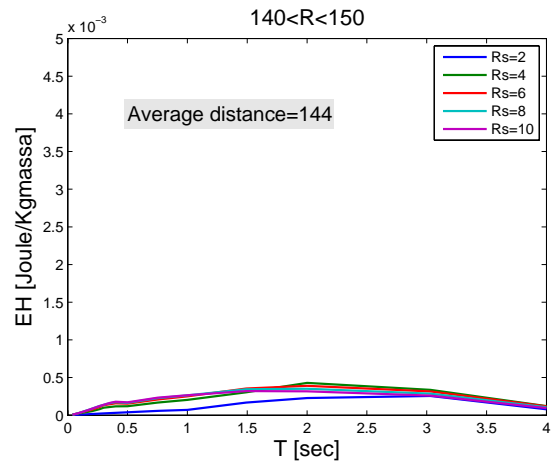
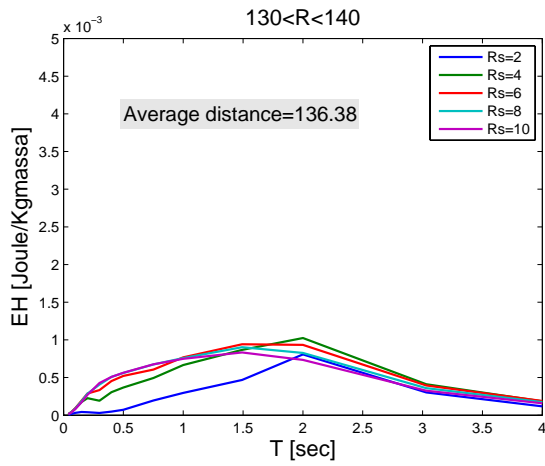


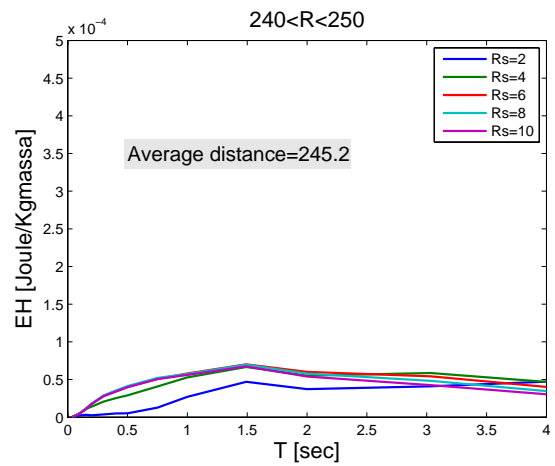
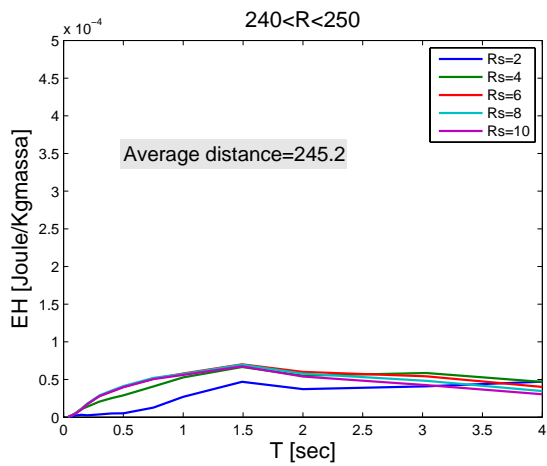
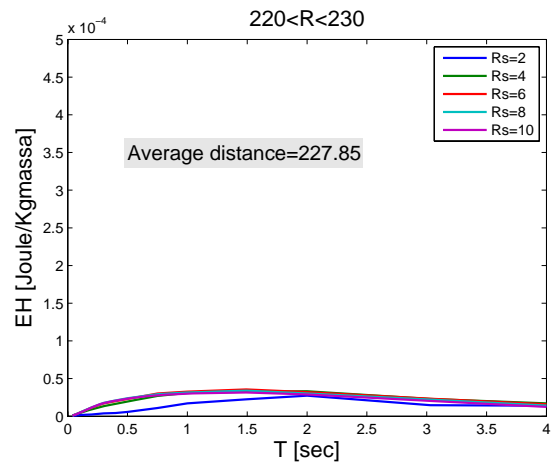
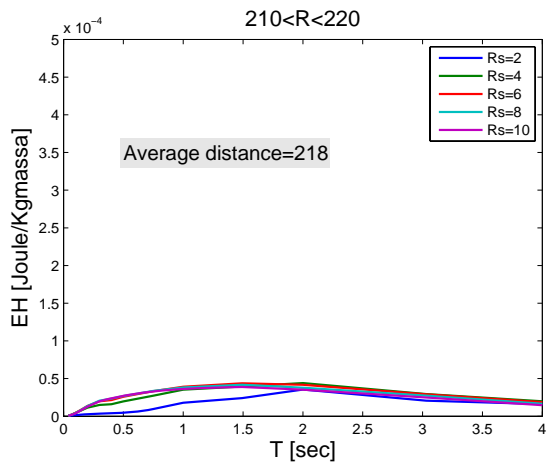
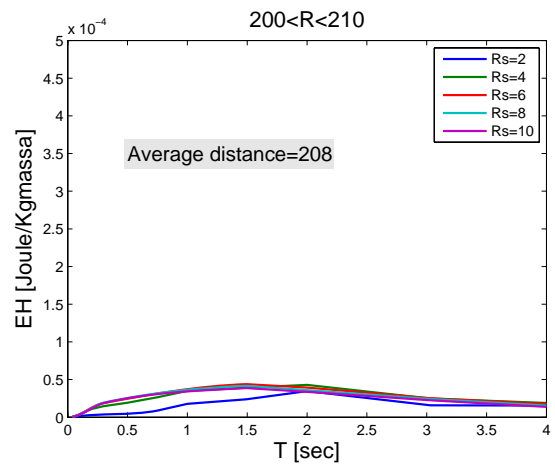
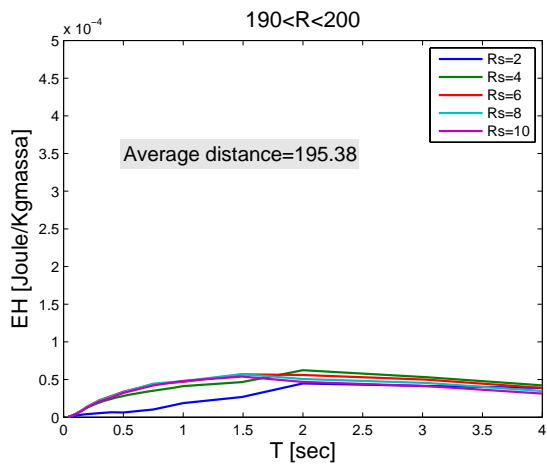
14. Vertical Component –Specific Hysteretic Energy Inelastic Spectra

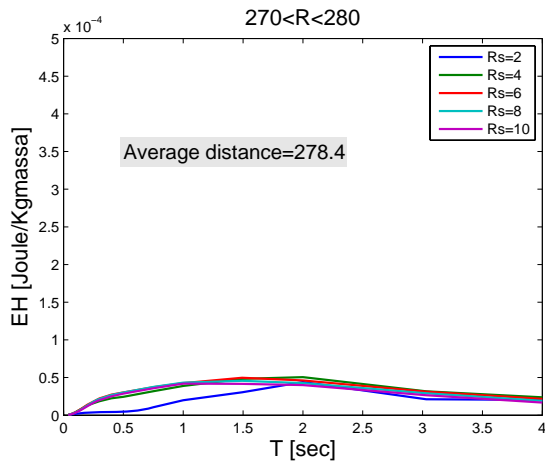
Vertical records are grouped in bins of 10 km of epicentral distance (R) and average specific hysteretic energy inelastic spectra of each bin are plotted for different values of the strength reduction factor R_s ($F_{el,max}/F_y$). Hardening ratio of inelastic system is equal to 0.03. Plots have been put in the same scale criteria assumed for horizontal component.



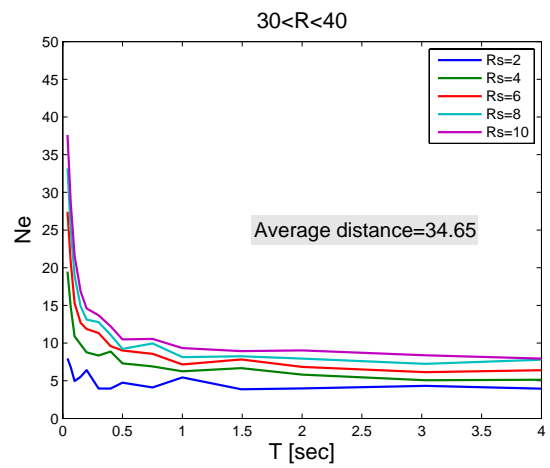
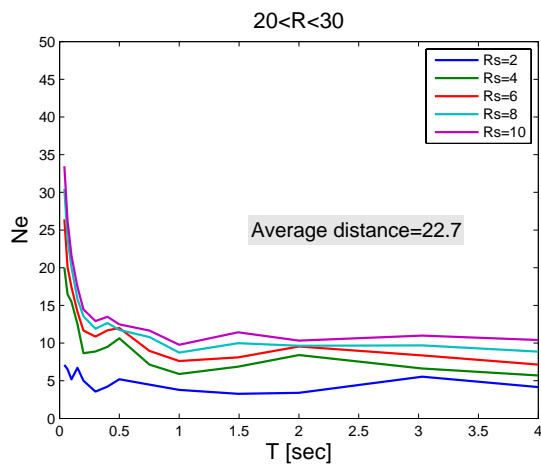
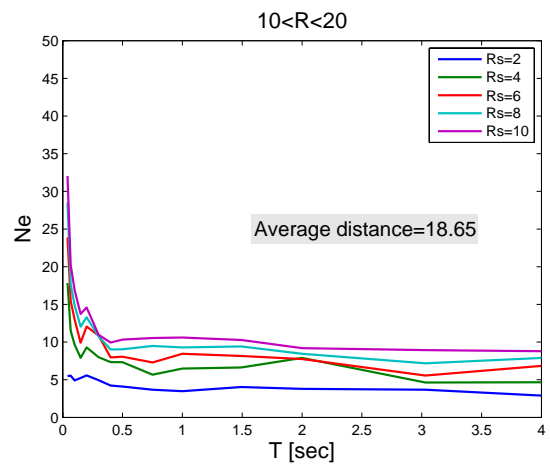
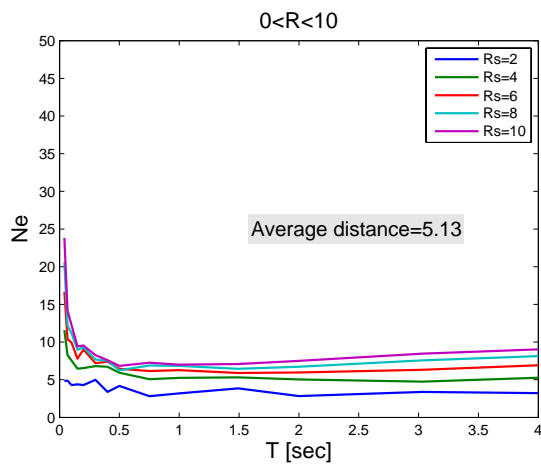


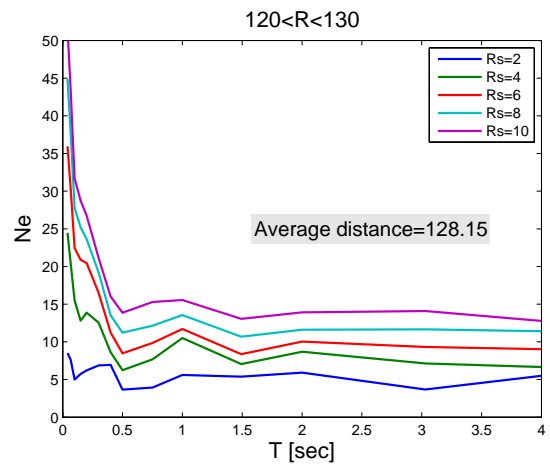
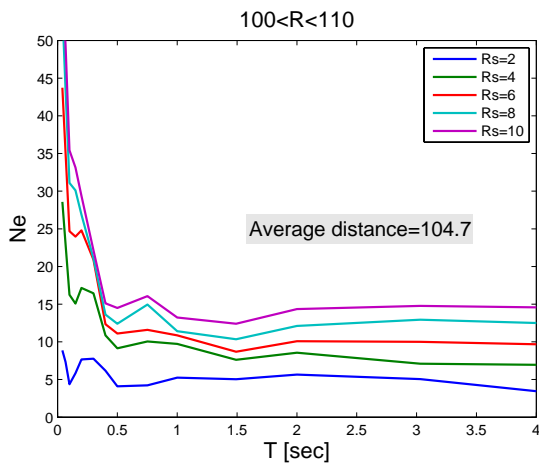
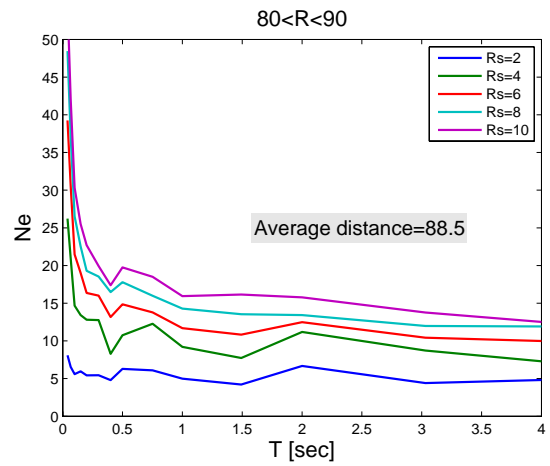
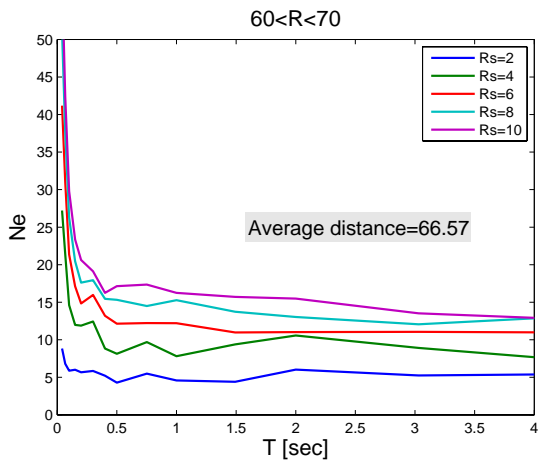
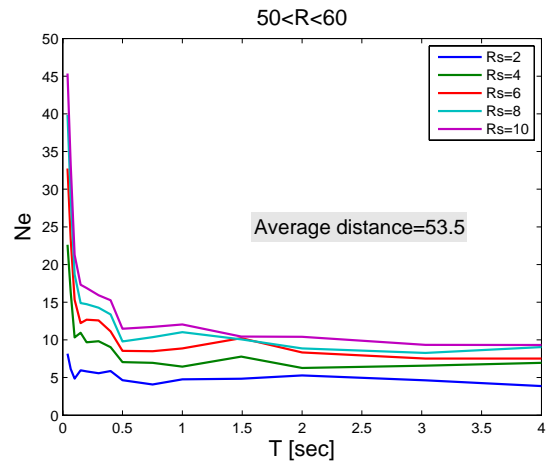
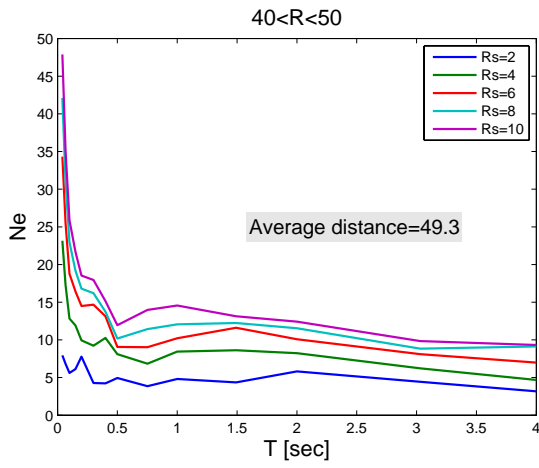


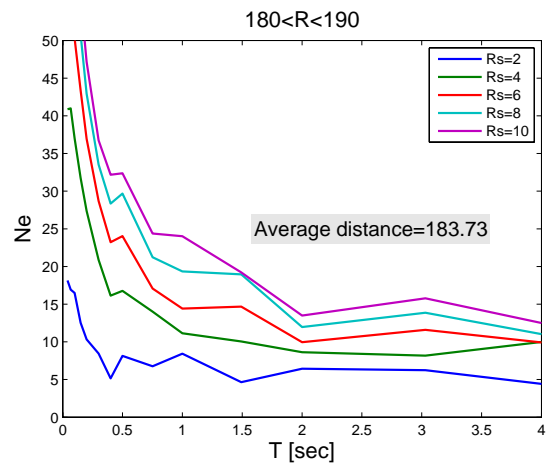
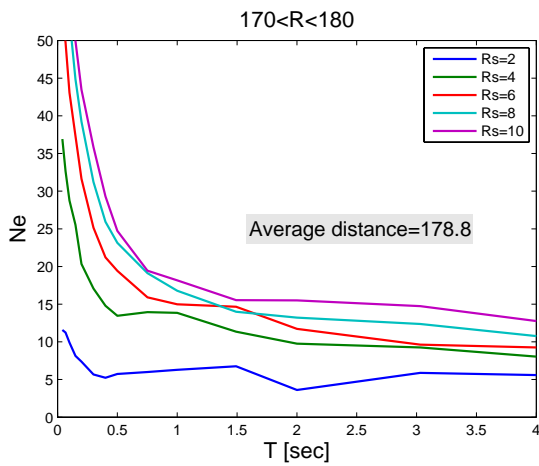
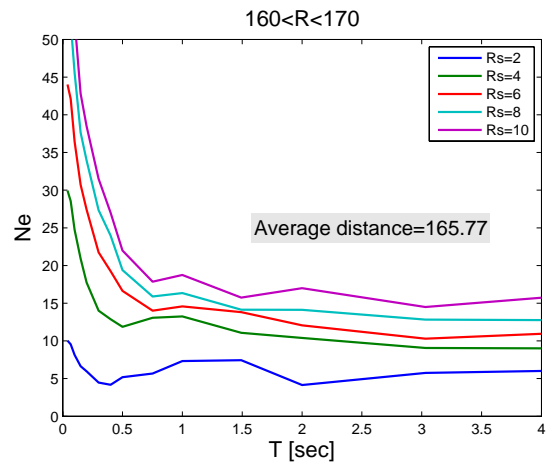
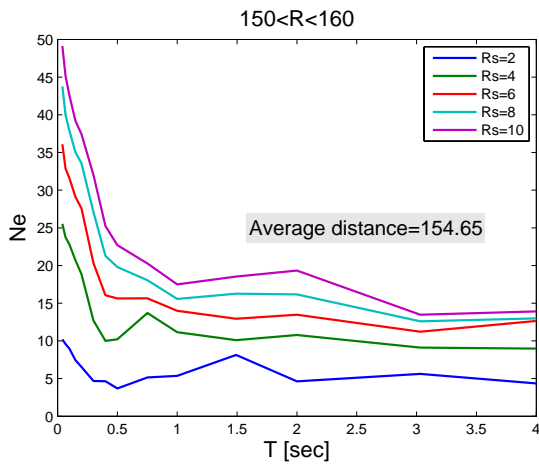
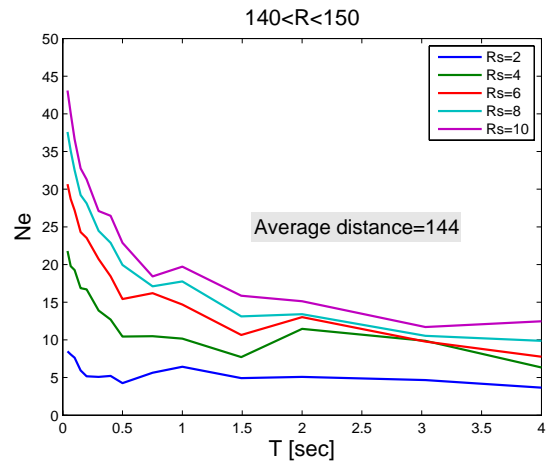
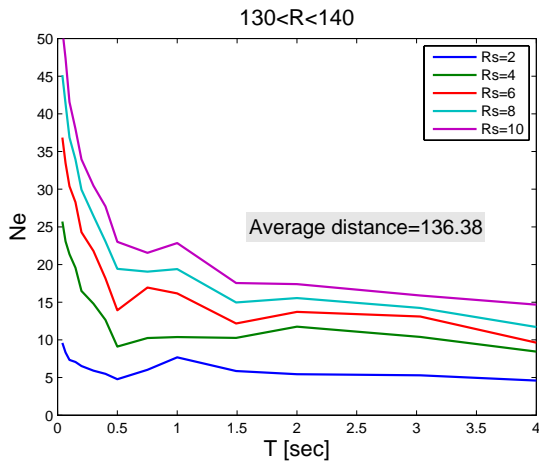


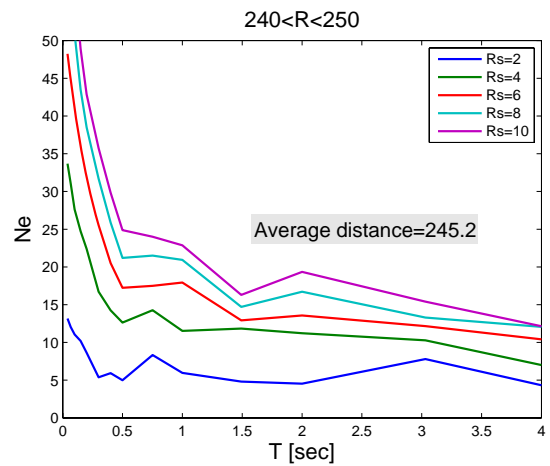
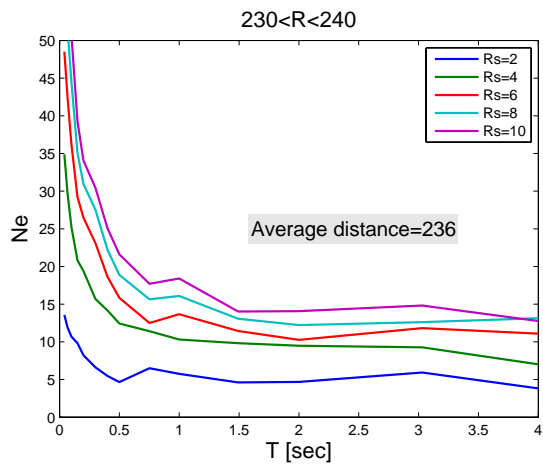
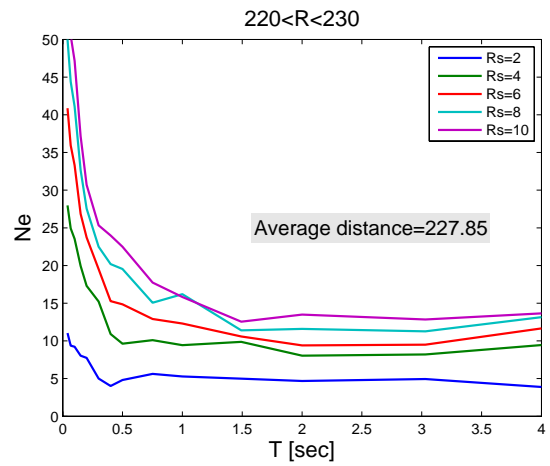
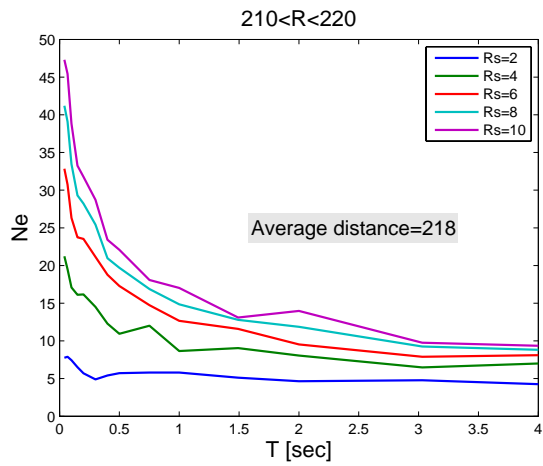
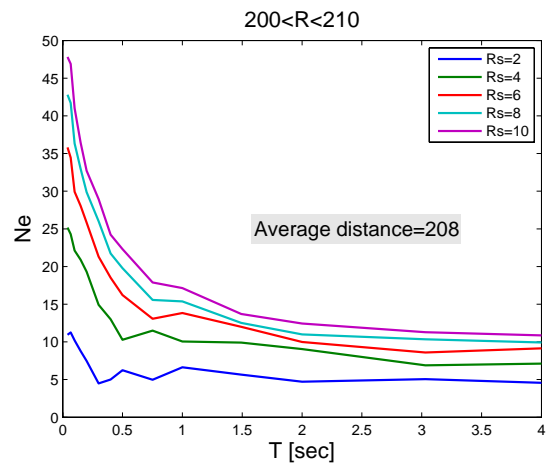
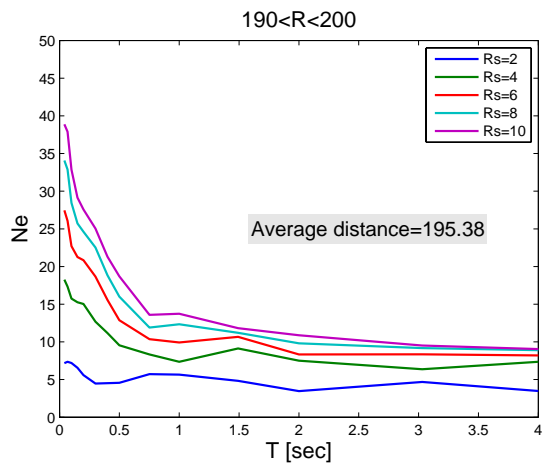


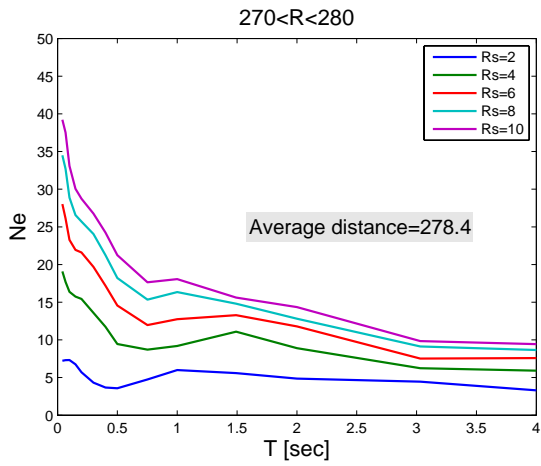
15. Horizontal Component – Number of Equivalent Cycles Spectra



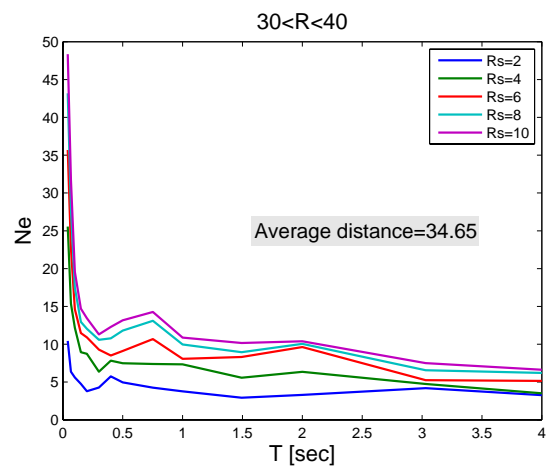
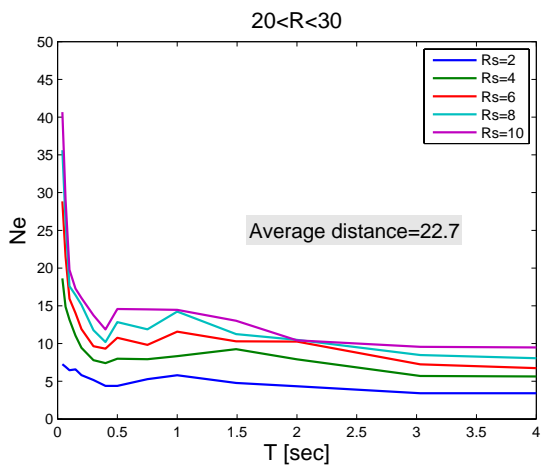
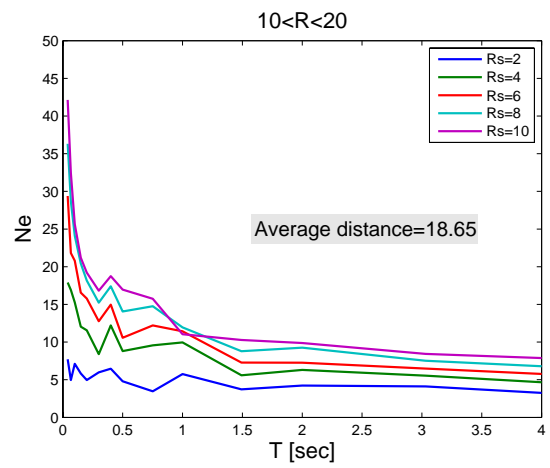
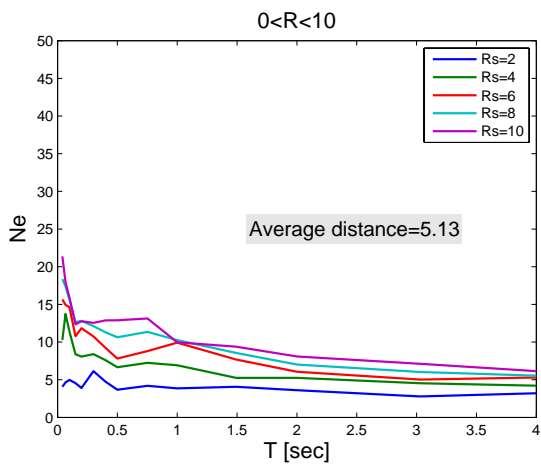


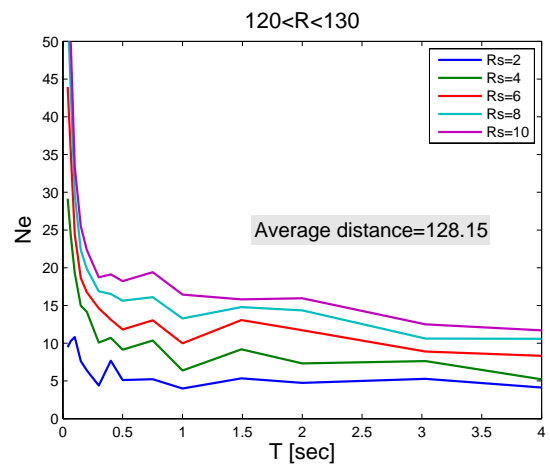
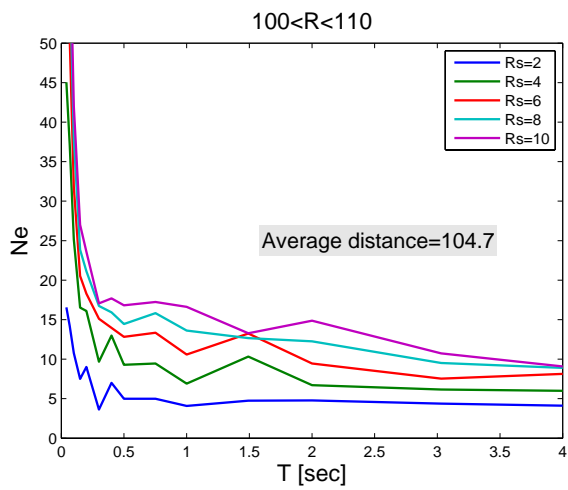
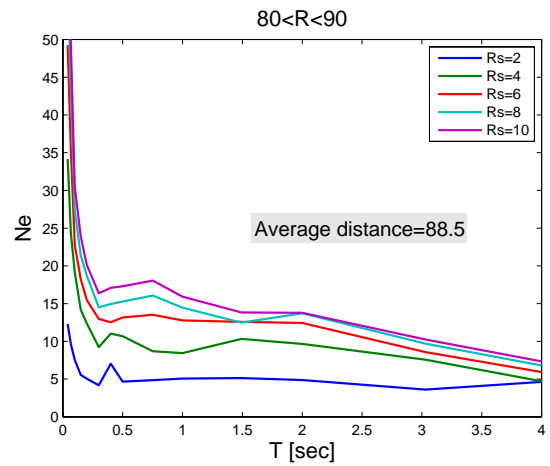
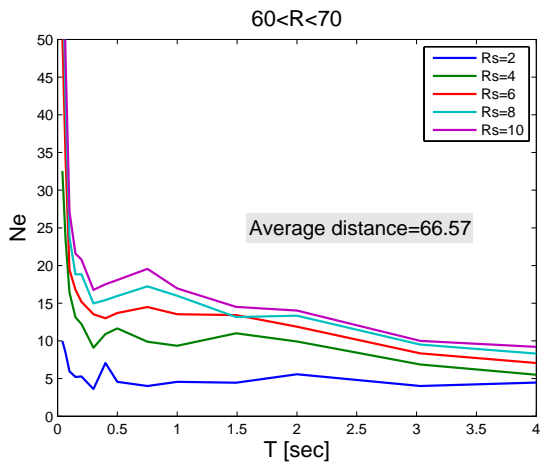
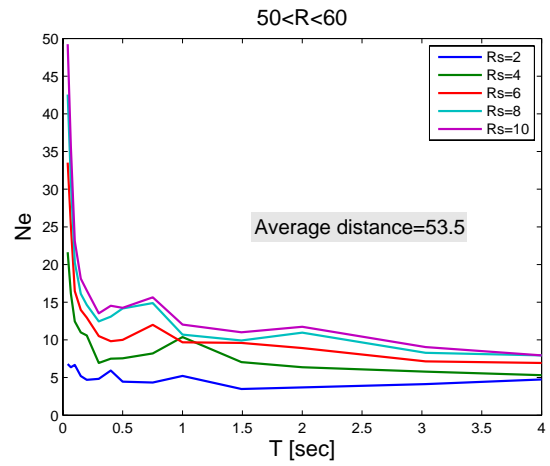
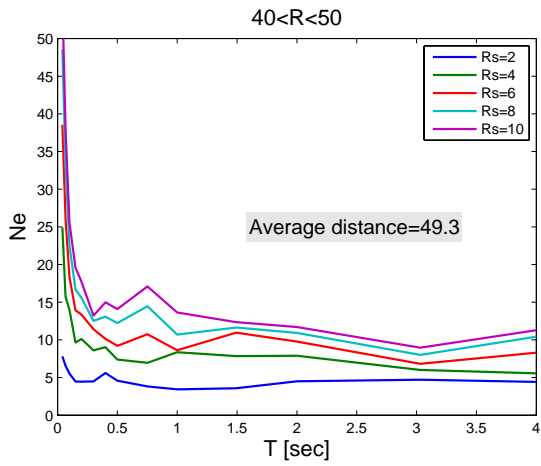


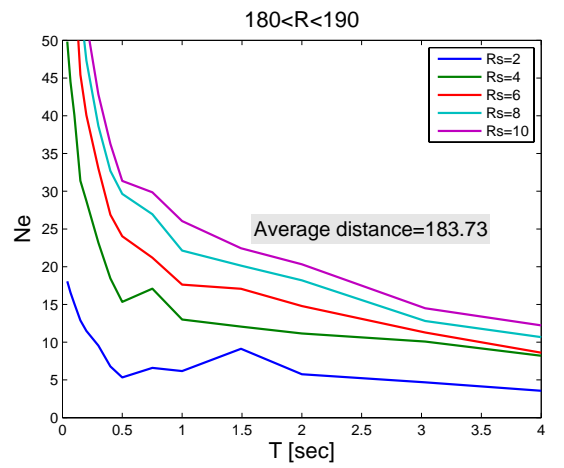
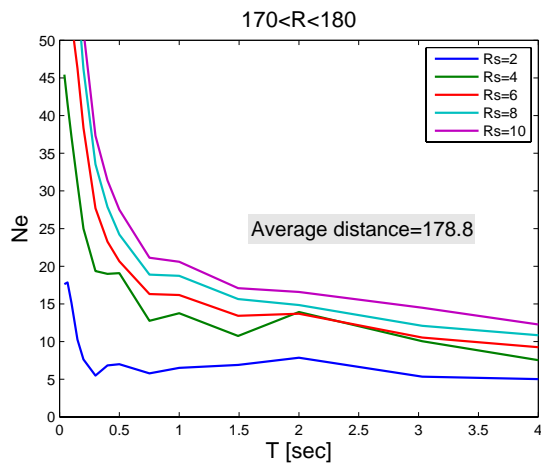
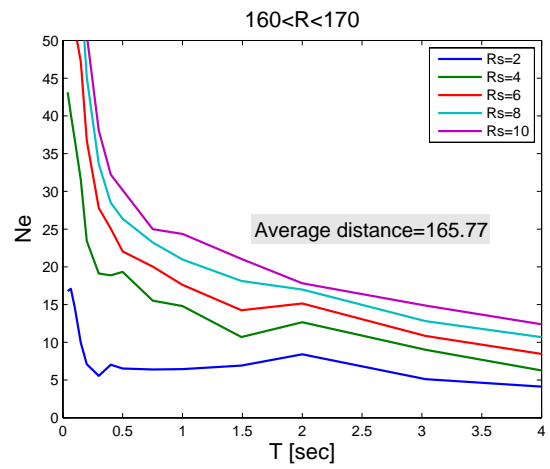
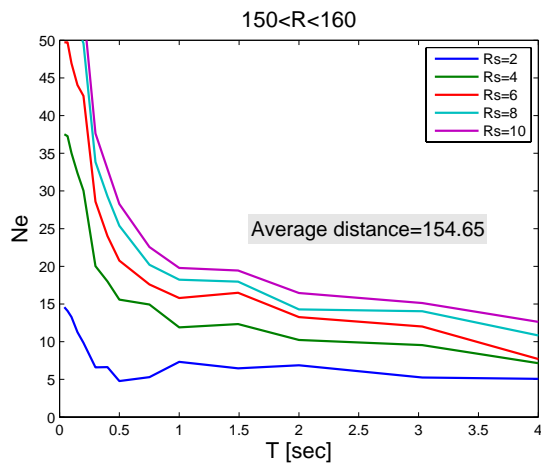
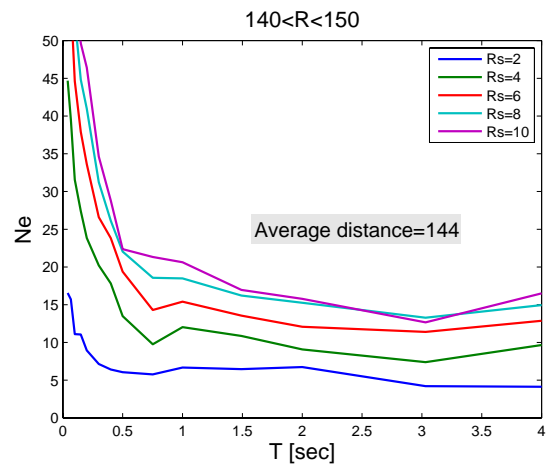
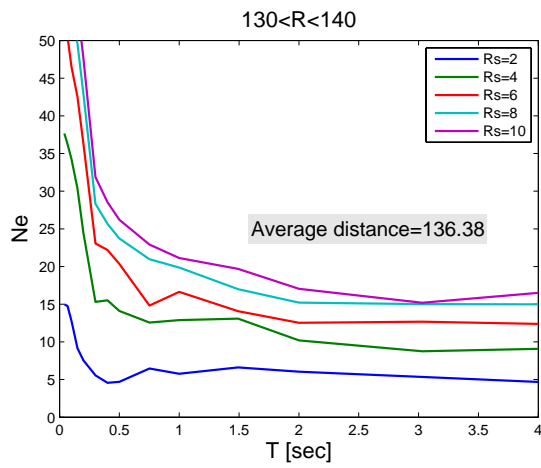


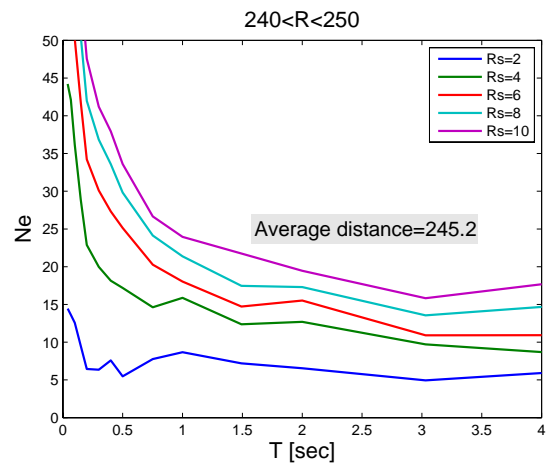
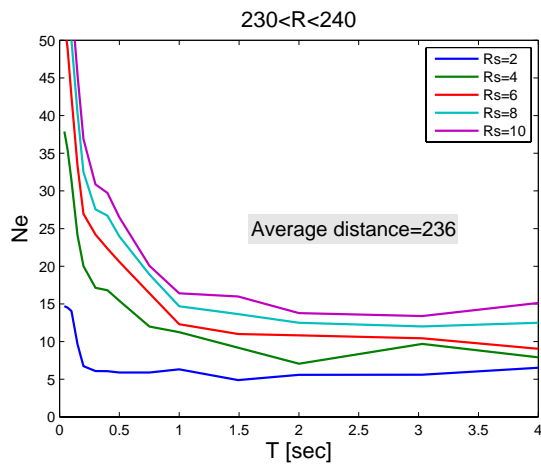
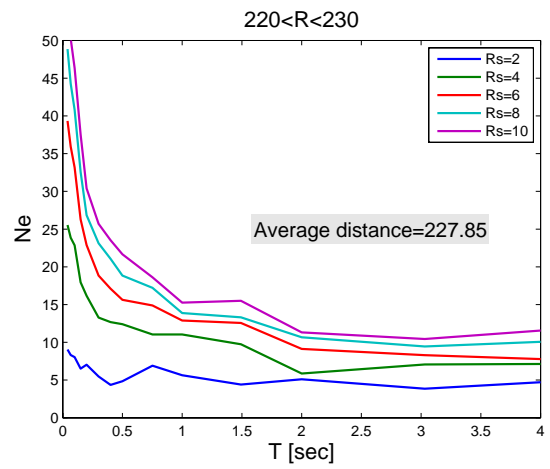
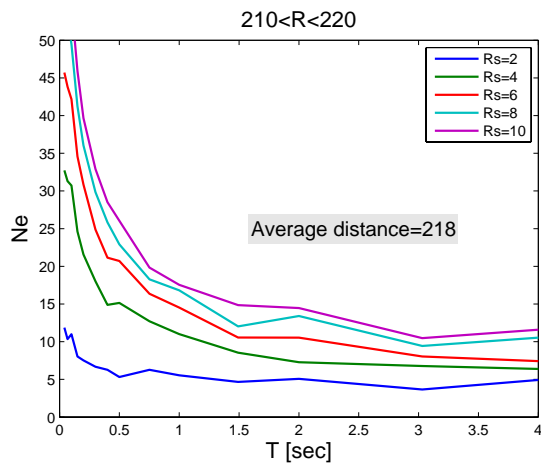
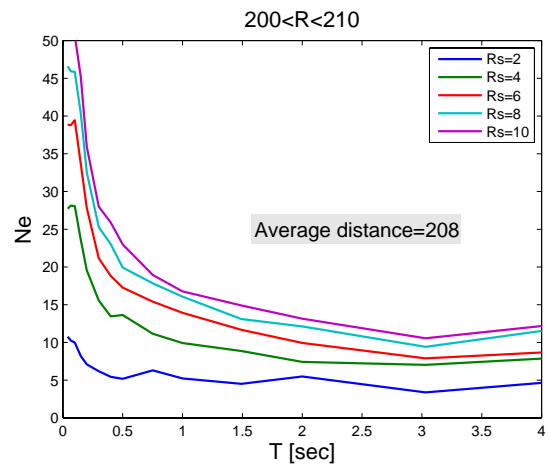
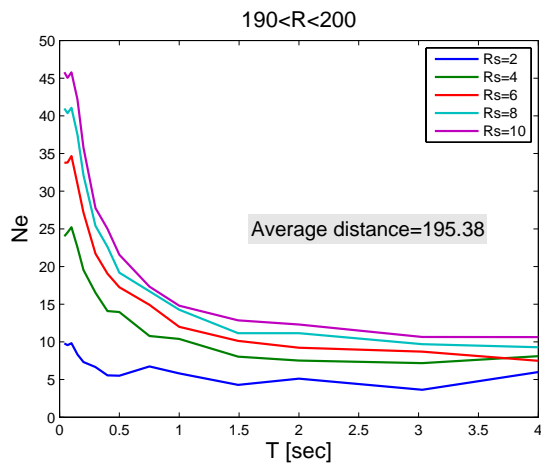


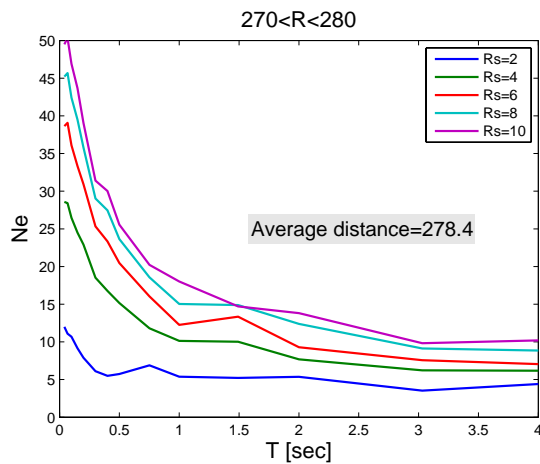
16. Vertical Component – Number of Equivalent Cycles Spectra











References

DPC-S4 project website, <http://esse4.mi.ingv.it/>.

Cosenza E., Manfredi G., Ramasco R, 1993: The Use of Damage Functionals in Earthquake Engineering: A Comparison between Different Methods. *Earthquake Engineering and Structural Dynamics*, 22 (10), 855-868.

Hancock J., 2006: The Influence of Duration and the Selection and Scaling of Accelerograms in Engineering Design and Assessment, Ph. D. Thesis.

Iervolino I.,Giorgio M., Galasso C. and Manfredi G., 2008: Prediction Relationships for a Vector-Valued Ground Motion Intensity Measure Accounting for Cumulative Damage Potential. *14th World Conference on Earthquake Engineering*, October 12-17, Beijing, China.

Sabetta F., Pugliese A., 1996: Estimation of Response Spectra and Simulation of Nonstationary Earthquake Ground Motion. *Bulletin of the Seismological Society of America*, 86, 337-352.

Iervolino I., Manfredi G. and Cosenza E., 2005: Ground motion duration effects on nonlinear seismic response. *Earthquake Engineering and Structural Dynamics*, 35, 21-38.